Report No. FRA-OR&D 75-84

TUNNEL DESIGN CONSIDERATIONS

ANALYSIS OF STRESSES AND DEFORMATIONS AROUND ADVANCING TUNNELS

AUGUST, 1975

FINAL REPORT

Prepared for

Department of Transportation
FEDERAL RAILROAD ADMINISTRATION
Washington, D.C. 20590

NOTICE

This document is disseminated under the sponsorship of the Department of Transportation in the interest of information exchange. The United States Government assumes no liability for its contents or use thereof.

Technical Report Documentation Page

1. Report No.	2. Government Accession No.	3. Recipient's Catalog No.
FRA OR&D 75-84		

4. Title and Subtitle	5. Report Date
Tunnel Design Considerations: Analysis of Stresses and Deformations Around Advancing Tunnels.	August 1975
	6. Performing Organization Code
7. Author(s)	8. Performing Organization Report No.
R. E. Ranken and J. Ghaboussi	UILU-ENG 75-2016
9. Performing Organization Name and Address	10. Work Unit No. (TRAIS)
Department of Civil Engineering University of Illinois at Urbana-Champaign Urbana, ILL. 61801	11. Contract or Grant No. DOT FR 30022
	13. Type of Report and Period Covered
12. Sponsoring Agency Name and Address	August 1974 - August 1975 Final Report
Federal Railroad Administration Department of Transportation Washington, D.C. 20590	14. Sponsoring Agency Code

15. Supplementary Notes

16. Abstract A truely comprehensive analysis of any ground-tunnel liner interaction problem requires that the three-dimensional nature (geometry, stress and displacement fields) of the problem be considered.

This report describes an investigation undertaken to study the complex distribution of stresses and displacements mobilized around and along unlined, partially lined, and completely lined tunnels being advanced through soils of various stress-strain behaviors. Circular tunnels with a depth to diameter ratio of five were considered. The unlined and lined tunnel analyses were divided into three subgroups on the basis of the simulated stress-strain behavior of the soil. One series of analyses considered linear-elastic behavior and involved the consideration of two different elastic modulus values and three different Poisson's ratio values. The soil in a second subgroup was assumed to exhibit elasto-plastic behavior corresponding to a shear strength independent of the mean stress and the angle of shearing resistance ($c \neq 0$, $\phi = 0$). An additional series of elasto-plastic analyses considered soil behavior to be a function of both cohesion and the angle of shearing resistance ($c \neq 0$, $\phi \neq 0$).

The finite element program GEOSYS was used in this investigation. The excavation and construction options of this computer program made it possible to simulate, with a minimum of effort, a tunnel being advanced through an initially stressed ground mass.

17. Key Words	18. Distribution Statement
Advancing Tunnel; Tunnel Liners; Finite Element; Soil-liner Interaction; Tunnel Analysis	Document is available to the public through the National Technical Information Service, Springfield, VA 22151

19. Security Classif. (of this report)	20. Security Classif. (of this page)	21. No. of Pages	22. Price
Unclassified	Unclassified	169	

Form DOT F 1700.7 (8-72) Reproduction of completed page authorized

PREFACE

The studies described in this report were performed by the Department of Civil Engineering of the University of Illinois at Urbana-Champaign, Urbana, Illinois during the period August 1974 to August 1975. The investigation was sponsored by the Federal Railroad Administration, Department of Transportation, through contract No. DOT FR 30022 under the technical direction of Mr. William N. Lucke. Prof. E. J. Cording, Dr. R. B. Peck and Mr. Lucke contributed ideas pertinent to the objectives and scope of the investigation. Their help is greatly appreciated.

The investigation described represents the continuing analytic studies performed with a computer program originally written by the firm of Agbabian Associates under the sponsorship of ARPA with ARPA Order No. 1579 and monitored by the Bureau of Mines. The program was modified for use on the IBM 360/75 computer at the University of Illinois. In this report the program has been called GEOSYS.

TABLE OF CONTENTS

LIST OF TABLES

LIST OF FIGURES

LIST OF SYMBOLS

a	tunnel radius
c	cohesion
c_u	undrained shear strength, apparent cohesion
C	Compressibility Ratio = $\frac{\text{extensional stiffness of the ground mass}}{\text{extensional stiffness of the liner}}$ (Eq. 4.4)
D_i	inside diameter of the tunnel liner
D_o	outside diameter of the tunnel liner
E_ℓ	modulus of elasticity of the tunnel liner
E_m	modulus of elasticity of the ground mass
H	depth from ground surface to axis of tunnel
J_2'	second invarient of the deviator stress tensor
K_o	coefficient of earth pressure at rest
ℓ_u	length of unsupported tunnel between face and liner
M_c	constrained modulus of the ground mass, $M_c = \frac{E_m (1 - \nu_m)}{(1 + \nu_m)(1 - 2\nu_m)}$
p_i	internal pressure
P	ground pressure acting on liner

r	radial coordinate, radial distance from tunnel centerline
R	maximum radius of the plastic zone
t	thickness of tunnel liner
t_b	thickness of bead on tunneling shield
t_s	thickness of shield tailskin
T	liner thrust
u	radial displacement
u_e	radial displacement of tunnel wall as given by elastic closed form solution
u_f	radial displacement at tunnel face
u_g	radial displacement at point of liner installation
u_l	radial displacement of liner under load
u_p	total potential radial displacement of tunnel wall
u_r	radial displacement of tunnel wall
u_u	radial displacement of tunnel wall occurring between the face and the point of liner installation
u^*	radial displacement just ahead of liner
v	tangential displacement

w	longitudinal displacement
z	longitudinal coordinate, longitudinal distance from tunnel face
z^*	distance between tunnel face and reference cross section
Z	distance behind tunnel face at which plastic zone reaches maximum radius
Z'	longitudinal extent of plastic zone ahead of tunnel
γ	unit weight
$\gamma_{rz}, \gamma_{z\theta}, \gamma_{r\theta}$	shear strains in the cylindrical coordinate system
δ	magnitude of net soil displacement
θ	circumferential coordinate
ν_ℓ	Poisson's ratio of the liner
ν_m	Poisson's ratio of the ground mass
$\sigma_r, \sigma_\theta, \sigma_z$	normal stresses in the cylindrical coordinate system
$\tau_{rz}, \tau_{r\theta}, \tau_{z\theta}$	shear stresses in the cylindrical coordinate system
ϕ	angle of shearing resistance

CHAPTER 1

INTRODUCTION

1.1 GENERAL

As a tunnel is advanced through a ground mass composed of either soil or rock the original state of stress existing in that ground mass is significantly altered around the tunnel. If the tunnel and its projected centerline are viewed in longitudinal section, three stress and displacement fields can be differentiated. Far ahead of the tunnel (and at large radial distances) the stresses remain in their undistrubed state. If one principal stress is vertical and the two horizontal principal stresses are of equal magnitude this natural stress field may be thought of as being two-dimensional. Around the tunnel face the two-dimensional stress field is transformed into a complex three-dimensional stress and displacement field. The spatial extent of this three-dimensional zone is controlled by the stress-strain behavior of the ground mass and the position and rigidity of the liner (if one is provided). Behind and out of range of the face's influence, the stresses and displacements return to a two-dimensional state, albeit of a completely different nature from the original two-dimensional state. If the ground and liner do not exhibit time-dependent behavior longitudinal variations of stress and displacement are confined to the three-dimensional zone. However, if the liner and/or the ground do demonstrate time-dependent behavior, these variations can continue far behind the face. The actual distance depends on the time required for the ground-liner system to return to equilibrium and the rate of tunnel advance.

Of the two components of the ground-liner system it is seldom the liner that is considered to exhibit time-dependent behavior of a nature significant enough to affect initial support of the tunnel opening. However, a proposed system for slipforming a concrete lining immediately behind a tunnel boring machine or shield, described by Parker, et al., [14], is a good example of such a case. Known as the Extruded Liner System, it has been proposed for both soil and rock tunnels. For tunnels in soft ground the system consists of an excavator, shield, slipform, and auxiliary concrete mixing and pumping equipment as illustrated in Fig. 1.1. As the tunnel is being advanced, a steel fiber-reinforced, regulated-set concrete is mixed and pumped into the slipform. This concrete sets rapidly after mixing and exhibits rapid strength gain during the time it is supported by the slipform. However, the concrete at a given tunnel section does not attain its ultimate strength until some time after the slipform has passed. In addition, while the liner is gaining strength the ground loads, more likely than not, will also be increasing. Thus, the concrete mix must be designed so that at any given time after leaving the slipform the liner will be strong enough to carry the ground loads acting at that time.

The initial loading to which any tunnel lining is subjected is strongly influenced by the amount of ground displacement that occurs before the liner and the ground come into contact and begin to interact. Since these displacements change with time and position along the axis of the advancing tunnel, the time and position of liner installation are important considerations in any analysis undertaken to estimate support loading. Add to this the possible variation of liner properties with time and position and it

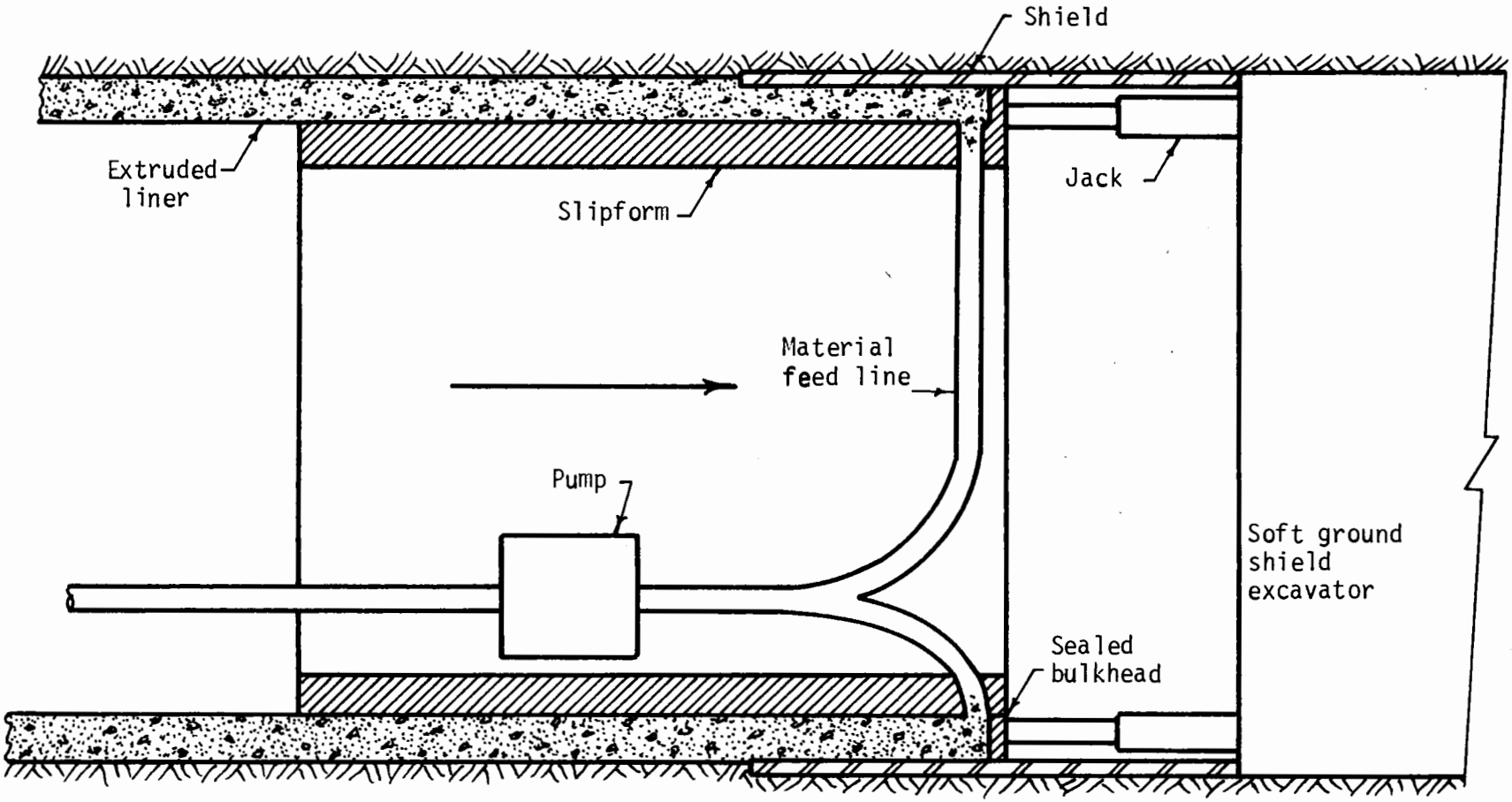

FIGURE 1.1 CONCEPTUAL EXTRUDED LINER SYSTEM FOR SOFT GROUND
(from PARKER, et al. [14])

becomes clear that analysis of the tunnel liner-ground interaction problem can become quite complex.

A comprehensive analysis of any ground-liner interaction problem requires that the three-dimensional nature (geometry, stress and displacement fields) and time-dependent nature (advance rate, behavior of ground and liner) of the problem be considered. Any method of analysis based only on the two-dimensional conditions that exist far behind the heading can represent only a part of the problem and will not provide the complete solution, nor even a necessarily reasonable partial solution.

To analyze the tunnel liner-ground interaction problem an investigation has been initiated in which the three-dimensional and time-dependent nature of the tunneling process are to be considered. Because of the extreme complexity of the problem, the finite element method of analysis and the following accumulative approach were decided upon.

The investigation is divided into a series of analyses in an ascending order of problem complexity. Initial analyses are of simple, idealized tunnel systems. Once these are evaluated an additional element of the problem is introduced to the system for analysis. This procedure continues until the complete system is considered.

The results obtained from the initial studies for the tunnel liner-ground interaction investigation are presented in this report. The first stage analyses were of an unlined tunnel in soils exhibiting idealized (linear-elastic and elasto-plastic) stress-strain behavior. In the second stage of the investigation the tunnel was assumed to be lined, with the liner extending either all the way to the tunnel face or to a section one radius behind the face. Again linear-elastic and elasto-plastic stress-strain behavior was

considered for the soil. One of the important features of these analyses is the simulation of a tunnel being advanced through an initially stressed ground mass.

1.2 OBJECTIVES

The general objectives of this investigation are to establish guidelines that can be used in the design of an extruded concrete tunnel liner. This involves, by means of ground-liner interaction analyses, the determination of the forces acting in the liner, along its length, for various ground conditions.

The specific objectives of the part of the investigation presented in this report are two fold: 1) to study the complex distribution of stresses and displacements mobilized around and along unlined, partially lined, and completely lined tunnels being advanced through soils, of various stress-strain behaviors; and 2) to relate these findings to the behavior of a tunnel lining placed by the Extruded Liner System.

1.3 SCOPE

For the purposes of the analyses reported herein, the modeled ground mass was assigned the properties of soil rather than rock. The soil was assumed to be isotropic, homogeneous and continuous. It was also stipulated that the soil remain continuous after excavation, thereby eliminating such phenomena as raveling and running ground from consideration.

Unlined, partially lined and fully lined tunnels of circular cross sections were considered. For the partially lined tunnels an unsupported length of tunnel, equal to one tunnel radius, was left between the face and the liner,

while for the fully lined tunnel the liner extended all the way to the face. The continuous, unreinforced concrete liner that was simulated in the analyses was assigned linear-elastic stress-strain properties.

The unlined and lined tunnel analyses were divided into three subgroups on the basis of the simulated stress-strain behavior of the soil. One series of analyses considered linear-elastic behavior and involved the use of two elastic modulus values and three Poisson's ratio values. The soil in a second subgroup of analyses was assumed to exhibit elasto-plastic behavior corresponding to a shear strength independent of the mean stress and the angle of shearing resistance ($c \neq 0$, $\phi = 0$). Another series of elasto-plastic analysis assumed soil behavior to be a function of these parameters ($c \neq 0$, $\phi = 0$).

The stress field existing in the undistrubed soil mass prior to excavation was assumed to be hydrostatic in all cases.

The data obtained from each analysis consisted of the soil and liner stresses and displacements. Thus, for each analysis the general distributions of stresses and displacements are presented for both the soil and the liner. In addition, the configuration of the plastic zone, the radial displacements of the actual and projected tunnel wall, and the longitudinal displacements of a reference cross section as the tunnel approached were isolated and presented separately.

1.4 RELATED RESEARCH

The three-dimensional distributions of stresses and displacements around an advancing tunnel and similar underground openings have been investigated to various extents by several researchers in the past. These studies

have consisted of laboratory model tests, field measurements, and finite element analyses. The following survey of this work represents the results of a necessarily brief literature search, and it is not intended that this be taken as a complete survey of all related research.

1.4.1 MODEL TESTS

Seeking the distribution of stresses around the bottom of a wellbore, Galle and Wilhoit [8] performed a series of three-dimensional photo-elastic experiments using the frozen stress technique. To simulate the wellbore (shaft, tunnel) cylindrical holes were machined into epoxy resin blocks. Two different model geometries were used. One in which the hole diameter to depth ratio was 4/11 and another in which this ratio was 5/12. Hole depth was half of the block length in all models. After each model was machined, external pressures were applied using nitrogen gas as the pressurizing fluid. Two types of external loading were considered: 1) hydrostatic compression and 2) uniaxial compression perpendicular to the centerline of the hole. No hole casing or liner was considered. It was found that the stresses around the bottom of the hole induced by a system of unequal principal stresses were considerably different from those induced by a hydrostatic stress system. With hydrostatic loading all stresses around the hole were compressive, whereas zones of tensile stresses were formed for certain combinations of unequal principal stresses. It was also found that stresses on the wall of the hole to within 2.9 radii of the bottom agreed well with those calculated by the elastic plane strain solution.

Abel and Lee [1] conducted a series of model tests in which they measured the stress changes occurring at a point as a cylindrical hole was successively deepened toward it. Three tests were performed, one for each of three different model materials, acrylic, concrete and Silver Blume granite. A hydraulic press was used to apply an external uniaxial compressive load to the model blocks. Stresses were measured by a solid inclusion borehole probe inserted within each block and positioned on the centerline of the model tunnel. It was not physically possible to advance the model tunnels while under load. Thus, after each measurement it was necessary to unload and remove the model from the press, drill the next increment of tunnel advance, and then reload the model. Abel and Lee compared their results to those of Galle and Wilhoit. A small compressive stress concentration located two diameters ahead of the model tunnel in the acrylic block (see Fig. 1.2), 1.25 diameters ahead of the model tunnel in the concrete block, and one diameter ahead of the model tunnel in the granite block was the only major difference between the two sets of data that could be compared. Abel and Lee concluded that the anomalous stresses could not be attributed to instrument error and that a true anomalous condition exists (ahead of the tunnel) that is not supported by available elastic theory or measurements. They also maintained that these stresses could not have been detected at the stress levels contoured by Galle and Wilhoit and that their models were too small, causing the results to be influenced by boundary effects.

1.4.2 FIELD MEASUREMENTS

Field measurements of the displacements and stress changes occurring in the ground mass around and ahead of an advancing tunnel have become

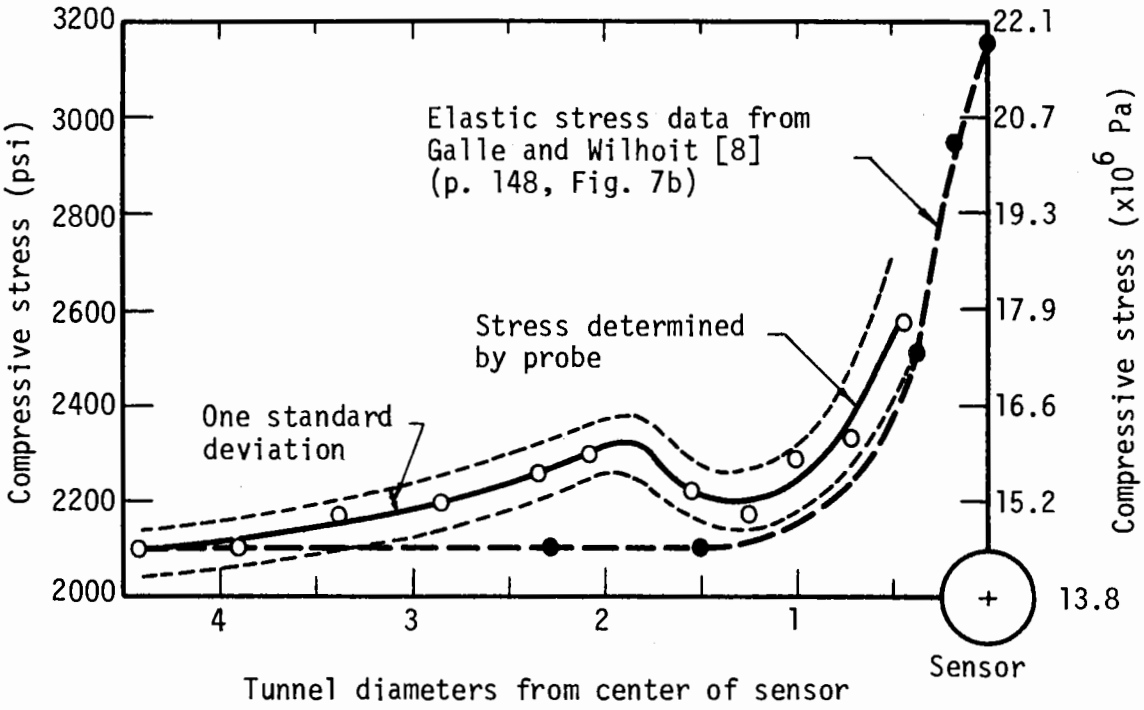

FIGURE 1.2 MAXIMUM PRINCIPAL STRESS IN ACRYLIC MODEL COMPARED TO THE RESULTS OF GALLE AND WILHOIT (MODIFIED FROM ABEL AND LEE [1])

more numerous in recent years. Difficulties associated with gaining access to the tunnel zone in order to place instrumentation have been the major obstacles to programs of this nature. In general, it has been possible to get around this problem only when the tunnel to be monitored was located at a shallow depth or aligned so as to pass close to an existing underground opening.

Abel and Lee [1] measured the stress changes that occured ahead of a 5 x 7 ft (1.6 x 2.1 m) tunnel as it was being advanced. The tunnel was driven roughly parallel to an existing tunnel located 70 ft (21.3 m) away. Two solid-inclusion borehole probes were placed approximately 50 ft (15.2 m) ahead of the advancing tunnel by means of a drill hole extending from the existing tunnel. The tunnel, at a depth of 350 ft (106.7 m), was advanced through metamorphic rock by the drill and blast method. Although there were numerous joints and one fault in the area, the most striking structural feature was reported to be the foliation of the metamorphic rock. It was found that the insitu stresses and the stress changes due to tunneling were controlled by this foliation. The measured stress changes showed an initial increase in compressive stress followed by a much larger decrease in compressive stress as the tunnel approached close to the probes. The trend of the data seemed to indicate that stress changes associated with the advancing tunnel were already taking place before the probes were installed (at points farther than 50 ft (15.2 m) ahead of the face).

Ward [18] presented data on displacements occurring around and ahead of a tunnel being advanced through London clay. The 80 ft (24.4 m) deep

tunnel was driven with a hand shield 13.5 ft (4.1 m) in diameter and behind which the tunnel was supported by a permanent cast iron liner. Two sets of displacement measurments were made by means of single-position extensometers anchored at one end in the clay near the tunnel line and extending to nearby underground structures. Lateral displacements were measured at axis level of the approaching tunnel. Three measuring points were established, each a different distance out from the projected tunnel wall. Measurements were first taken when the shield was 20 ft (6.1 m) away and were continued until the tail of the shield was 20 ft (6.1 m) past the extensometers. All displacements were toward the tunnel opening and the largest of these (0.49 in. = 12 mm) was recorded by the probe closest to the tunnel wall (1.6 ft = 0.5 m). The first significant movements occurred approximately one diameter ahead of the face, while displacements had essentially ceased one radius behind the tail of the shield. The most rapid inward displacements occurred just behind the bead and just behind the tail of the shield. A set of three axial displacement measurements were made at axis level in front of the face of the same tunnel. Extensometers were placed on the tunnel centerline, at the left springline, and 1 ft (0.3 m) outside the right springline. Measurements began when the tunnel face was 25 ft (7.6 m) away and continued until the anchoring points were destroyed by excavation. Displacements were very small until the shield approached to within one diameter of the probes. Final displacement at the left springline was approximately 40 percent of the centerline displacement (0.68 in. = 17 mm), while the maximum displacement 1 ft (0.3 m) outside the right springline was only about 7.5 percent of the centerline value.

A. M. Muir Wood [13] presented data on the vertical displacements associated with the passage of a shield in London clay. Displacements were monitored at the ground surface, 9.5 ft (2.9 m) and 3 ft (1 m) above the tunnel crown, and 20 in. (0.5 m) below the tunnel invert. The shield had a diameter of 35 ft 9 in. (10.9 m) and was 10 ft (3.1 m) long. The liner, which was placed immediately behind the shield consisted of precast concrete segments 1 ft (0.3 m) thick. The crown was overlain by about 12 ft (3.7 m) of clay with approximately 12 ft (3.7 m) of gravel above that. Measurements were made with single position extensometers installed from the ground surface. Displacements were first detected when the shield was approximately 1.67 diameters away from the measuring points, but remained small until the shield approached to only one diameter away. Just before the shield reached the instrumented station the measured displacements were 0.40 in. (10 mm) downward at 3 ft (1 m) above the crown, 0.28 in. (7 mm) downward at 9.5 ft (2.9 m) above the crown, and 0.12 in. (3 mm) upward at 20 in. (0.5 m) below the invert. As the shield's cutting edge passed the probes, a 0.24 in. (6 mm) upward displacement occurred at the point 3 ft (1 m) above the crown, while no movement was recorded at the higher probe and the invert probe was destroyed. By the time the tail of the shield had passed the measuring points, essentially all of the displacements had occurred. The maximum displacements measured were 0.54 in. (13.7 mm) at the point 3 ft (1 m) above the crown and 0.49 in. (12.5 mm) at 9.5 ft (2.9 m) above the crown.

Hansmire and Cording [11] presented results from a very extensive program to record ground displacements associated with a soft-ground tunnel

on the Washington Metro. The tunnel, 21 ft (6.4 m) in diameter (O. D.), was located at a depth of 38 ft (11.6 m) (to crown) in essentially granular soils. The face was excavated with a ripper-bucket on an articulated arm mounted inside a shield. The overall length of the shield, including poling plates and hood, was 23.5 ft (7.2 m). The primary support consisted of expanded steel ribs with full timber lagging. A 100 ft (30.5 m) test section consisting of three instrument lines was established across the path of the tunnel. Each instrument line consisted of a number of inclinometer casings and multiple position extensometers to measure horizontal and vertical displacements, respectively. As the shield approached and passed through the test section, sufficient data (vertical displacements, longitudinal and lateral horizontal displacements) were obtained to provide the full three-dimensional pattern of displacements around the advancing tunnel.

It was found that very little of the final total displacements occurred ahead of the shield and that the bulk of the displacements could be related to the details of the excavation and construction process. Displacements were greatest right around the shield and were due primarily to the tendency of the shield to plow through the soil and to the void behind the poling plates. Additional displacements occurred behind the shield and were due primarily to incomplete expansion of the lining. The maximum vertical displacement at the tunnel crown was approximately 13 in. (33 cm), while the maximum lateral inward displacement at the springline was on the order of 2 in. (5 cm).

Attewell and Farmer [3] discuss a similar program of field measurements made on a tunnel in London. In this case, a 13.5 ft (4.1 m) diameter shield driven tunnel was excavated by hand at a depth of 89 ft (27.2 m) (to

crown) in stiff, fissured, heavily overconsolidated London clay. The tunnel was lined with rings of cast-iron segments which were assembled within the tailpiece of the shield. Horizontal subsurface displacements were measured with an inclinometer. Vertical subsurface displacements were measured with an electronic system that utilized magnetic rings located at intervals along the inclinometer casings.

In general the measured displacements were very small, reflecting both the stiff nature of the clay and the fact that the closest measuring points were positioned at least several feet outside the tunnel opening. The maximum measured vertical displacements just above the crown (5 ft = 1.5 m) were on the order of 0.65 in. (16.5 mm). Measurements at a point at axis level and 5.6 ft (1.7 m) outside the left springline indicated an inward displacement of approximately 0.3 in. (8 mm). The unmeasured displacements right at the tunnel opening were undoubtedly larger than these measured values, but still probably did not exceed an inch (25 mm) or so.

1.4.3 FINITE ELEMENT STUDIES

To establish the theoretical basis for a method of determining the state of stress in a rock mass de la Cruz and Goodman [6] used the finite element method to analyze the deformations occurring around the bottom of a borehole. The three-dimensional problem was modeled with an axisymmetric finite element mesh, but nonaxisymmetric as well as axisymmetric stress fields were considered. On the basis of the results obtained from several linear-elastic analyses they derived (using nonlinear regression analysis and polynominal interpolation) expressions for radial displacements at several points along the borehole axis.

Descoeudres [7] investigated the distribution of displacements and stresses around an unlined tunnel in rock using a three-dimensional finite element analysis. Displacements of the tunnel wall were given for various ratios of initial vertical stress and radial and axial horizontal stresses. The results (displacements) of six linear-elastic analyses and one elasto-plastic analysis were presented.

The distributions of radial displacements obtained in these two investigations were very similar. They indicate that first displacements occur approximately two diameters ahead of the tunnel face and that complete displacement has occurred at a distance of about two diameters behind the face. The magnitudes of the radial displacement at any point within this zone is a function of initial stress state, the elastic properties of the medium, circumferential and longitudinal position of the point, and the tunnel diameter.

CHAPTER 2

METHOD OF ANALYSIS

2.1 GENERAL

The finite element program GEOSYS [10], which is a modified form of a program written for the U. S. Bureau of Mines by Agbabian Associates [2], was used in this investigation.

Because of the great expense associated with the use of three-dimensional finite elements in the analysis of an advancing tunnel, these elements were not used in this investigation. Instead, the three-dimensional problem was modeled with axisymmetric finite elements.

The quadrilateral, isoparameteric axisymmetric finite element [20] used in this study are circular rings, called toroidal elements (Fig. 2.1a). Although an assemblage (mesh) of these elements can be constructed in a wide variety of forms, here a simple solid cylindrical shape (Fig. 2.1b) was considered the most suitable for the problem at hand. The position of any point within such a mesh is defined by the three cylindrical coordinates: r, θ and z. When such a mesh is subjected to an axially symmetric loading the problem becomes mathematically two-dimensional. Because of symmetry, the stress components are independent of the angular (θ) coordinate and, thus, all derivatives with respect to θ vanish and the components v, $\gamma_{r\theta}$, $\gamma_{\theta z}$, $\tau_{r\theta}$, and $\tau_{\theta z}$ are zero. The nonzero stress components are σ_r, σ_θ, σ_z, and τ_{rz} (see Fig. 2.1c).

Because of the restrictions on geometry and loading the axisymmetric

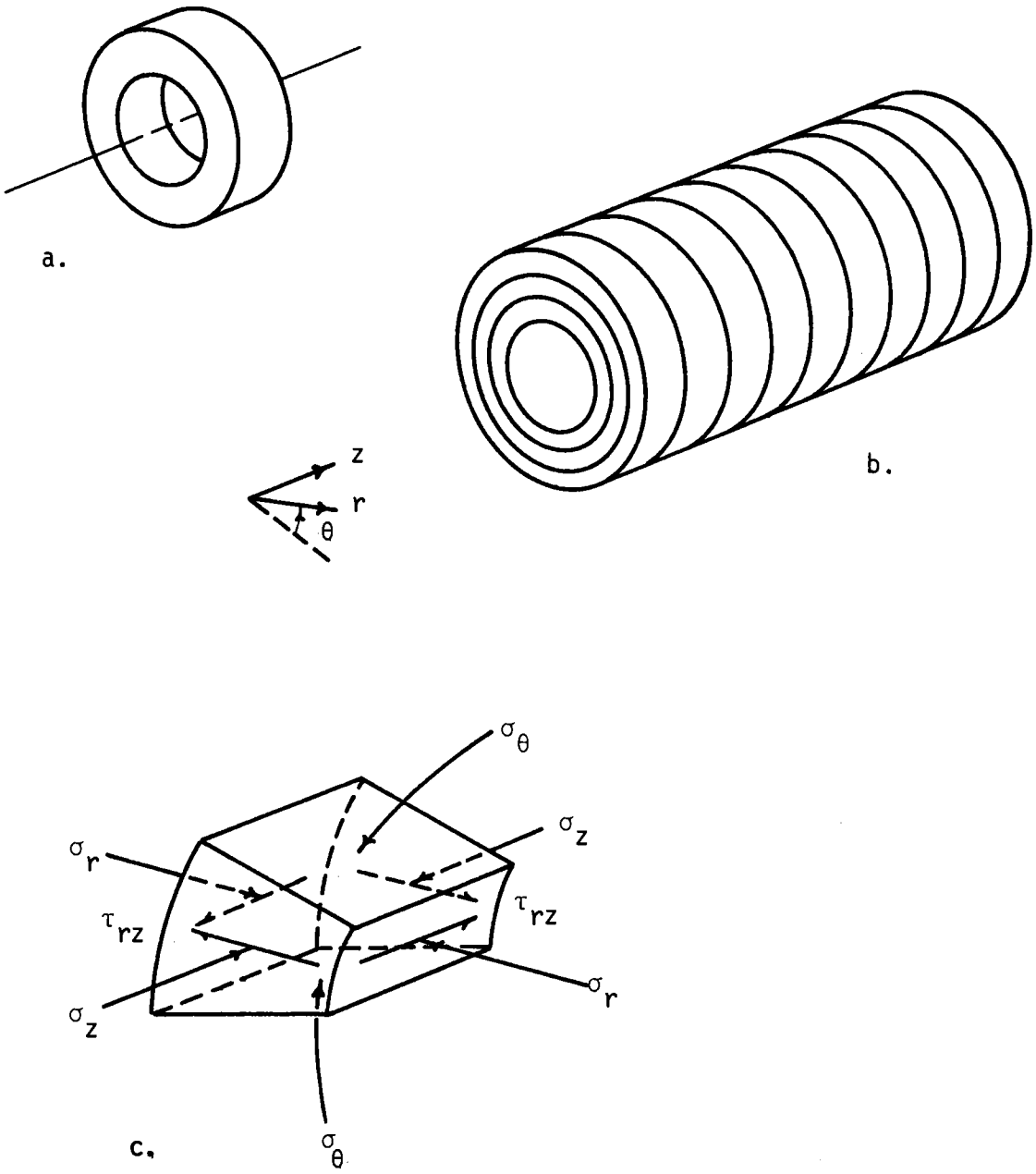

FIGURE 2.1 a. AXISYMMETRIC FINITE ELEMENT, b. CONCEPTUAL AXISYMMETRIC FINITE ELEMENT MESH AS USED HERE, c. NON-ZERO STRESS COMPONENTS

analysis cannot be applied to shallow tunnels. It is not possible to simulate the boundary effects imposed by the ground surface nor the increase of stress with depth from crown to invert that become significant at shallow depth. Thus, these analyses correspond to the special case of a deep tunnel (depth > several diameters) located in a ground mass subjected to a uniform stress field in which $K_o = 1$.

2.2 FINITE ELEMENT MESH

Figure 2.2 represents one half of a longitudinal cross-section through a typical finite element mesh used in this investigation. Boundary stresses were applies so as to achieve an initial uniform hydrostatic stress state throughout the mesh, $\sigma_r = \sigma_\theta = \sigma_z = \gamma H$, where γ is the unit weight of the soil and H is the depth of the tunnel axis below the ground surface. At the beginning of each analysis all elements were assigned soil properties. The shaded elements are the soil elements which were "excavated" to form the tunnel. The elements with diagonals indicate the positions where liner elements were installed after excavation.

2.3 EXCAVATION AND LINER INSTALLATION SEQUENCE

Each analysis consisted of a series of steps in which the mesh and/or its boundary conditions were modified to simulate advancement of the tunnel through the soil. In step one the boundary stresses were applied to the mesh, all elements of which were assigned soil properties. At the end of this step the mesh represented a fully stressed, undisturbed ground mass. The first excavation into this ground mass occurred in step two when the

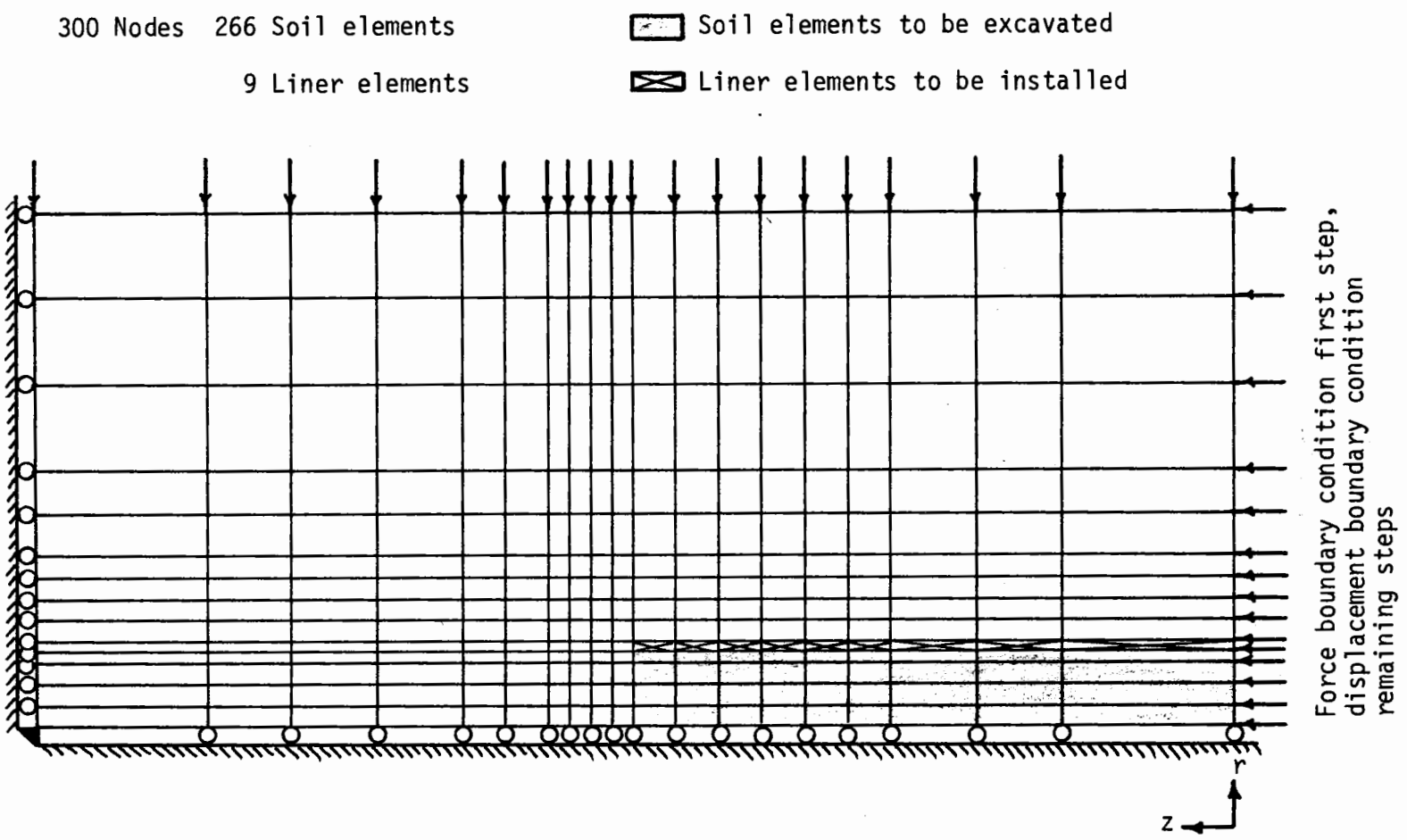

FIGURE 2.2 TYPICAL FINITE ELEMENT MESH

first set of soil elements were removed. Also in this step the force boundary condition along the right boundary was replaced by a displacement boundary condition to prevent longitudinal displacements there and to maintain the stress field in the soil. If the tunnel was to be lined a liner element was inserted at this step also. In each of the remaining steps the tunnel was advanced a distance equal to the length of the next ring of soil elements.

The excavation and construction sequence is achieved through the deactivation or activation of the elements involved. When the mesh is generated all elements (soil and liner) are assigned to the positions that they are to occupy at one time or another throughout the analysis. An activity number is assigned to each element that will be removed from or added to the mesh. The activity number indicates the step at which the element will be removed or added. In the case of excavation. the soil elements involved will have the appropriate material properties and will contribute to the global stiffness of the system up to the indicated step, beyond which the contribution of these elements to the global stiffness of the system will be zero. The reverse of this procedure is applied to those elements (liner) to be added to the mesh.

2.4 MATERIAL BEHAVIOR MODELS

Linear-elastic and elastic-perfectly plastic (elasto-plastic) material behavior models were considered in this investigation. The characteristics of these two models, as incorporated in the finite element program GEOSYS have been described in a previous report [10].

The yield function which defines the elasto-plastic model is a

function of the shear strength parameters: cohesion, c, and angle of shearing resistance, ϕ. For this study the elasto-plastic analyses were divided into two categories; one for which it was assumed that $c \neq 0$, $\phi = 0$, and another for which it was assumed that $c \neq 0$, $\phi \neq 0$.

The $\phi = 0$ assumption is valid only for saturated soils and only for as long as the moisture content of the soil remains unchanged. Any change in moisture content would be accompanied by a change in effective stresses and would introduce an effective frictional component of shear strength. Thus, the results from an analysis that assumes $\phi = 0$ apply only to the short term behavior of a tunnel. Theoretically, the $\phi = 0$ analysis could be used for any saturated soil. However, this type of analysis becomes practical only if the permeability of the soil is low enough so that the condition of no change in moisture content is satisfied for a reasonable length of time. A soil composed of particles larger than silt size would experience a change in water content almost immediately upon excavation. Thus, the $\phi = 0$ analysis would not be justified for such a soil. However, most clays and some silts possess sufficiently small permeabilities so that the no drainage condition can be satisfied for a time (days or weeks) after excavation. It is to these soils that this type of analysis can be applied.

CHAPTER 3

RESULTS OF ANALYSIS

3.1 GENERAL

The results obtained from the finite element analyses performed in this investigation are presented in this chapter. The following data are provided for each analysis:

--configuration of the plastic zone (elasto-plastic analyses)

--distribution of soil stresses

--distribution of soil displacements

--radial displacements of the actual and projected tunnel wall

--longitudinal displacements of a reference cross section as the tunnel approaches

--liner thrust (lined tunnel analyses)

It should be pointed out here that minor distortions of the data due to boundary and other procedural effects have been removed in order to isolate and clarify the information related solely to the behavior of an advancing tunnel.

3.2 UNLINED TUNNELS

3.2.1 GENERAL

Ten of the analyses performed considered the tunnel to be unlined. Four of these assumed the soil to behave linear-elastically, while the remaining six assumed elasto-plastic stress-strain behavior. Table 3.1 gives

TABLE 3.1

MATERIAL PROPERTIES FOR THE UNLINED TUNNEL ANALYSES

Case	ν_m	c_u psi	c_u (Pa)	ϕ degrees
ULLE 1	0.30	---	--	---
ULLE 2	0.40	---	--	---
ULLE 3*	0.40	---	--	---
ULLE 4	0.49	---	--	---
ULEP 1	0.49	14	(9.65×10^4)	0
ULEP 2	0.49	28	(1.93×10^5)	0
ULEP 3+	0.49	31.5	(2.17×10^5)	0
ULEP 4	0.49	37	(2.55×10^5)	0
ULEP 5	0.40	14	(9.65×10^4)	15
ULEP 6	0.40	14	(9.65×10^4)	30

E_m = 5000 psi (3.45×10^7 Pa)

Tunnel diameter = 20 ft (6.1 m)

Initial stress state: $\sigma_r = \sigma_\theta = \gamma H$, $\tau_{rz} = 0$

γH = 83.33 psi (5.75×10^5 Pa)

* E_m = 15,000 psi (1.03×10^8 Pa)

\+ Excavation sequence was not used

a summary description of these various analyses. The four letter code in the case number designation that is used in Table 3.1 and the following text indicates the type of analysis to which it refers. The letters UL indicate that the tunnel is unlined, while linear-elastic and elasto-plastic analyses are indicated by LE and EP, respectively.

3.2.2 LINEAR-ELASTIC ANALYSES

In performing four linear-elastic analyses, three values for Poisson's ratio, ν_m and two values for the elastic modulus, E_m, were considered.

As expected, it was found that the medium stresses were independent of E_m, while the displacements of the opening were inversely proportional to the modulus. Strictly speaking, different values of Poisson's ratio yielded different distributions of stresses and displacement. However, the effect on stresses was confined to a region around the tunnel face and was almost unnoticeable until the limit $\nu_m = 0.5$ (incompressible material) was approached. The effect on displacements, although not uniform and not exceptionally great, was noticeable throughout the soil mass. In general, the effect of Poisson's ratio was not significant when compared to the effect of the other parameters (modulus, magnitude of initial stress state, liner) that influenced tunnel behavior in these analyses.

SOIL STRESSES

The distributions of stress in the medium surrounding the tunnel for cases ULLE1, ULLE2, and ULLE3 are shown in the form of nondimensionalized

stress contours in Fig. 3.1. Cases ULLE2 and ULLE3 differ only in the magnitude of E_m, thus the stress distributions are the same for these two cases. Case ULLE1 had a smaller Poisson's ratio, but the differences between the stress distributions are so small that they can be considered negligible. The stress distribution for case ULLE4 ($\nu_m = 0.49$) are given in Fig. 3.2. Differences between the stress distributions, due to a difference in ν_m, occur only in a specific region, the longitudinal extent of which is approximately one and a half tunnel diameters either side of the tunnel face.

Figures 3.1 and 3.2 indicate that the zone of three-dimensional stress and strain (displacement) around an advancing tunnel extends out to approximately 2 diameters ahead of the face and back approximately 1-1/2 diameters behind the face. Far ahead of the face the two-dimensional free-field stress state ($\sigma_r = \sigma_\theta = \sigma_z = \gamma H$, $\tau_{rz} = 0$) remains undisturbed. At points farther than 1-1/2 diameters behind the face the stresses correspond closely to the two-dimensional, plane strain distribution.

It is common to illustrate the stress distribution around a tunnel by a plot of stress versus radial distance from the tunnel axis. This has been done for the stress distribution shown in Fig. 3.1. Figures 3.3, 3.4 and 3.5 are nondimensional plots of σ_r, σ_θ, and σ_z and τ_{rz}, respectively. To illustrate the change in stress with longitudinal distance from the tunnel face each figure consists of a number of curves, each for a given distance behind or ahead of the face (z/a). Only cross sections that are located in the three-dimensional stress-strain zone are shown.

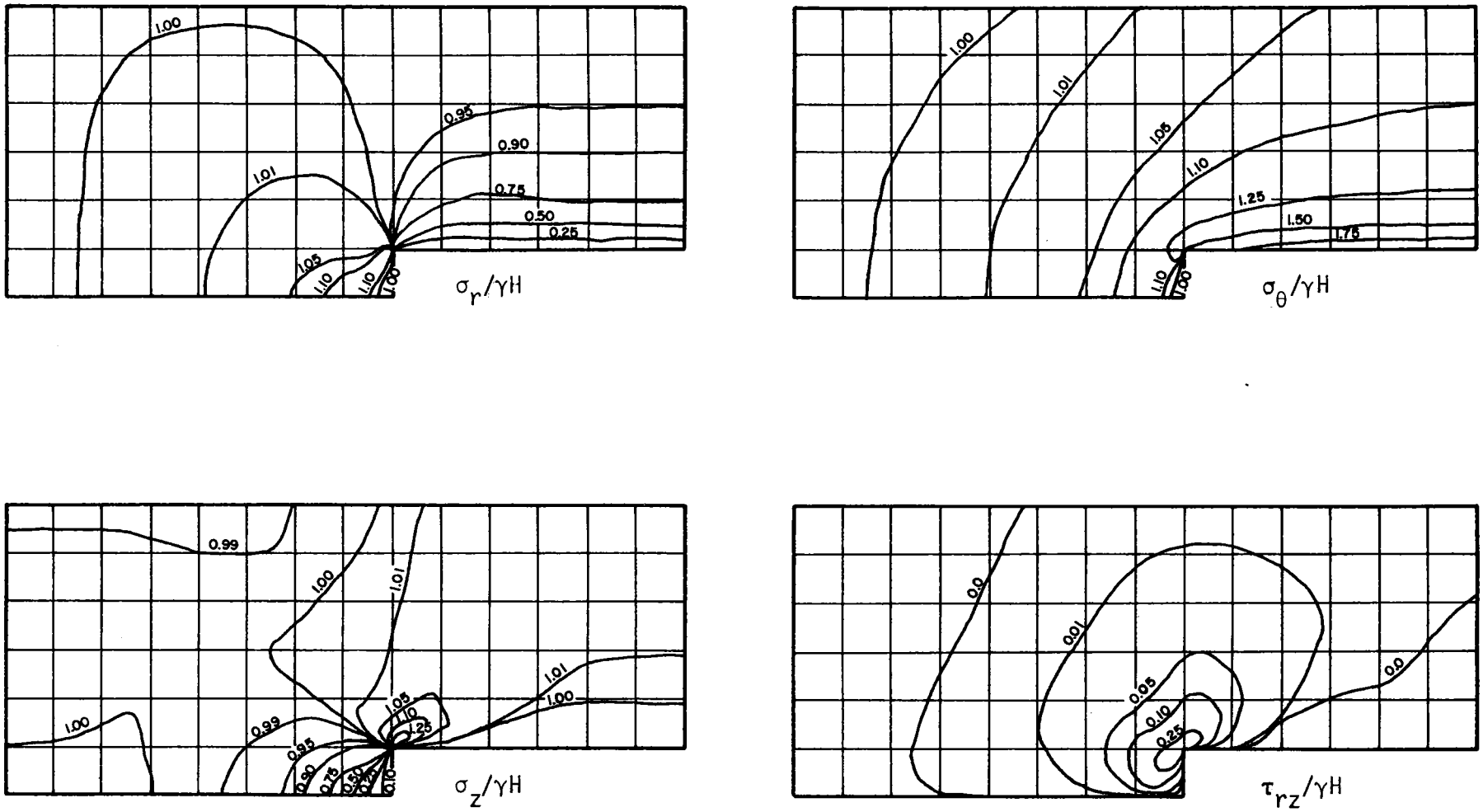

FIGURE 3.1 DISTRIBUTION OF STRESSES AROUND AN UNLINED TUNNEL IN A LINEAR-ELASTIC MEDIUM (CASES ULLE1, 2, 3)

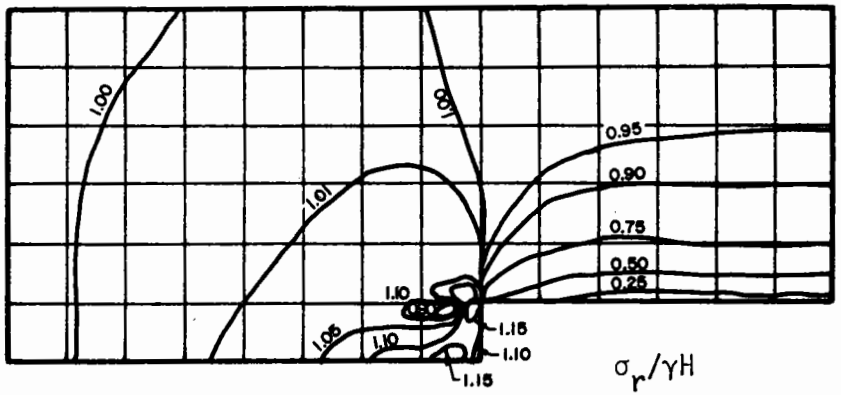

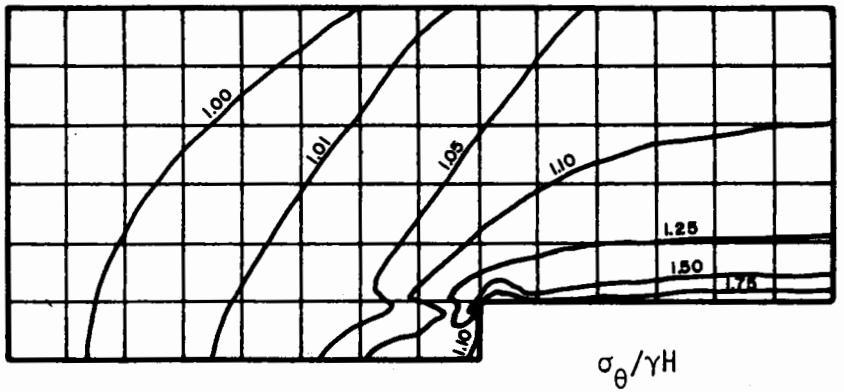

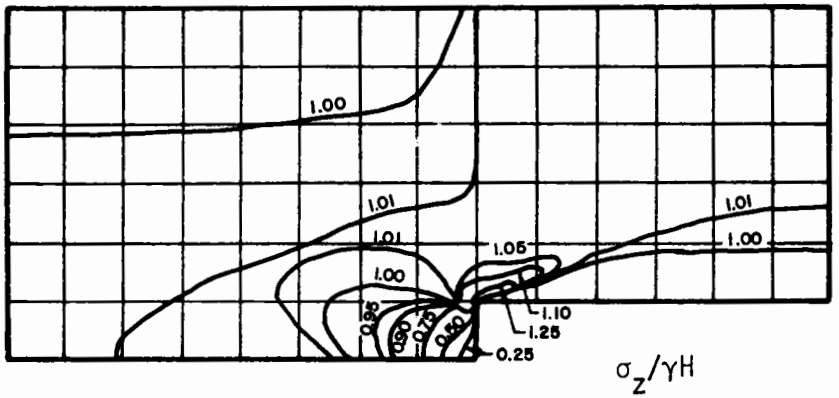

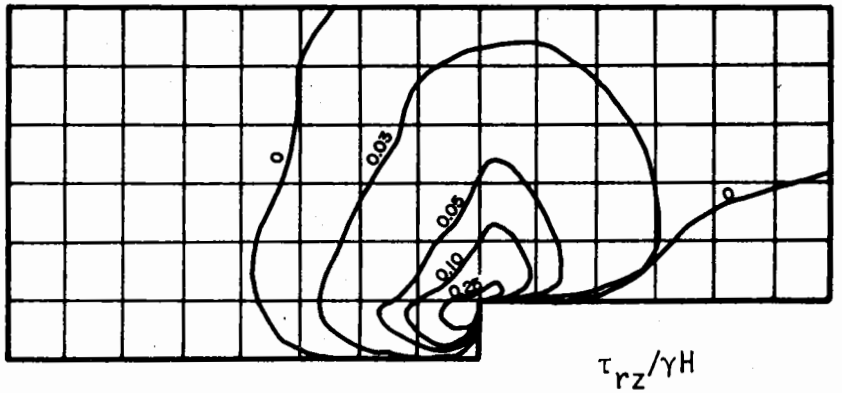

FIGURE 3.2 DISTRIBUTION OF STRESSES AROUND AN UNLINED TUNNEL IN A LINEAR-ELASTIC MEDIUM (CASE ULLE 4)

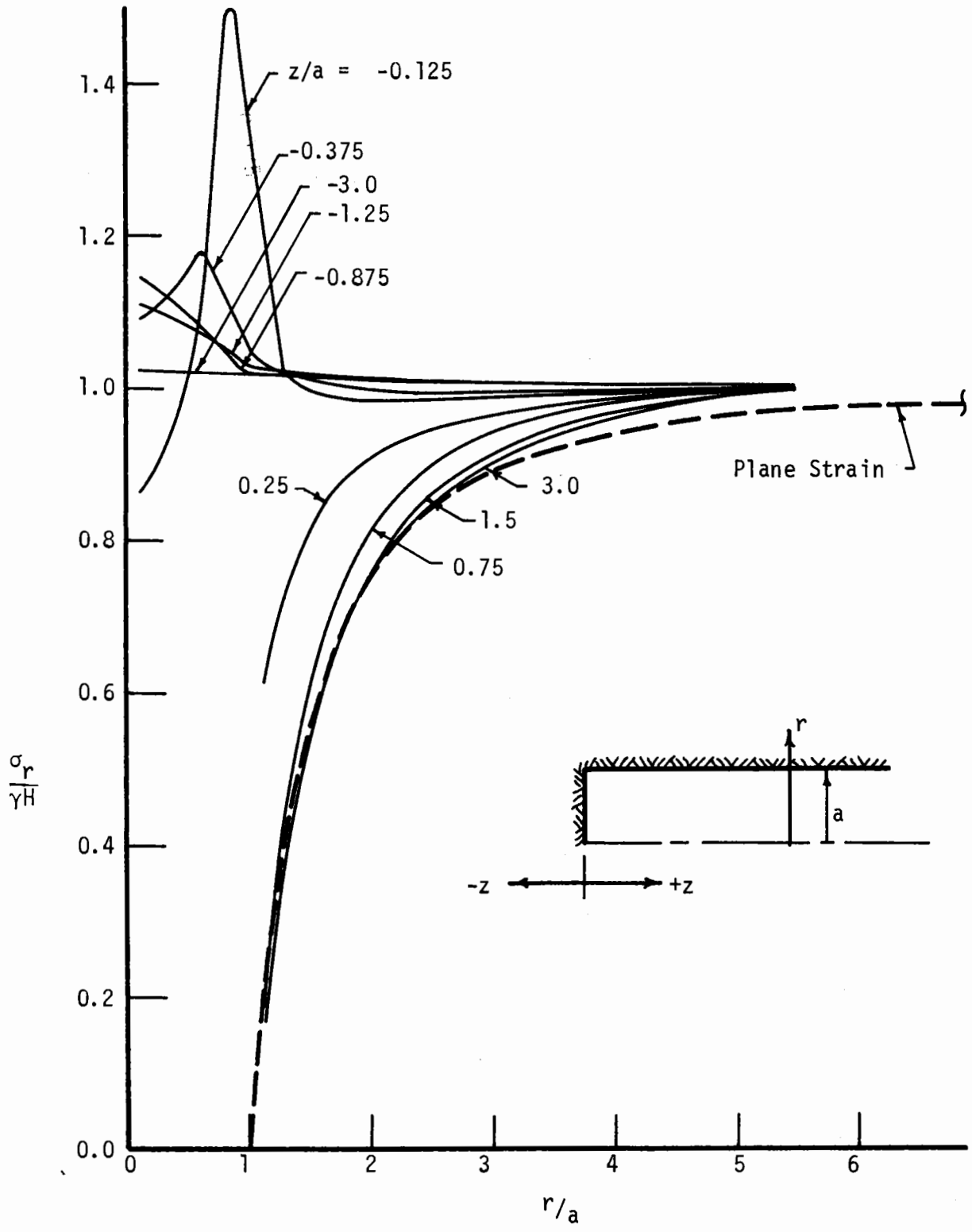

FIGURE 3.3 RADIAL DISTRIBUTION OF RADIAL STRESSES AROUND AN UNLINED TUNNEL IN A LINEAR-ELASTIC MEDIUM (CASES ULLE 1, 2, 3)

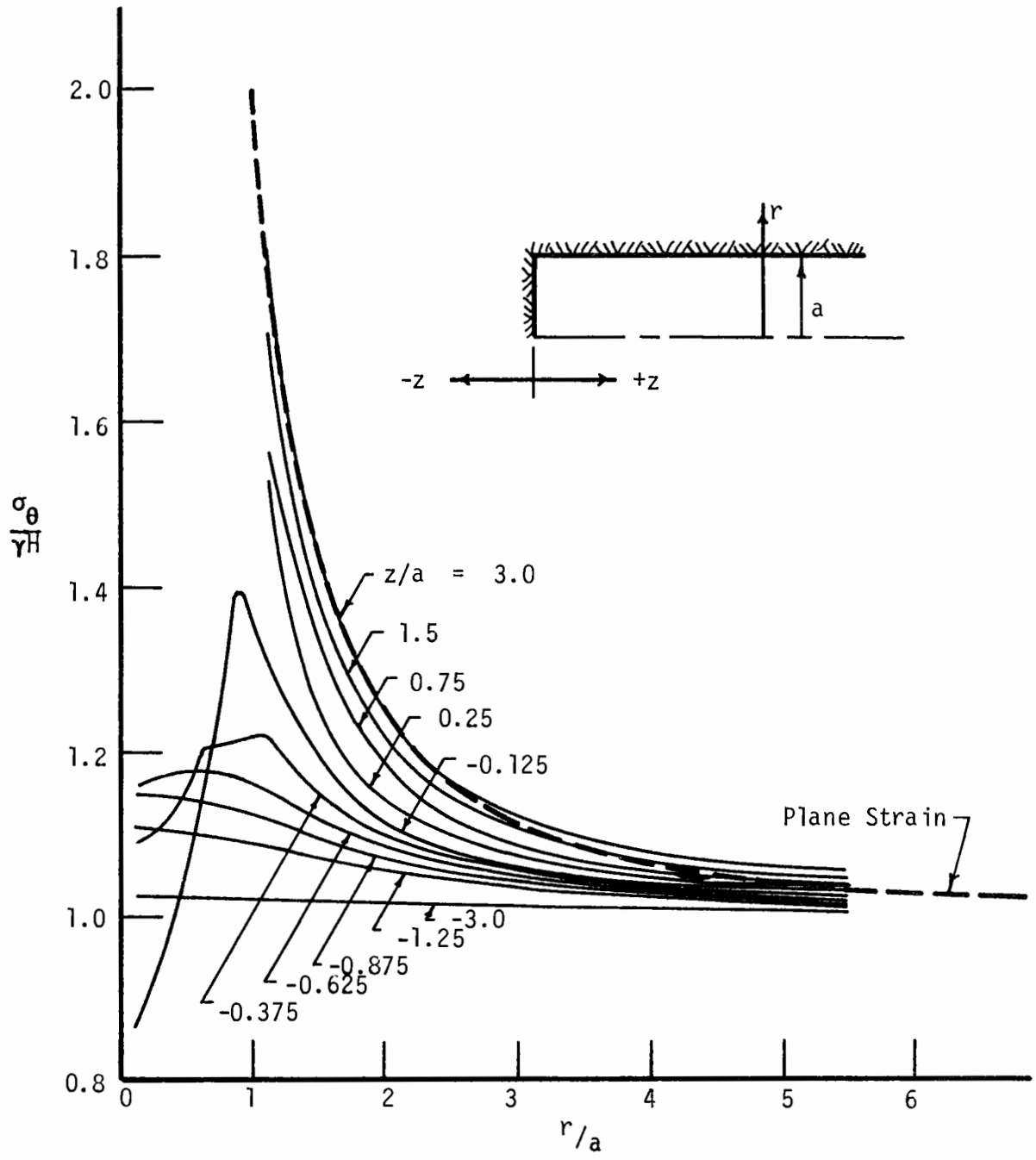

FIGURE 3.4 RADIAL DISTRIBUTION OF CIRCUMFRENTIAL STRESSES AROUND AN UNLINED TUNNEL IN A LINEAR-ELASTIC MEDIUM (CASES ULLE 1,2,3)

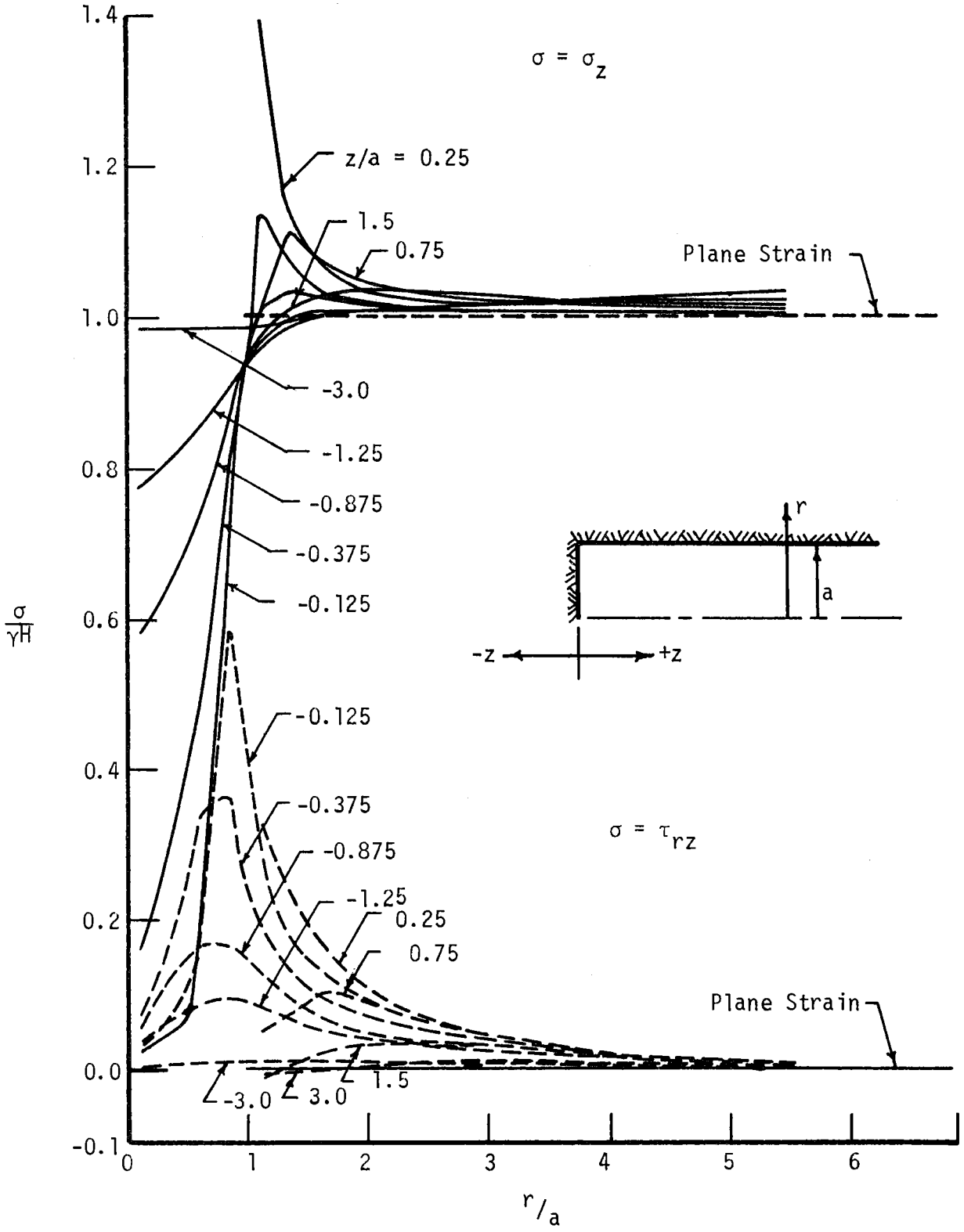

FIGURE 3.5 RADIAL DISTRIBUTION OF LONGITUDINAL AND SHEAR STRESSES AROUND AN UNLINED TUNNEL IN A LINEAR-ELASTIC MEDIUM (CASES ULLE 1, 2, 3)

It can be seen from Figs. 3.3 and 3.4 that the curves for z/a = 3 diverge from the plane strain curves at r/a > 3 or 4. This divergence from the theoretical solution results because the finite element boundary stresses (equal to the free-field stresses) were applied at a radial distance of only six radii, whereas the closed-form, plane strain solution assumes the free-field stresses to be applied at a radial distance of infinity.

SOIL DISPLACEMENTS

A representative pattern of the soil displacements that were initiated by advancement of the unlined tunnel in case ULLE1 is shown in Fig. 3.6. Part a of this figure gives the total displacements that resulted as the tunnel was driven through the full length indicated. Part b gives the incremental displacements that the soil experienced when the face was advanced through only a short distance (one-half tunnel radius). At a given point the displacement is represented by an arrow. The insert in part a of the figure illustrates that the arrows represent net displacements--direction and distance between original and final positions of a point--and not the actual displacement paths. Arrow length is keyed to net displacement magnitude and arrow direction corresponds to net displacement direction. At those locations where no arrow is given the displacements were very small--less than one-twentieth of one percent of the tunnel radius.

The distribution of total displacements shows that the soil moves both longitudinally and radially toward the tunnel opening. The

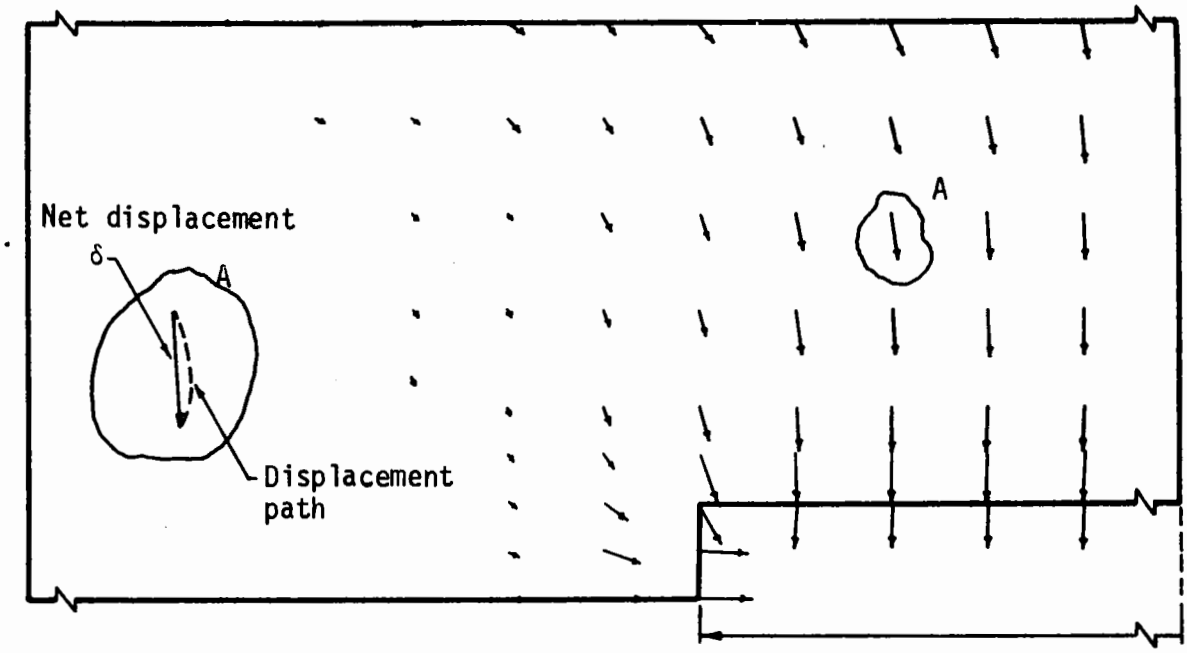

$\Delta = \frac{\delta}{a} \times 100$

.050 ≤ Δ < .125
.125 ≤ Δ < .250
.250 ≤ Δ < .375
.375 ≤ Δ < .500
.500 ≤ Δ

a) Total displacements

Δ < .050 Not shown

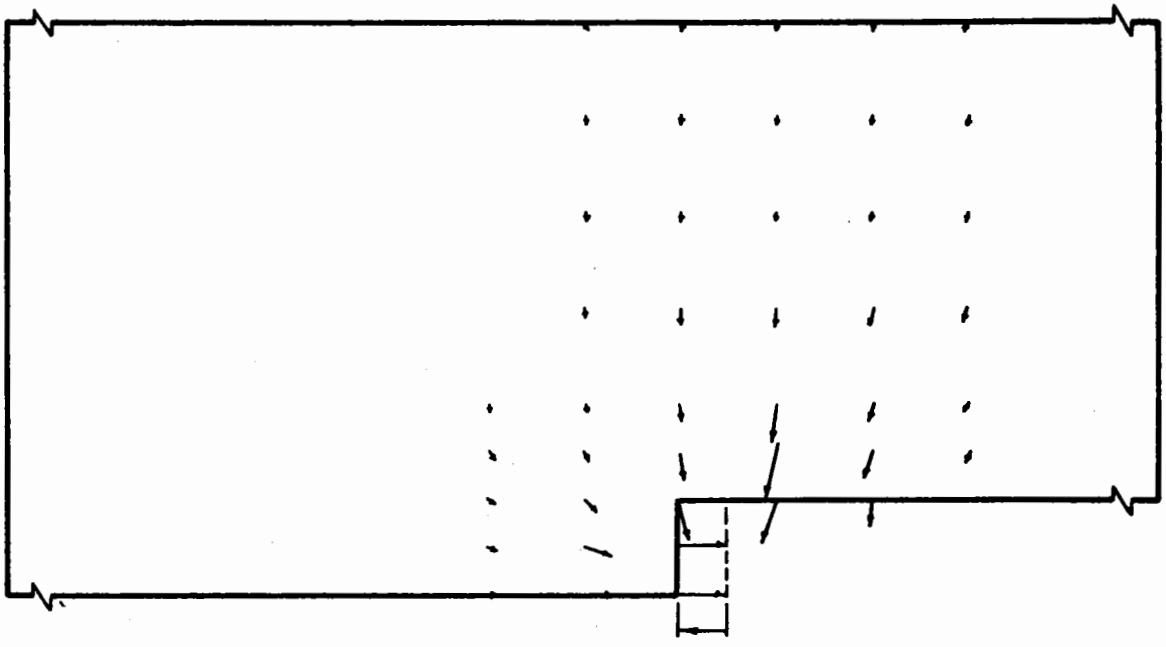

b) Incremental displacements

FIGURE 3.6 DISTRIBUTION OF DISPLACEMENTS AROUND AN UNLINED TUNNEL IN A LINEAR-ELASTIC MEDIUM (CASE ULLE 1)

largest displacements occur behind the tunnel face and are almost entirely radial. Along the tunnel axis significant movements occur out to a distance of about one tunnel diameter ahead of the face, but with increasing radial distance from the axis these displacements extend out farther ahead of the face.

The largest incremental displacements are clustered around the newly excavated portion of the tunnel. The largest of these displacements are located just behind the pre-excavation position of the face where support provided by the face was lost when the tunnel was advanced. These large radial displacements at the tunnel opening resulted in the propagation of significant displacements ($\Delta \geq .05$) all the way out to the mesh boundary, six radii from the tunnel centerline.

The displacement distributions obtained from the linear-elastic analyses ULLE1 through 4 did not differ from each other in any unusually drastic manner. Thus, only the one distribution is shown.

It was found that displacement magnitude at any given point varies linearly with elastic modulus, while the direction of the displacement is independent of the modulus. Poisson's ratio, which is an indicator of elastic compressibility, affects both displacement magnitude and direction. However, the affect is not great, and it is not uniform throughout the soil mass.

RADIAL DISPLACEMENTS

The radial displacements obtained from the linear-elastic analyses are given in Fig. 3.7. The displacements, u_r, have been normalized with

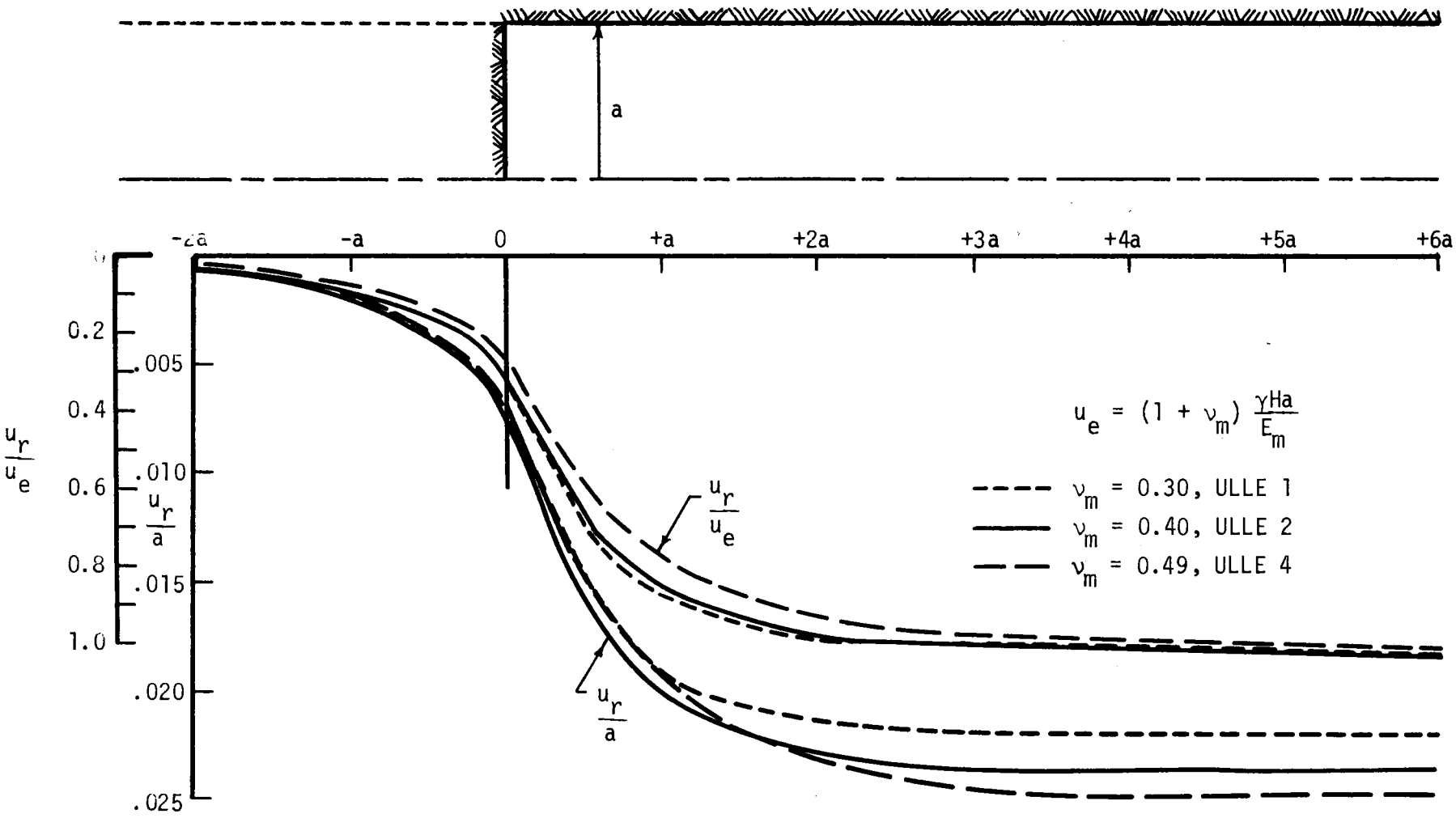

FIGURE 3.7 RADIAL DISPLACEMENTS FOR AN UNLINED TUNNEL IN A LINEAR-ELASTIC MEDIUM

respect to two different quantities. The upper set of curves represent the displacements normalized with respect to u_e, which is the radial displacement given by the closed form, plane strain, elastic solution for cross sections far behind the tunnel face [5]. The lower set of curves give the displacements normalized by dividing by the tunnel radius, a. These curves give a better indication of the affect of Poisson's ratio and they are in a form suitable for comparison to similar curves from the nonlinear analyses that will be discussed later.

The displacements u_r and u_e are those due to excavation of the tunnel opening only. They do not include the displacements that result from application of the free-field stresses to the intially unstressed medium. The expression for u_e is

$$u_e = (1 + \nu_m) \frac{\gamma H a}{E_m} \tag{3.1}$$

The results of the analyses indicated that significant radial displacements did not occur beyond a point about three tunnel radii ahead of the face. It can be seen from Fig. 3.7 that even at a distance of only two radii ahead of the face the displacements are very small. Likewise, when the face has advanced a distance of three radii beyond a given point, displacements at that point have essentially ceased. These maximum displacements correspond to the values (u_e) predicted by the two-dimensional, closed-form solution. Approximately 25 to 30 percent of the total displacement occurs ahead of the tunnel face.

In Fig. 3.8 the displacement curve AB' C', which is an idealization of the curves shown in Fig. 3.7, represents the displacement of the

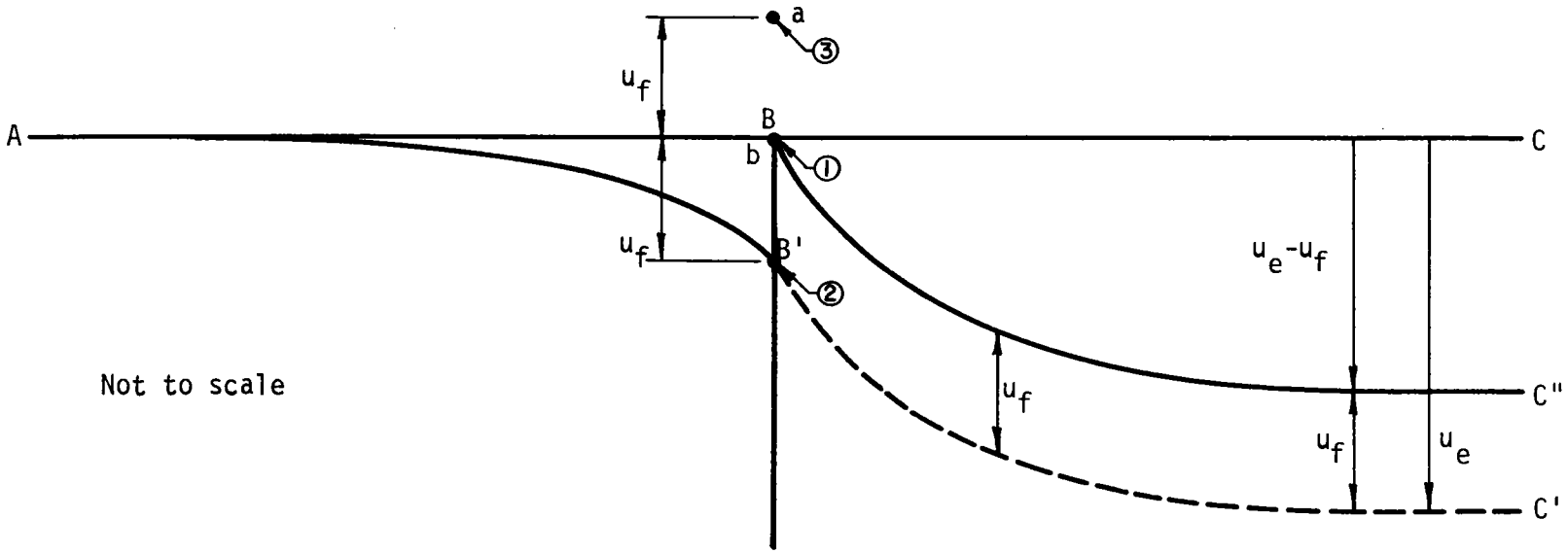

FIGURE 3.8 RELATIONSHIP BETWEEN CALCULATED RADIAL DISPLACEMENTS AND ACTUAL POSITION OF THE TUNNEL WALL

projected tunnel perimeter, ABC, due to excavation of the tunnel up to cross section B. As the tunnel face was advanced to cross section B, soil particle b, originally located at point 1, displaced inward to point 2. At the same time, assuming no attenuation of displacement with distance from the tunnel, particle a, originally at point 3, moved to point 1. As the face advances ahead of section B, soil particle b will be removed by the excavation process and particle a will be located on the exposed tunnel wall. Thus, the $B'C'$ portion of curve $AB'C'$ is purely theoretical and does not represent the position of the tunnel wall. If the face is advanced in very small increments (as with a tunnel boring machine) the position of the actual tunnel wall is given by the continuous curve BC''. If the tunnel is advanced in large increments the curve will be discontinuous.

LONGITUDINAL DISPLACEMENTS

The longitudinal displacements, w, that occur at a cross section ahead of the tunnel face, as the face approaches, are given in Fig. 3.9 for the various linear-elastic analyses. Shown in the figure are three plots of nondimensionalized displacement versus distance of the face from the reference cross section. Each plot is for a different value of r/a (0, 1/2, 1). Since there is no closed form solution for these displacements, the values obtained were normalized by dividing them by the tunnel radius, a. Several factors related to the method of analysis (length of initial excavation, size of finite element mesh, boundary conditions) combined to render the longitudinal displacements for $z^* > 2a$ somewhat suspect, and thus

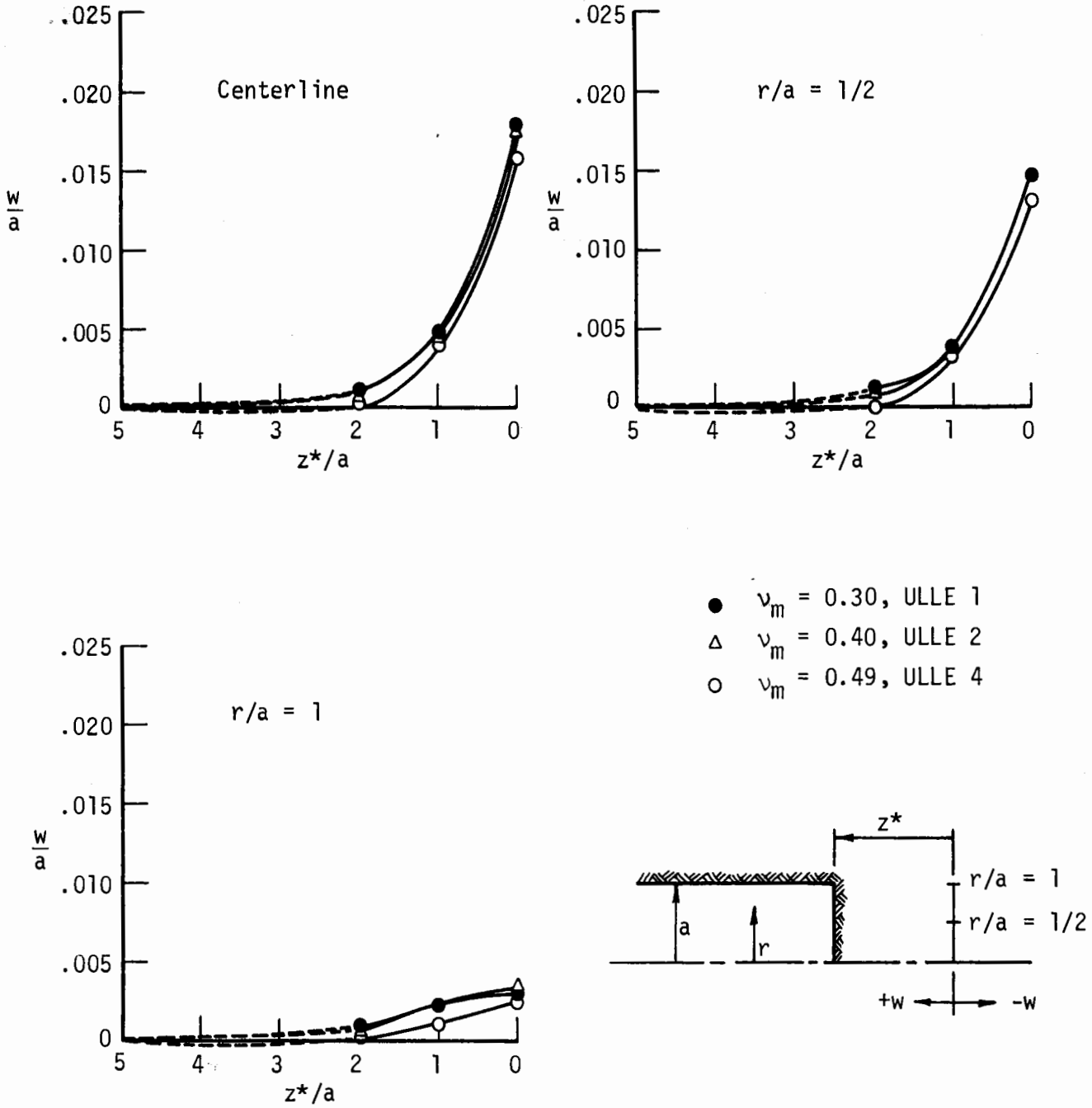

FIGURE 3.9 LONGITUDINAL DISPLACEMENTS ASSOCIATED WITH AN UNLINED TUNNEL IN A LINEAR-ELASTIC MEDIUM

they have been represented by dashed curves. Although these displacements may have been influenced by factors other than just the presence of the tunnel opening, they are of the correct order of magnitude relative to the values given by the solid curves.

Figure 3.9 shows that the displacements remained small until the tunnel face approached to within approximately one tunnel diameter of the reference cross section. It appears that as the face approached this location ($z^* = 2a$) the reference cross section displaced uniformly (i.e., with little variation in displacement with radial distance from the tunnel centerline). However, as the face approached to within $z^* < 2a$, a pattern of differential displacements appeared, with the greatest displacement along the tunnel centerline and progressively less displacement as r increased to r = a.

3.2.3 ELASTO-PLASTIC ANALYSES, $\phi = 0$

For the first four elasto-plastic analyses (cases ULEP1, 2, 3 and 4) it was assumed that $\phi = 0$. A different value of c_u was used in each case, while all other parameters were kept constant. The relationship between c_u and E_m (E_m = 200-300 q_u = 400-600 c_u) was ignored in order to evaluate the influence of c_u alone, a task which would have been more difficult if variation of other parameters had entered the analyses. As a check on the effect of changing the elastic modulus with the value of c_u an additional analysis, identical to ULEP1 except for the value of E_m, was made. It was found that the distribution of soil stresses and the configuration of the plastic zone were identical to those given by ULEP1,

while the ratio of displacements at any point from the two analyses was approximately equal to the inverse of the modulus ratio ($u_1/u_2 \simeq E_{m2}/E_{m1}$).

Sequential excavation was not used to simulate the formation of the tunnel opening in case ULEP3. Instead, the finite element mesh was generated with the complete tunnel in place and then the boundary stresses were applied. This method of analysis had little effect on the distribution of stresses and the plastic zone (the configuration of which was the primary objective of this particular analysis), but gave incorrect displacements.

PLASTIC ZONE

When the shear stress, or stress difference, exceeds the shear strength of a soil, plastic yielding occurs. The extent of the plastic zone that forms around a tunnel is a function of the tunnel radius, the shear strength of the soil and the magnitude of the stress difference.

For the elasto-plastic analyses performed in this study $\sqrt{J_2'}$ is a measure of the stress difference at a given point, where J_2' is the second invarient of the deviator stress tensor. Since it is assumed that $\phi = 0$, the shear strength of the soil is given by c_u, the undrained shear strength. Thus, plastic yielding occurs if $\sqrt{J_2'} > c_u$. The radius of the plastic zone that forms is proportional to the ratio $\sqrt{J_2'}/c_u$.

The approximate position of the boundary between the elastic and plastic zones around an unlined tunnel in a given medium can be estimated from the distribution of $\sqrt{J_2'}$ provided by a linear-elastic analysis of the soil-tunnel system. To illustrate this, Fig. 3.10 gives the distribution of $\sqrt{J_2'}$ around the unlined tunnel of case ULLE4 which considered the same

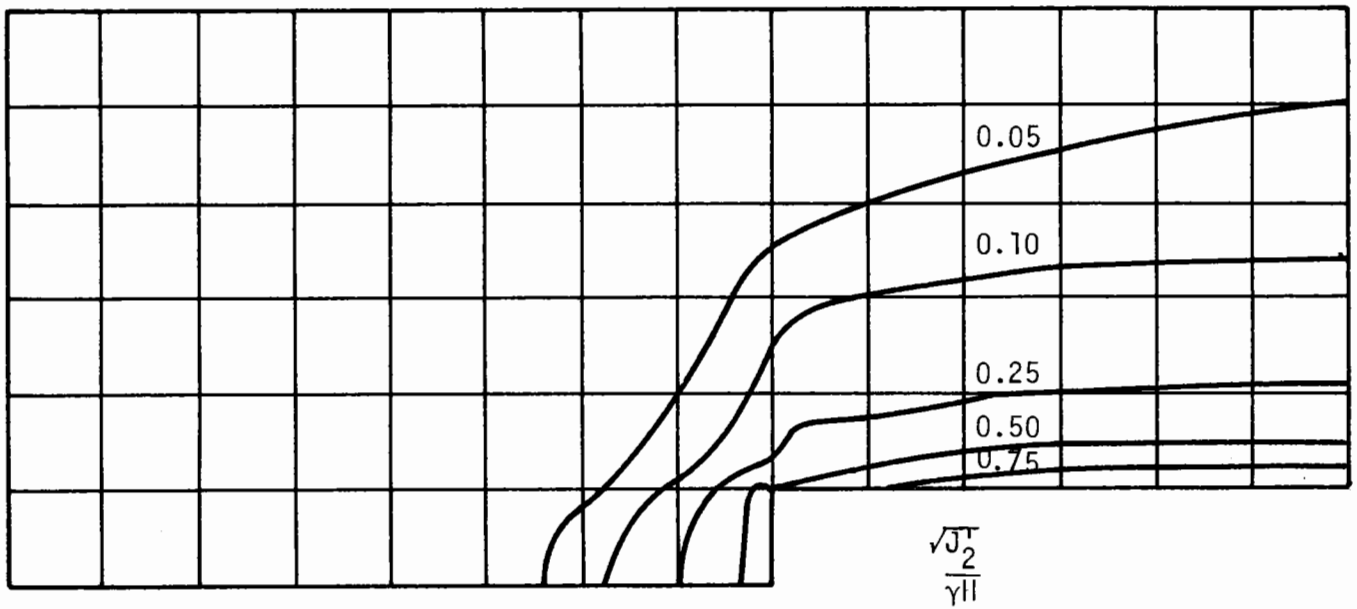

FIGURE 3.10 DISTRIBUTION OF $\sqrt{J_2'}$ AROUND AN UNLINED TUNNEL IN A LINEAR ELASTIC MEDIUM (CASE ULLE 4)

elastic properties as used in the elasto-plastic analyses of this section. At the elastic-plastic boundary, $\sqrt{J_2'} = c_u$ and $\sqrt{J_2'} / \gamma H = c_u/\gamma H$. Thus, if the value of c_u is such that $c_u/\gamma H = 0.25$, for example, an approximation to the elastic-plastic boundary that will form is given by the $\sqrt{J_2'} /\gamma H = 0.25$ contour in Fig. 3.10. This contour line is only an approximation because the actual elastic-plastic boundary is influenced by the redistribution of stress that occurs as the plastic zone forms.

A typical configuration of the plastic zone that developes around an unlined tunnel is shown in Fig. 3.11. In the longitudinal direction the plastic zone extends out ahead of the tunnel face a distance $z = Z'$. Because the hydrostatic, free-field stress state is rapidly approached with increasing distance ahead of the face, the distance Z' is not exceptionally large. In addition, Z', relative to the radial extent of the plastic zone, is not very sensitive to variation of the shear strength parameter for the same reason. Behind the face the plastic zone extends longitudinally back to the point where the tunnel first entered the soil mass being considered.

In the radial direction the extent of the plastic zone increases from a minimum radius of zero at $z = Z'$ to a maximum radius, R, at $z = Z$ behind the face. There is a dip in the boundary curve right near the "corner" formed by the intersection of the tunnel wall and the face. This irregularity is caused by stress concentrations that form around the "corner." For $z > Z$ the stress-strain state is two-dimensional and the radius of the plastic zone, R, is independent of z. A closed form solution [5] for the two-dimensional, plane strain condition is available. According to this

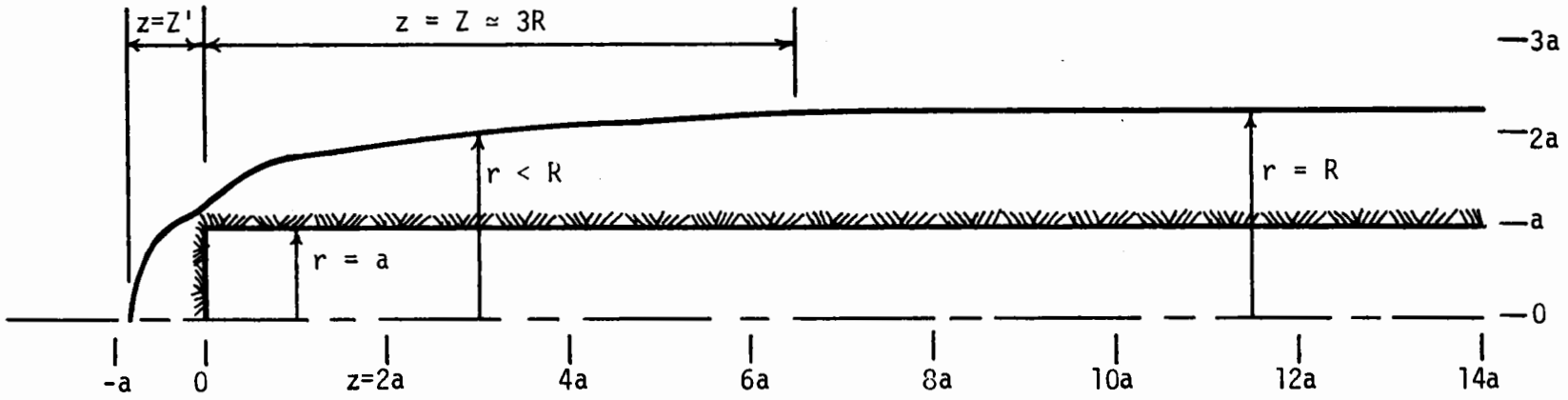

FIGURE 3.11 TYPICAL PLASTIC ZONE AROUND AN UNLINED TUNNEL

solution, the radius of the plastic zone is given by the expression,

$$R = a \exp[\frac{\gamma H}{c_u} - 1/2]. \qquad (3.2)$$

This expression is not exactly correct because it does not consider the redistribution of stress that occurs with the yielding. In Eq. 3.2 γH is the value of $\sqrt{J_2'}$ at r = a and far behind the face, where $\sigma_r = 0$, $\sigma_\theta = 2\gamma H$, $\sigma_z = \gamma H$ and $\tau_{rz} = 0$.

When a plastic zone forms the redistribution of stresses results in a much larger zone of three-dimensional stress and strain around the tunnel face than when there is no plastic zone. In Fig. 3.11 this three-dimensional zone extends out an unknown distance ($> Z'$) ahead of the face and back a distance z = Z behind the face. From the linear-elastic analyses of section 3.2.2 it was found that the zone of three-dimensional stress-strain effects extended behind the tunnel face for a distance of approximately three tunnel radii. Relative to this, the elasto-plastic ($\phi = 0$) analyses can give (depending on the amount of yielding) three-dimensional zones that extend much farther behind the face. It was found from the elasto-plastic analyses that the distance Z is approximately equal to three times the maximum radius of the plastic zone ($Z \simeq 3R$). However, this relationship is based on analyses in which R was relatively small. It is not known for certain that the same relationship holds when R is large.

Figure 3.12 shows the elastic-plastic boundaries obtained for the various values of c_u considered. As expected, for a given value of γH,

A: c_u = 14 psi (9.65 x 10^4Pa), ULEP 1

B: c_u = 28 psi (1.93 x 10^5Pa), ULEP 2

C: c_u = 31.5 psi (2.17 x 10^5Pa), ULEP 3

D: c_u = 37 psi (2.55 x 10^5Pa), ULEP 4

γH = 83.33 psi (5.75 x 10^5Pa)

E_m = 5000 psi (3.45 x 10^7Pa)

ν_m = 0.49

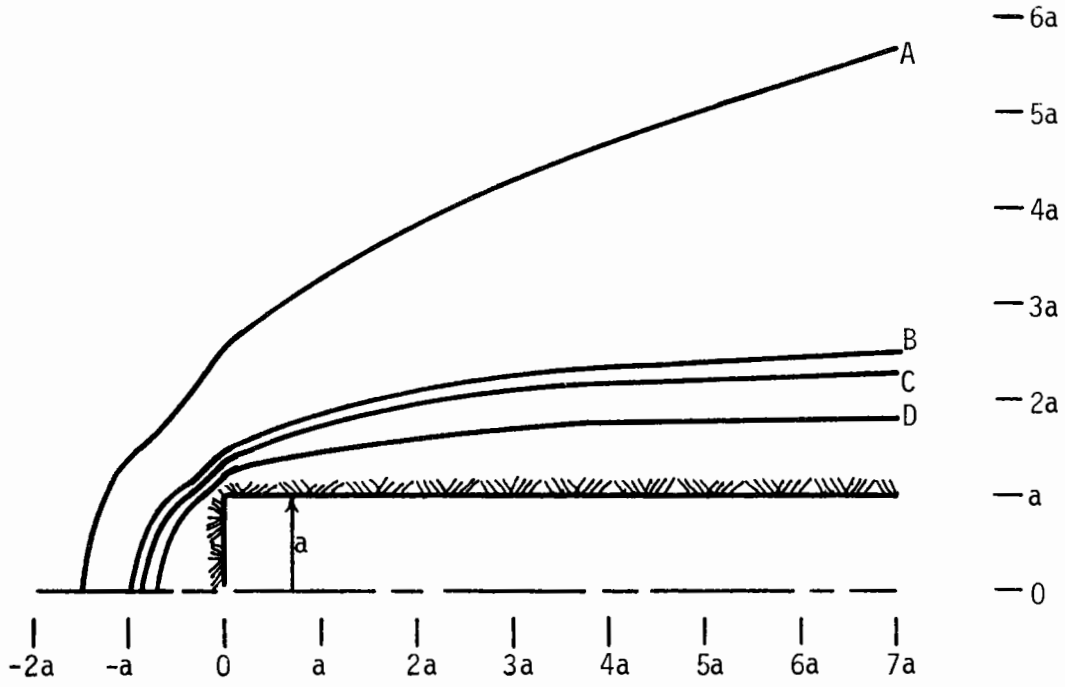

FIGURE 3.12 PLASTIC ZONES AROUND AN UNLINED TUNNEL IN AN ELASTO-PLASTIC MEDIUM - ϕ = 0 FOR VARIOUS c_u VALUES

the extent of the plastic zone increases as c_u decreases. Also, it is clear that the elastic-plastic boundary at points far behind the tunnel face is more sensitive to changes in c_u than it is at points near and ahead of the face. Table 3.2 compares the results obtained from the finite element analyses and the closed form solution. Very good agreement was obtained for

TABLE 3.2

c_u psi	c_u (Pa)	R_{cf}	R_{fe}	$Z=3R_{cf}$	Z_{fe}
14	(9.65×10^4)	12a	--	36a	--
28	(1.93×10^5)	2.7a	--	8.1a	--
31.5	(2.17×10^5)	2.25a	2.2a	6.75a	6.5a
37	(2.55×10^5)	1.88a	1.75a	5.64a	5.25a

cf = closed form solution

fe = finite element solution

a = tunnel radius

c_u values of 31.5 psi (2.17×10^5Pa) and 37 psi (2.55×10^5Pa). For c_u values of 14 psi (9.65×10^4Pa) and 28 psi (1.93×10^5Pa) the length of tunnel considered ($z = 7a$) was not sufficient for observation of the maximum radius of the plastic zone or the distance behind the tunnel face at which this radius is achieved. However, the boundaries plotted in Fig. 3.12 indicate that had the length of tunnel been extended sufficiently far behind the face good agreement with the calculated values would have been obtained.

SOIL STRESSES

The stress distributions obtained for case ULEP2 for which γH = 83.33 psi (5.75×10^5 Pa) and c_u = 28 psi (1.93×10^5 Pa) are shown in Fig. 3.13. These stress contours may be compared with those in Fig. 3.2 which are for the linear-elastic analysis of a soil with the same elastic properties as case ULEP2.

Figure 3.13 shows that with the formation of the plastic zone there is a general reduction of stress magnitude in the vicinity of the tunnel. Similar stress reductions were observed for cases ULEP1, 3, and 4, with the extent of the stress reduction varying with the value of c_u. As would be expected, the degree of stress redistribution increased with decreasing values of c_u.

According to the closed form solution [5] the stresses in the medium at cross sections located far behind the tunnel face ($z \geq Z$), where the stress state is two-dimensional, are given by two sets of equations.

In the plastic zone: $a \leq r \leq R$,

$$\sigma_r = 2\, c_u\, \ell n\, r/a + p_i \tag{3.3a}$$

$$\sigma_\theta = 2\, c_u\, (1 + \ell n\, r/a) + p_i \tag{3.3b}$$

$$\sigma_z = c_u\, (1 + 2\, \ell n\, r/a) \tag{3.3c}$$

In the elastic zone: $r \geq R$,

$$\sigma_r = \gamma H - c_u (a/r)^2 \exp\left[\frac{\gamma H}{c_u} - 1\right] \tag{3.3d}$$

$$\sigma_\theta = \gamma H + c_u (a/r)^2 \exp\left[\frac{\gamma H}{c_u} - 1\right] \tag{3.3e}$$

$$\sigma_z = 2\nu_m\, \gamma H \tag{3.3f}$$

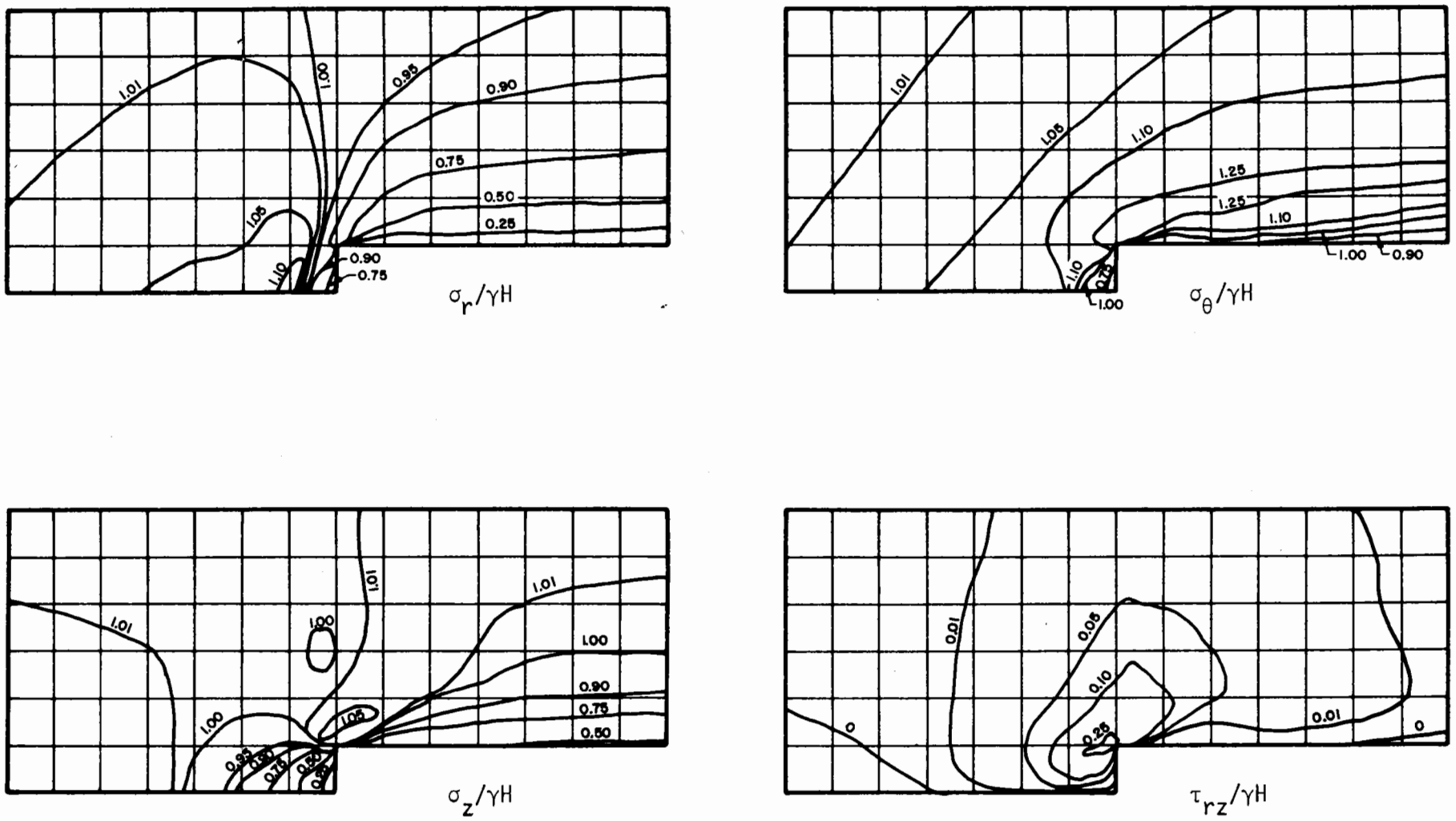

FIGURE 3.13 DISTRIBUTION OF STRESSES AROUND AN UNLINED TUNNEL IN AN ELASTO-PLASTIC MEDIUM - $\phi = 0$ (CASE ULEP 2)

The stress distributions that are obtained from these equations for the parameter values of case ULEP2 are given by the dashed curves in Fig. 3.14. Also plotted in this figure are the stress distributions obtained from the finite element analysis for a cross section at a distance of six tunnel radii behind the face. Due to the configuration of the finite element mesh this was the greatest distance behind the face for which stress values were provided. The two sets of curves differ primary because the two cross sections do not coincide (closed form solution: $z \geq Z$, finite element solution $z = 6a < Z$).

Comparing Figs. 3.13 and 3.2 it can be seen that plastic yielding ahead of the tunnel has reduced the stress magnitudes there and forced the higher stresses out farther ahead of the face. The extent of the three-dimensional stress-strain zone ahead of the tunnel has correspondingly been increased. Whereas this zone extended out approximately two diameters ahead of the face in the linear-elastic analyses, it extends out at least three diameters ahead of the face in Fig. 3.13. This distance is a function of the same vaiables that control the extent of the plastic zone.

SOIL DISPLACEMENTS

Figure 3.15 illustrates the soil displacements that occur as an unlined tunnel is advanced through the elasto-plastic medium of case ULEP1 ($\phi = 0$, $c_u = 14$ psi $= 9.65 \times 10^4$ Pa).

In general, the displacement directions are the same as those observed for the linear-elastic analysis, while the displacement magnitudes are considerably larger in the elasto-plastic case.

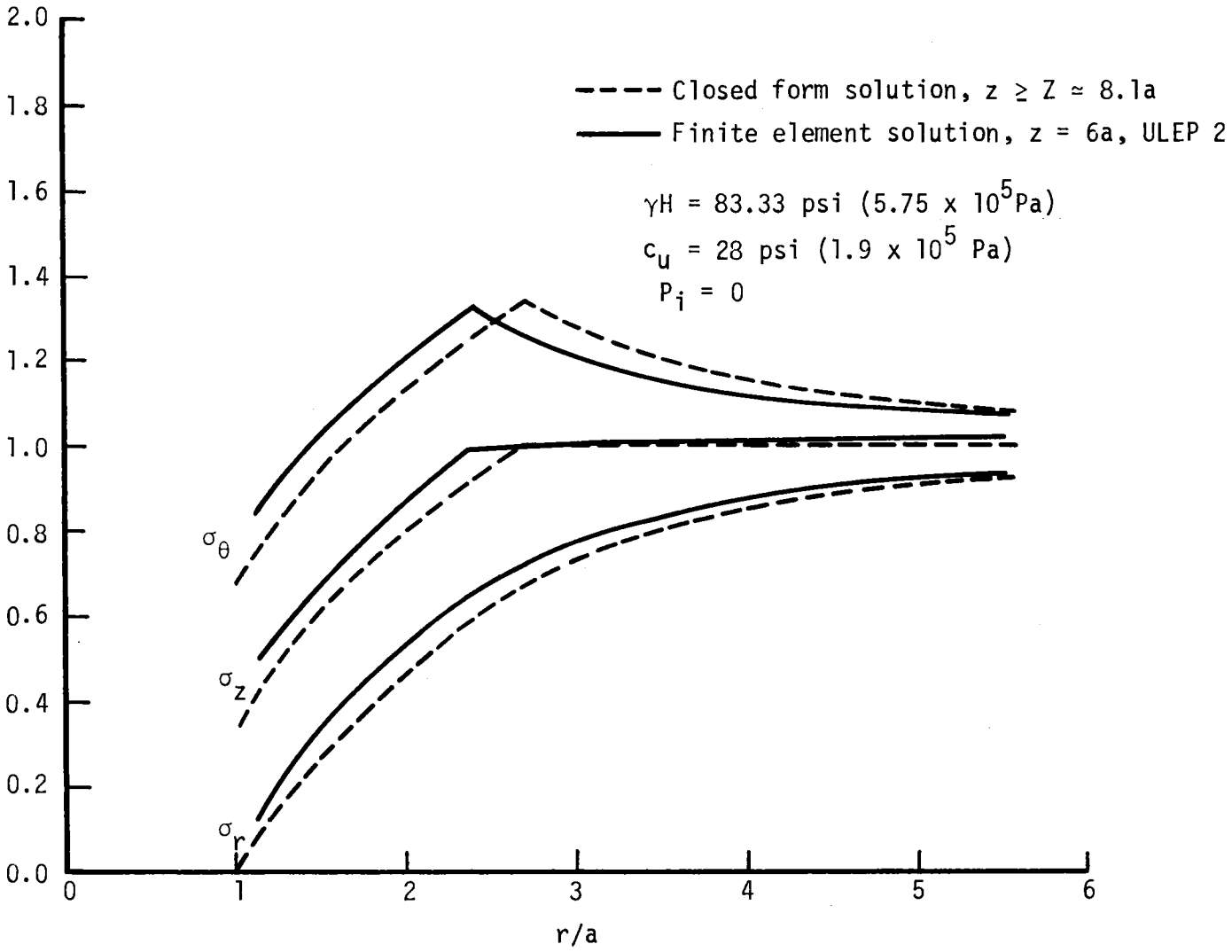

FIGURE 3.14 RADIAL DISTRIBUTION OF STRESSES AROUND AN UNLINED TUNNEL IN AN ELASTO-PLASTIC MEDIUM - $\phi = 0$, $z \simeq Z$

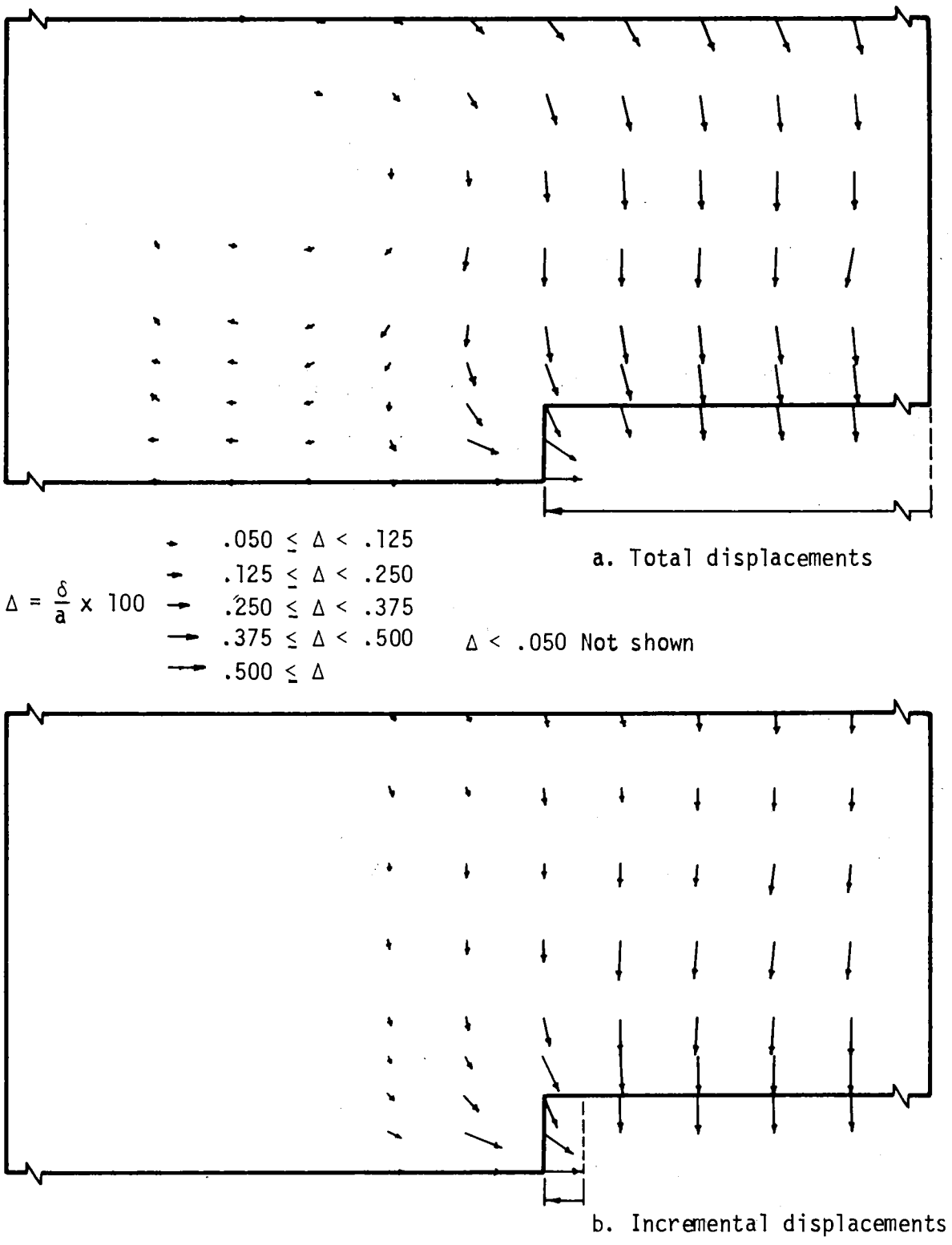

FIGURE 3.15 DISTRIBUTION OF DISPLACEMENTS AROUND AN UNLINED TUNNEL IN AN ELASTO-PLASTIC MEDIUM - ϕ = 0 (CASE ULEP 1)

The negative displacements (away from the tunnel) in Fig. 3.15 are the result of mesh boundary conditions and Poisson's ratio effects. They were also observed in the linear-elastic analyses, but were so small that they did not show up in Fig. 3.6. They are most widespread when the material is incompressible ($\nu_m \simeq 0.50$, see Fig. 3.9), but they are also strongly affected by the boundary conditions. In cases ULEP3 and 4, in which the radius of the mesh was expanded, no such displacements were observed (see Fig. 3.17).

RADIAL DISPLACEMENTS

The radial displacements obtained for the elasto-plastic, $\phi = 0$, analyses (cases ULEP1, 2 and 4) are given in Fig. 3.16. The displacements for case ULEP3, for which excavation simulation was not used, are not included. The displacements have been normalized with respect to the tunnel radius, a.

Throughout the longitudinal distance ($-1.5a \leq z \leq 7a$) shown in Fig. 3.16 there has been an increase in radial displacements, relative to those for the linear-elastic case (dashed curve), due to yielding of the soil around the tunnel. At every cross section, as the extent of plastic yielding increased (or c_u decreased), the radial displacement increased. Not only does the amount of inward displacement increase with the decrease in c_u, but also the distance behind the tunnel face at which the maximum displacement is attained. For ULEP4 the inward radial movement finally ceased at a point approximately 5.5 tunnel radii behind the face. For ULEP1 and ULEP2 the radial displacements continued to increase throughout the length of tunnel considered. Assuming that the radial displacements,

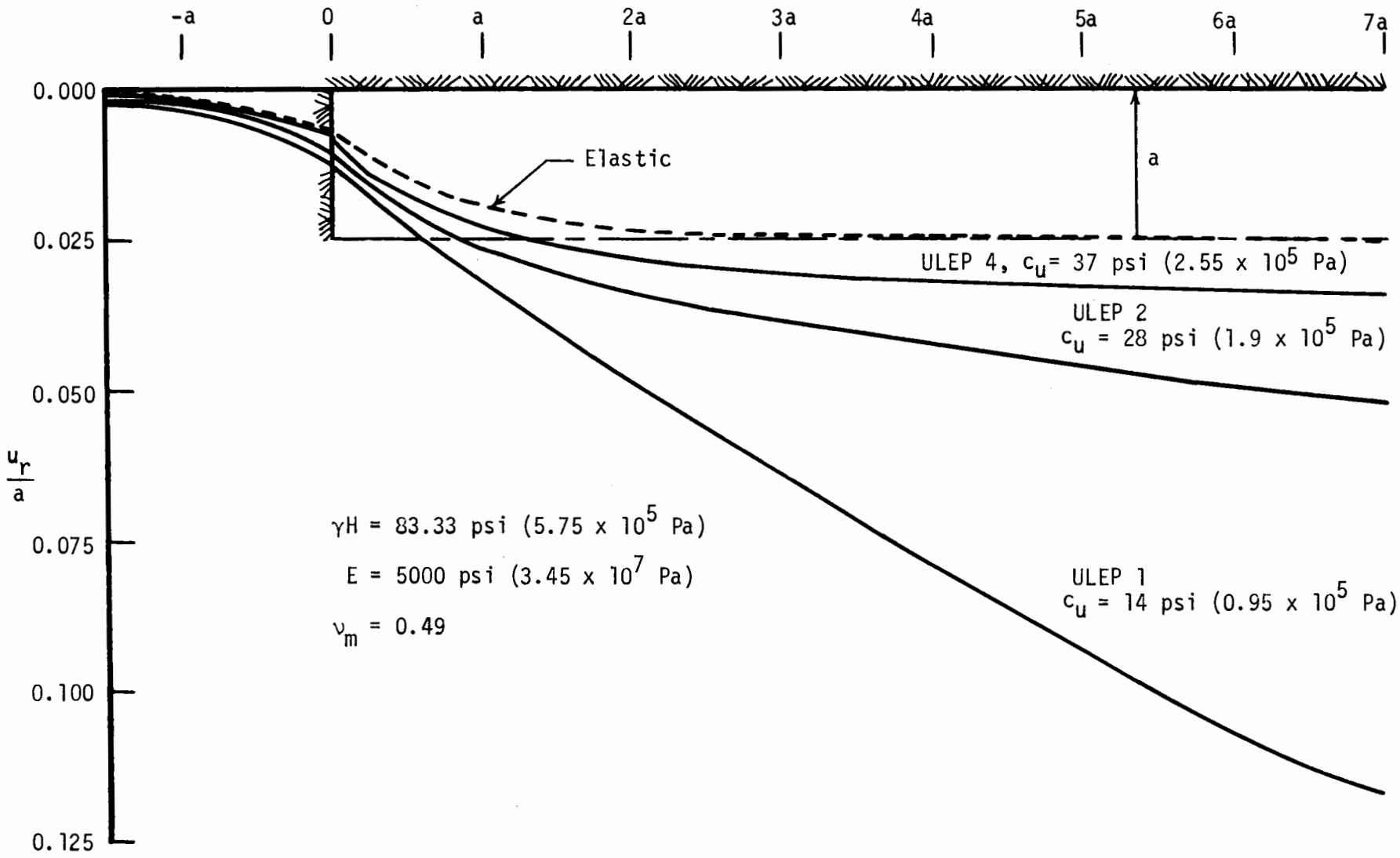

FIGURE 3.16 RADIAL DISPLACEMENTS FOR AN UNLINED TUNNEL IN AN ELASTO-PLASTIC MEDIUM, ϕ = 0

like the radius of the plastic zone, do not reach their maximum values until the zone of two-dimensional stress-strain is encountered, ≈3R behind the face, the maximum u_r for ULEP1 and ULEP2 will occur at distances of 36a and 8.1a behind the face, respectively.

As indicated in Fig. 3.16 the displacements for case ULEP1 were very large. The two-dimensional, closed form solution [5] predicts a total inward radial displacement of 39 in. (1m) for this case. According to the assumptions on which the closed form solution is based, and as indicated by the finite element analysis results, this maximum displacement would be attained only at points far behind the tunnel face. Even so, it is unlikely that a tunnel could be constructed in such a soil without some form of immediate internal support such as air pressure, a liner installed close to the face, or both.

It is likely that the displacements in the vicinity of the tunnel face for case ULEP1 are smaller than those which would occur in a real tunnel excavated in this soil without internal support. For a real tunnel the weight of the overburden would probably be great enough, relative to the shear strength of the soil, that the soil would squeeze or flow into the opening. The occurrence of this type of soil movement, which was not modeled in the analysis, would result in larger displacements than those shown in Fig. 3.16

The discussion pertaining to Fig. 3.8, as applied to Fig. 3.7, also applies here. In fig. 3.16 the displacement curves behind the tunnel face do not represent the position of the displaced tunnel wall, because a portion of that total displacement (that occuring ahead of the face) was removed by the excavation process. The position of the tunnel wall at any

point behind the face is obtained by subtracting the radical displacements at the face from the total displacement at that point.

LONGITUDINAL DISPLACEMENTS

Figure 3.17 gives the longitudinal displacements of a cross section ahead of the tunnel face as the tunnel approaches. The displacements, w, have been normalized with respect to the tunnel radius, a.

It is clear from Fig. 3.17 that the formation of a plastic zone around the tunnel does not significantly alter certain basic displacement patterns that were indicated by the linear-elastic analyses. The longitudinal displacements at the reference cross section are small and essentially uniform over the radial distance considered ($0 \leq r \leq a$) until the face approaches to within about one tunnel diameter. As the distance between the face and the reference cross section becomes less than one diameter the displacements increase rapidly and a pronounced pattern of differential displacements becomes apparent.

The primary effect of plastic behavior of the medium is to increase the magnitude of the displacements. In general, the longitudinal displacements at the face are larger when a plastic zone forms around the tunnel than they are when the soil remains elastic. In addition, greater displacements result when the plastic zone is large than when it is small.

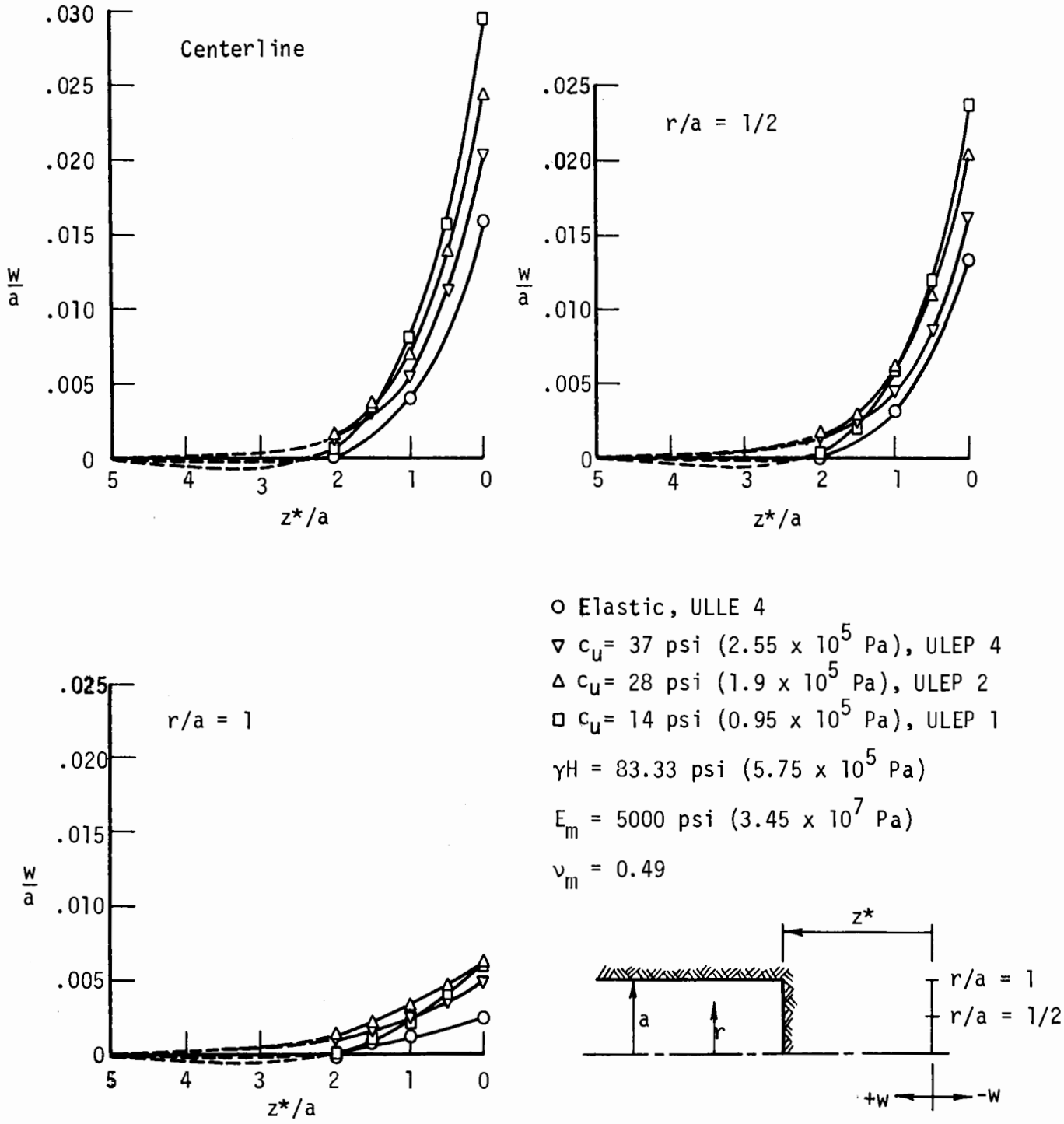

FIGURE 3.17 LONGITUDINAL DISPLACEMENTS ASSOCIATED WITH AN UNLINED TUNNEL IN AN ELASTO-PLASTIC MEDIUM - $\phi = 0$

3.2.4 ELASTO-PLASTIC ANALYSES, $\phi \neq 0$

Two elasto-plastic analyses of an unlined tunnel (ULEP5 and ULEP6) were conducted in which both cohesion and angle of shearing resistance were considered. A cohesion value of 14 psi (9.65×10^4 Pa) was used in both cases, while two values for the angle of shearing resistance were considered ($\phi = 15°$ and $\phi = 30°$).

PLASTIC ZONE

The plastic zones obtained in cases ULEP 5 and ULEP6 are shown in Fig. 3.18. It can be seen in this figure that the size of the plastic zone is sensitive to the magnitude of the angle of shearing resistance. When it was assumed that $\phi = 0$ (case ULEP1) the radius of the plastic zone at a point seven tunnel radii behind the face was approximately 6a. Increasing the angle of shearing resistance from zero to 15 degrees reduces the plastic zone to a radius of only 2.6a at the same distance behind the face. The plastic zone in Fig. 3.18a is very similar to that obtained in case ULEP2 for which C = 28 psi (1.93×10^5 Pa) and $\phi = 0$. Doubling the angle of shearing resistance from 15 to 30 degrees resulted in an approximately 50 percent decrease in the extent of the plastic zone (see Fig. 3.18b) in these analyses. For this case the plastic zone obtained is slightly smaller than that which resulted in case ULEP4 where C = 37 psi (2.55×10^5 Pa) and $\phi = 0$.

For the $\phi = 0$ elasto-plastic analyses of Section 3.2.3 in which the shear strength of the soil was a constant, it was possible to estimate beforehand the extent of the plastic zone that would form on the basis of the known shear strength value and the distribution of $\sqrt{J_2'}$ obtained from an elastic

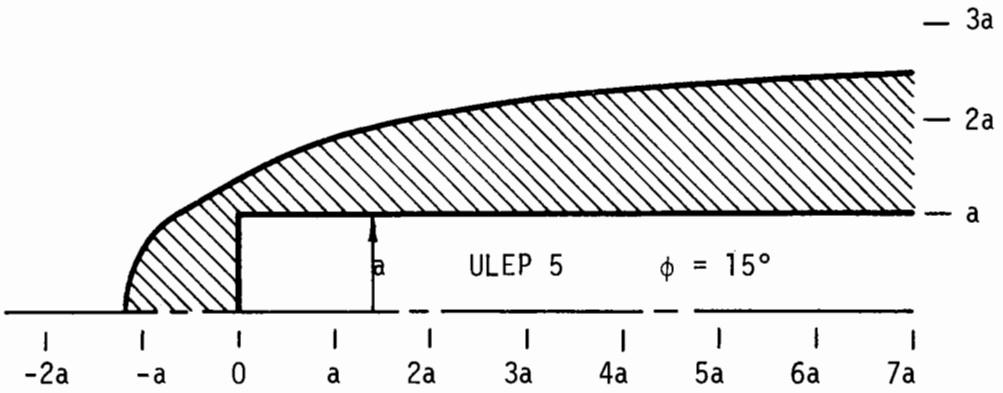

c = 14 psi (9.65×10^4 Pa)

E_m = 5000 psi (3.45×10^7 Pa)

ν_m = 0.40

γH = 83.33 psi (5.75×10^5 Pa)

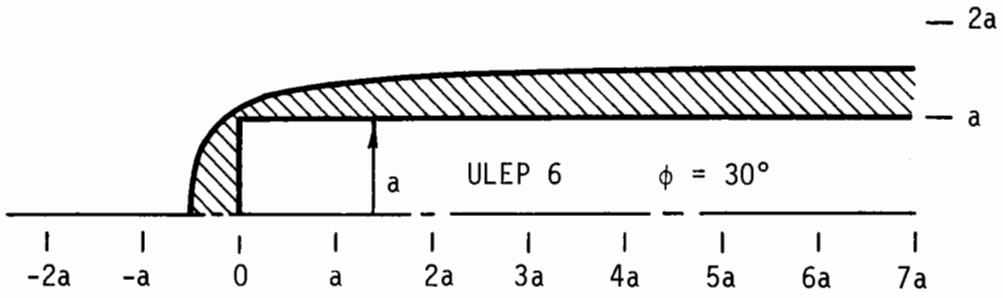

FIGURE 3.18 PLASTIC ZONES AROUND AN UNLINED TUNNEL IN AN ELASTO-PLASTIC MEDIUM - $\phi \neq 0$.

analysis of the tunnel. Here this was not possible because the shear strength of the soil was not a constant. When the angle of shearing resistance has a value greater than zero the shear strength at a point is a function of the mean normal stress acting at that point. Thus, the extent of plastic yielding cannot be predicted from the distribution of $\sqrt{J_2'}$ alone. Both $\sqrt{J_2'}$ and the mean normal stresses must be considered.

SOIL STRESSES

The stress distributions obtained for case ULEP6 are given in Fig. 3.19. For this analysis $\phi = 30°$, c = 14 psi (9.65×10^4 Pa) and γH = 83.33 psi (5.75×10^5 Pa). Because the plastic zone around the tunnel in this case was relatively small there has not been an extensive redistribution of the stresses around the tunnel due to plastic yielding. The stress distributions in Fig. 3.19 are similar to those of Fig. 3.1 for the linear-elastic analysis. Although there has been a general reduction of all stresses in the vicinity of the tunnel opening due to yielding, the most obvious is that shown in Fig. 3.19b, corresponding to the circumferential stresses.

SOIL DISPLACEMENTS

The total and incremental soil displacement distributions for case ULEP6 are shown in Fig. 3.20. The displacement directions are similar to those obtained in previous analyses (Figs. 3.6 and 3.15). Displacement magnitudes are intermediate between those for the linear-elastic analysis and those for elasto-plastic analysis ULEP1 ($\phi = 0$, c = 14 psi (9.65×10^4 Pa)), but are closer to the elastic magnitudes.

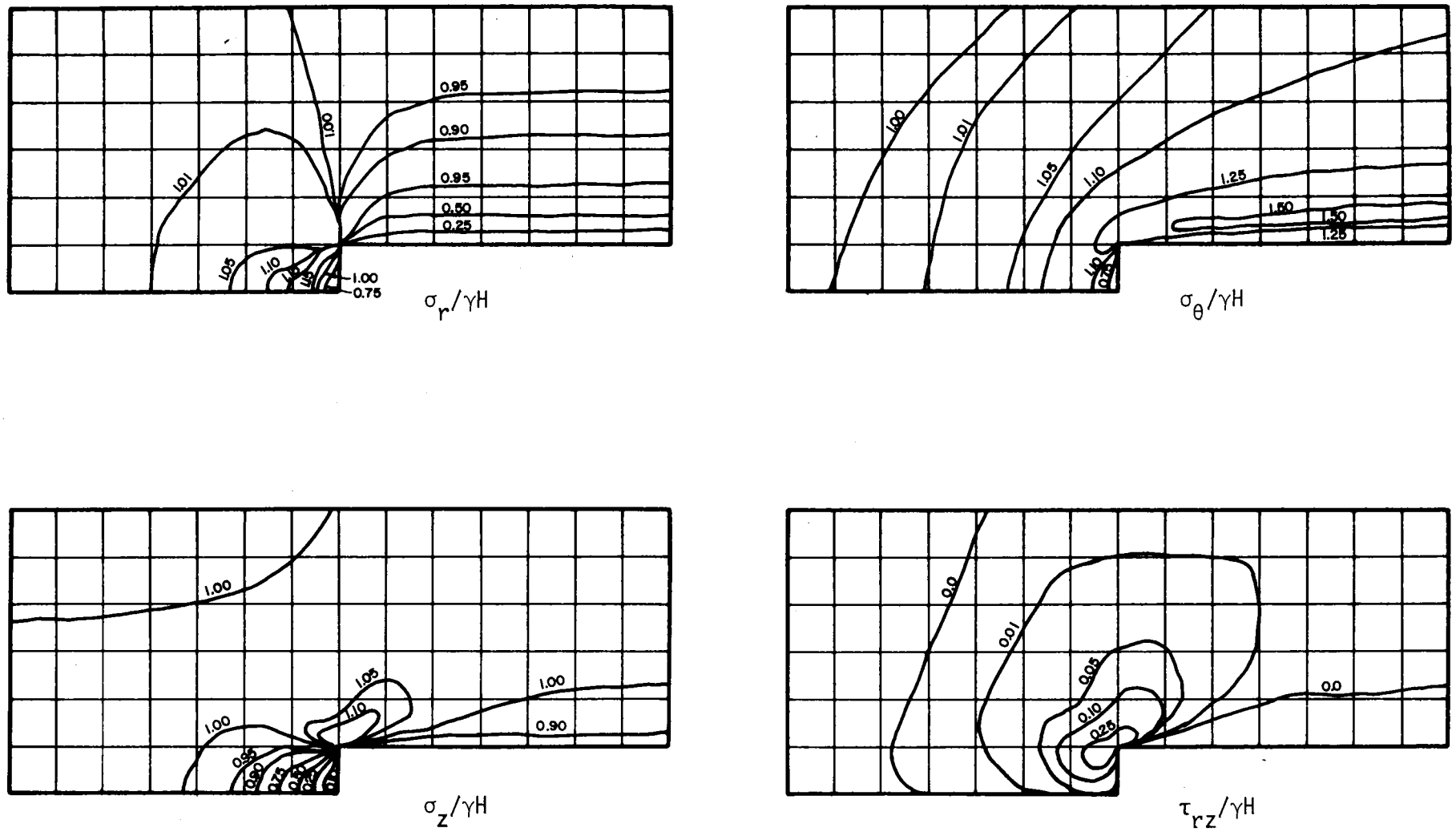

FIGURE 3.19 DISTRIBUTION OF STRESSES AROUND AN UNLINED TUNNEL IN AN ELASTO-PLASTIC MEDIUM - $\phi \neq 0$ (CASE ULEP 6)

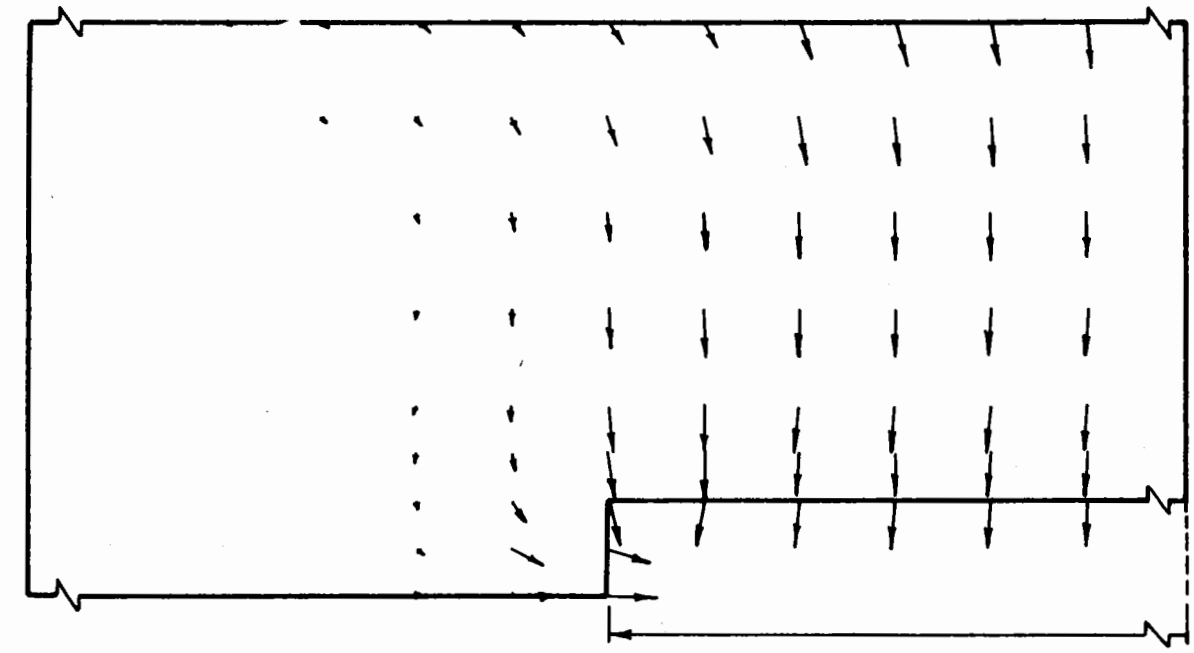

$\Delta = \frac{\delta}{a} \times 100$

.050 ≤ Δ < .125
.125 ≤ Δ < .250
.250 ≤ Δ < .375
.375 ≤ Δ < .500
.500 ≤ Δ <

a.) Total displacements

Δ < .050 Not shown

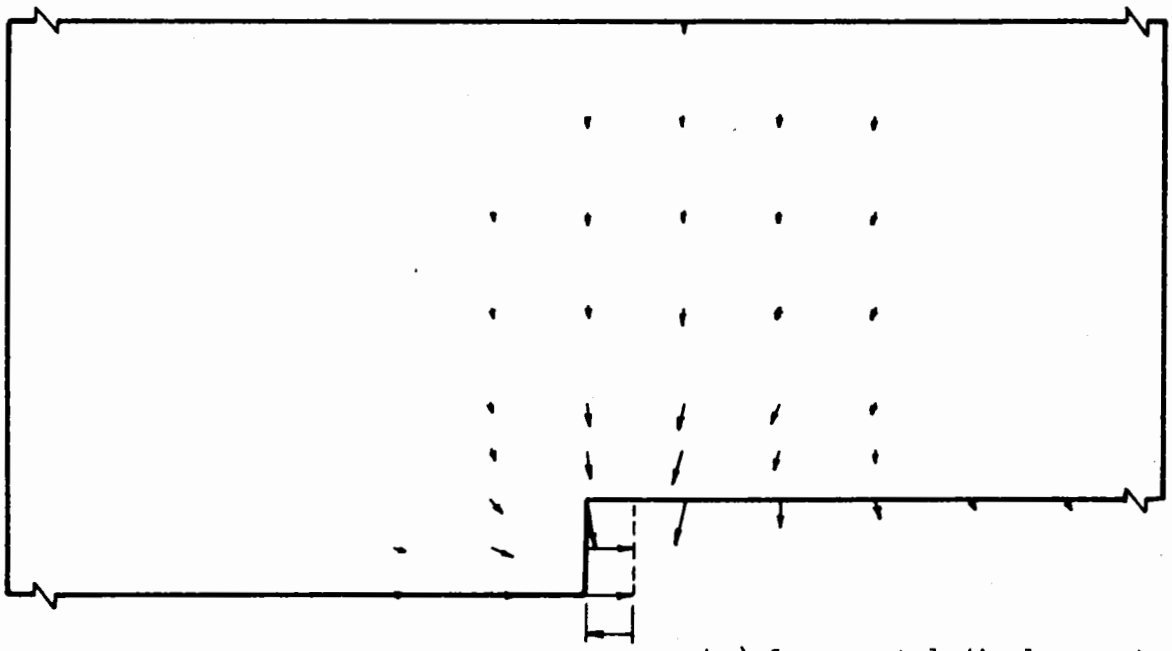

b.) Incremental displacements

FIGURE 3.20 DISTRIBUTION OF DISPLACEMENTS AROUND AN UNLINED TUNNEL IN AN ELASTO-PLASTIC MEDIUM - $\phi \neq 0$ (CASE ULEP 6)

RADIAL DISPLACEMENTS

Figure 3.21 gives the radial displacements of the tunnel opening for the two $c \neq 0$, $\phi \neq 0$ elasto-plastic analyses. For a value of the angle of shearing resistance of only 15° very large radial displacements were obtained, larger even than those that resulted when $\phi = 0$ (case ULEP1, Fig. 3.16). In order to estimate which of two elasto-plastic analyses ($c \neq 0$, $\phi = 0$ vs. $c \neq 0$, $\phi \neq 0$) should yield the larger radial displacements, there are two counter-acting factors that must be considered. Everything else being equal, the $c \neq 0$, $\phi \neq 0$ soil has a greater shear strength than the $c \neq 0$, $\phi = 0$ soil at the stress levels considered and thus should exhibit smaller radial displacements. On the other hand, the $\phi = 0$ soil is assumed to be incompressible ($\nu_m \simeq 0.5$) whereas the $\phi \neq 0$ soil exhibits both elastic volume increase upon load removal (tunnel excavation) and plastic volume increase due to yielding. It would appear that for the two cases (ULEP1 and ULEP5) considered here the effect of the volume changes exceeded that of the differences in shear strength. There is some question, however, as to whether the same relative results would be obtained with real soils. In these finite element analyses of elasto-plastic soils, plastic volume changes are modeled using the concept of the associated flow rule of the theory of plasticity, which implies that the plastic strain increments are normal to the yield surface. This gave plastic volume increases in the $c - \phi$ analyses performed here. It is generally held, however, that the associated flow rule leads to volume strains much in excess of reality, especially when the plastic zone is large as in case ULEP5. Therefore, it may well be that the radial displacements obtained for case ULEP5 are larger than they should be.

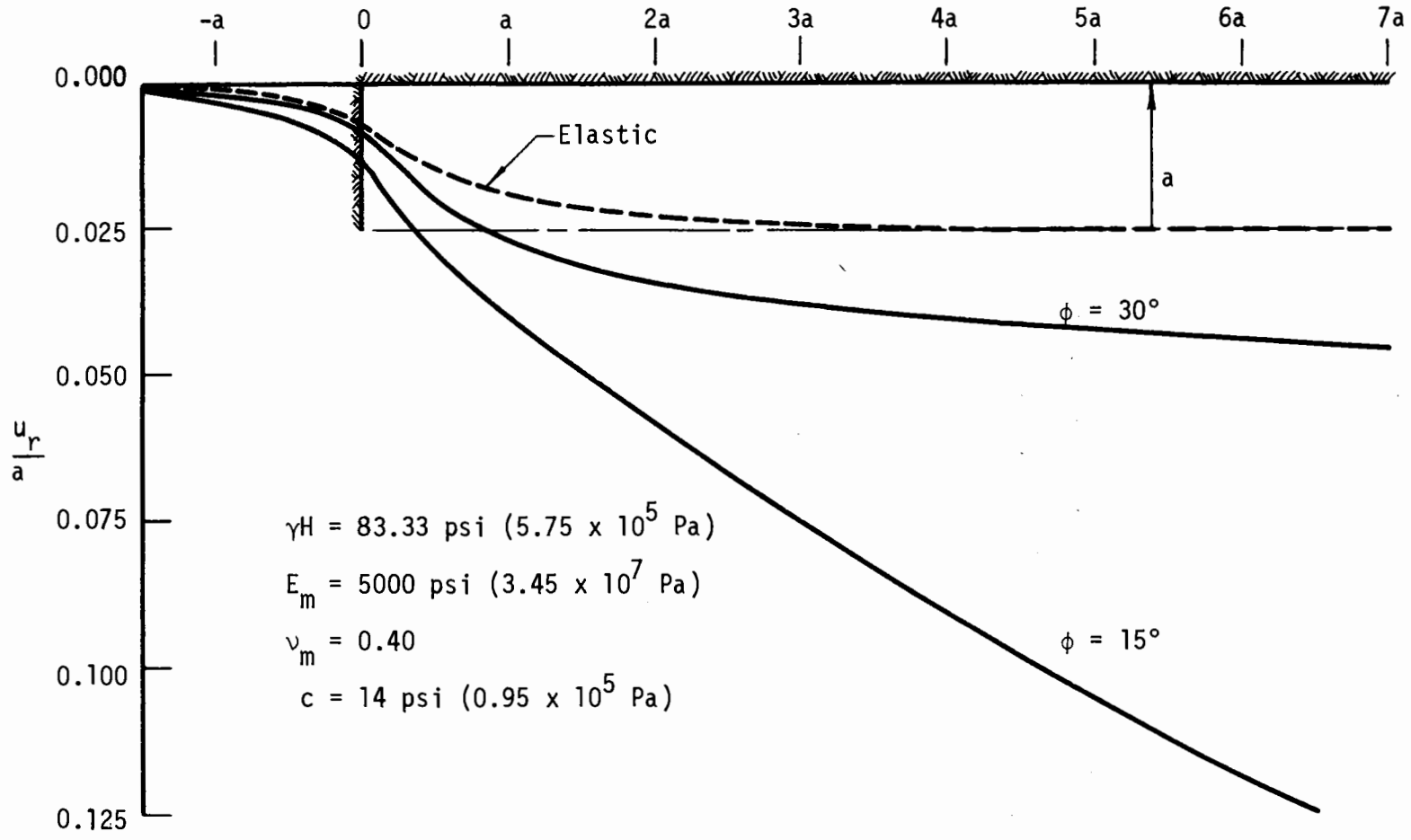

FIGURE 3.21 RADIAL DISPLACEMENTS FOR AN UNLINED TUNNEL IN AN ELASTO-PLASTIC MEDIUM - $\phi \neq 0$

Since the plastic zone for case ULEP6 was relatively small, it is likely that the radial displacements obtained for $\phi = 30°$ are more reliable, although indications are that these displacements, far behind the face, are slightly larger than they should be. Figure 3.18 shows that for this case the plastic zone has reached its maximum radius at a point approximately 4.5a behind the tunnel face, indicating that for $z > 4.5a$ the plane strain condition exists. Figure 3.21 shows, however, that the radial displacements are still increasing slightly in this zone.

LONGITUDINAL DISPLACEMENTS

The longitudinal displacements of a cross section as it is approached by the advancing tunnel are given in Fig. 3.22. The analysis yielded very large displacements at points near the center of the face, away from the tunnel wall, for case ULEP5. At longitudinal distances greater than one radius between the face and the reference cross section the $\phi = 15°$ displacements are less than the $\phi = 0$ displacements. However, as z^*/a decreases to less than one the longitudinal displacements away from the tunnel wall increase rapidly. At the tunnel centerline the face displacements for $\phi = 15°$ are almost 100 percent greater than those for $\phi = 0$. As with the radial displacements, these displacements may be excessive due to the way the plastic volume strains were modeled.

3.3 LINED TUNNELS

3.3.1 GENERAL

A series of six finite element analyses were performed for the lined

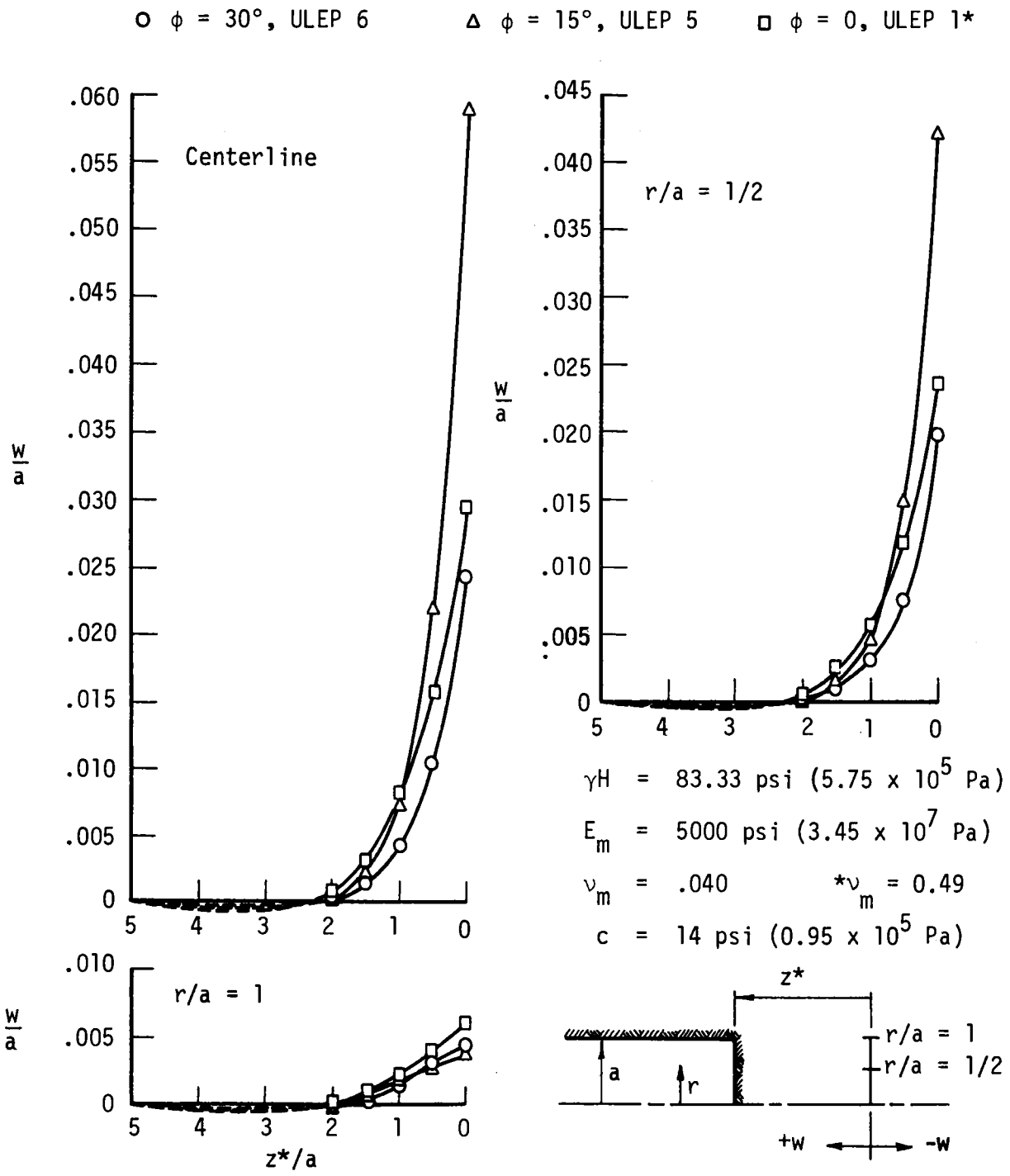

FIGURE 3.22 LONGITUDINAL DISPLACEMENTS ASSOCIATED WITH AN UNLINED TUNNEL IN AN ELASTO-PLASTIC MEDIUM - $\phi \neq 0$.

tunnel case. Table 3.3 gives the material properties of the medium and liner for each analysis. The dimensions and elastic properties of the liner, the elastic modulus of the medium, and the magnitude of the hydrostatic free-field stress were the same for all six analyses.

As with the unlined tunnel series, three types of material behavior were considered for the medium. The first two cases, LLE1 and LLE2, assumed the medium to be linear-elastic. Cases LEP1 and LEP2 considered elasto-plastic behavior in which $\phi = 0$, corresponding to the undrained loading of a cohesive soil. Elasto-plastic behavior for a soil whose shear strength is a function of mean stress and the angle of shearing resistance as well as cohesion was considered in cases LEP3 and LEP4. In all cases the liner was assumed to behave linear-elastically.

For each material type two positions of the forward end of the liner with respect to the tunnel face were investigated. It was first assumed that the liner is continuously installed all the way to the face as the tunnel is advanced. It was then assumed that the liner lags behind the advancing face so that there is always an unlined gap of one tunnel radius length between the face and the end of the liner.

The lined tunnel results are compared to those from the corresponding unlined tunnel analyses and to the results obtained from a two-dimensional closed-form solution [15,17] and two-dimensional finite element analyses. The two-dimensional solutions apply only to cross sections far behind the face, and both assumed the soil to be linear-elastic. The two-dimensional solution methods are discussed in more detail in Chapter 4.

TABLE 3.3

MATERIAL PROPERTIES FOR THE LINED TUNNEL ANALYSES

Case	ν_m	c_u psi	c_u (Pa)	ϕ degrees	$\frac{\ell_u}{a}$
LLE 1	0.40	---	--	--	0
LLE 2	0.40	---	--	--	1
LEP 1	0.49	14	(9.65×10^4)	0	0
LEP 2	0.49	14	(9.65×10^4)	0	1
LEP 3	0.40	14	(9.65×10^4)	30	0
LEP 4	0.40	14	(9.65×10^4)	30	1

Initial stress state: $\sigma_r = \sigma_\theta = \sigma_z = \gamma H = 83.33$ psi $(5.75 \times 10^5$ Pa), $\tau_{rz} = 0$

Soil modulus: $E_m = 5000$ psi $(3.45 \times 10^7$ Pa)

Liner properties: $E_\ell = 2 \times 10^6$ psi $(1.38 \times 10^{10}$ Pa), $\nu_\ell = 0.15$

Liner dimensions: $D_o = 20$ ft (6.1 m), $D_i = 18$ ft (5.5 m), $t = 1$ ft (0.305 m)

3.3.2 LINEAR-ELASTIC ANALYSES

For these analyses the soil was given the same elastic properties that were used for the unlined tunnel case ULLE2.

The compressibility ratio (see Chapter 4) for the soil-liner system is very low ($C = 0.087$), primarily because the soil has a low elastic modulus whereas the liner has a high modulus. The low C value indicates that the liner is very stiff with respect to the soil. Because the liner is very stiff it has a considerable restraining effect on the surrounding soil.

Thus, once the liner is installed significant displacements of the soil, and related stress changes, can occur only ahead of the liner. An unlined gap between the tunnel face and the liner allows a considerably greater amount of displacement and stress change to occur than if no gap existed.

SOIL STRESSES

The distributions of stresses in the soil surrounding the completely lined tunnel are shown in Fig. 3.23. By comparing these normalized stress contours to those in Fig. 3.1 for the unlined tunnel, the restraining effect of the liner can be readily discerned.

Stresses in the soil change from their undisturbed, free-field values when displacements toward the tunnel are allowed. For this analysis the stiff liner permitted only a small amount of radial displacement to occur after the liner was installed. Thus, this type of deformation contributed little to the stress distributions shown in Fig. 3.23. The relatively large displacements, both radial and longitudinal, that occurred ahead of the face and liner were the major causes of the stress changes observed both ahead and behind the tunnel face (the tunnel is advanced through a zone of altered stress).

By comparing the stress contours in the zone ahead of the tunnel face for the unlined and completely lined cases, it can be seen that one effect of the liner is to reduce the magnitude of the stresses in this zone. This is especially true for the radial (σ_r) and circumferential (σ_θ) stresses. If the tunnel is unlined there is a region about 3/4 of a tunnel radius ahead of the face where the radial stress reaches magnitudes of about 110 percent of the free-field stress. When a stiff liner is installed up to

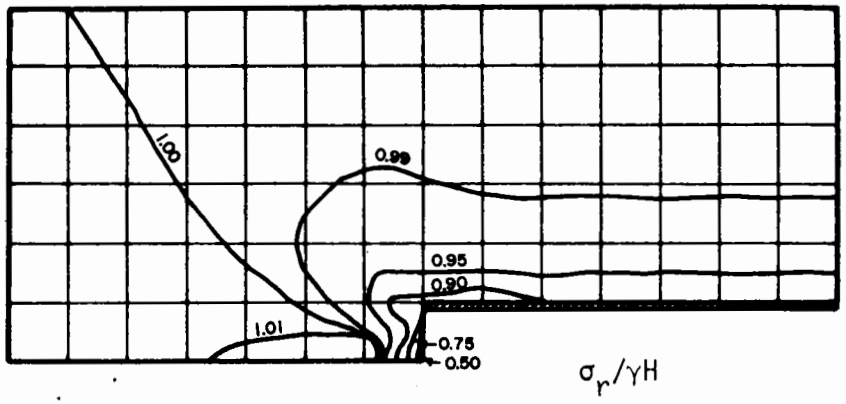

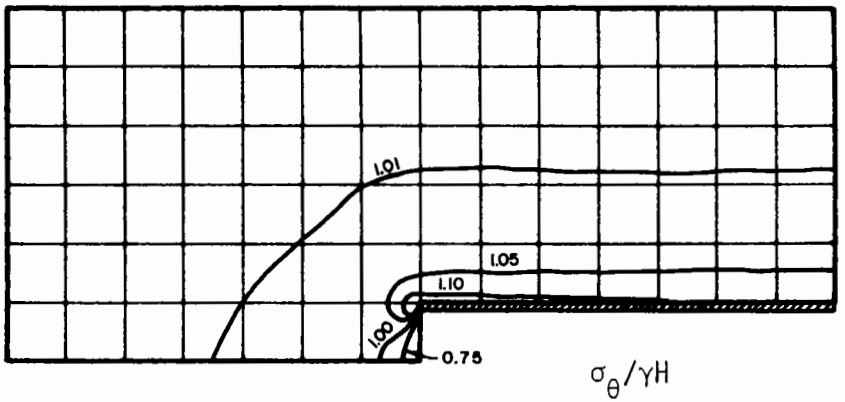

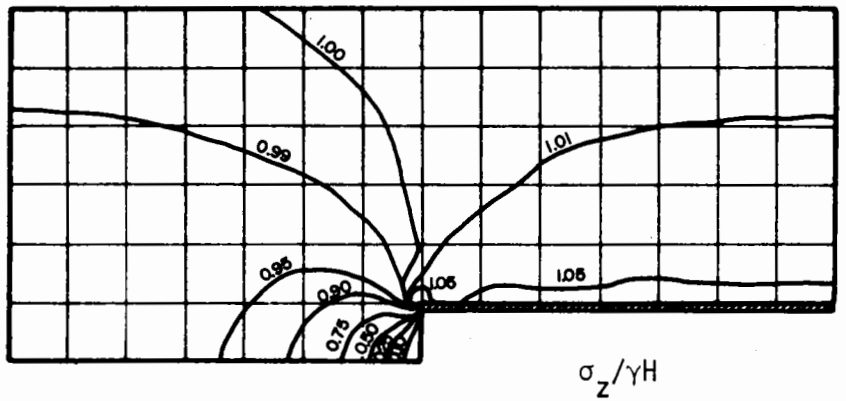

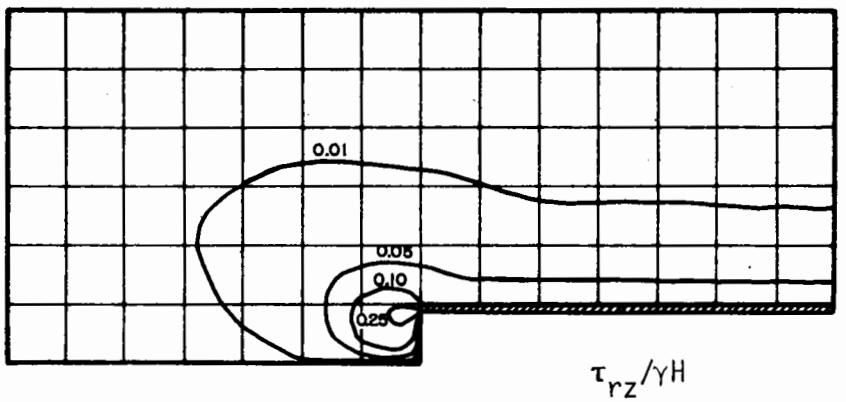

FIGURE 3.23 DISTRIBUTION OF STRESSES AROUND A FULLY LINED TUNNEL IN A LINEAR-ELASTIC MEDIUM (CASE LLE 1)

the face the radial stress in the same region is actually several percent less than the free-field magnitude and at no point does it exceed the free-field value by more than two or three percent. The circumferential stresses in this same region are reduced from 110-125 percent of the free-field magnitude when the tunnel is unlined to only 100-105 percent of the free-field stress when the liner is kept up to the face.

Stresses in the soil surrounding the tunnel behind the face are controlled primarily by the magnitude of the stresses ahead of the face. It is assumed in these analyses that the tunnel and liner are advanced simultaneously and that this advancement takes place in a series of steps, each of which occurs instantaneously. When the tunnel is advanced a portion of the soil in the altered stress zone ahead of the face is removed and an additional length of liner is installed. Since these operations occur instantaneously, no stress changes can occur in the soil around the newly excavated volume of soil until after the liner is in place. Then, since the liner is very stiff it deforms only a small amount, resulting in only a slight change in the stresses. Thus, the stresses behind the face are only slightly different than those ahead of the face.

The stress distributions for the partially lined tunnel in a linear-elastic medium are given in Fig. 3.24. This figure shows that if the tunnel is left unlined for a distance of only one tunnel radius behind the face the disruption of the initially undisturbed stress state that results due to the presence of the tunnel closely approximates that found for the unlined tunnel case (Fig. 3.1). This could have been anticipated from the results observed for the unlined case. Figures 3.7 and 3.1 show that at

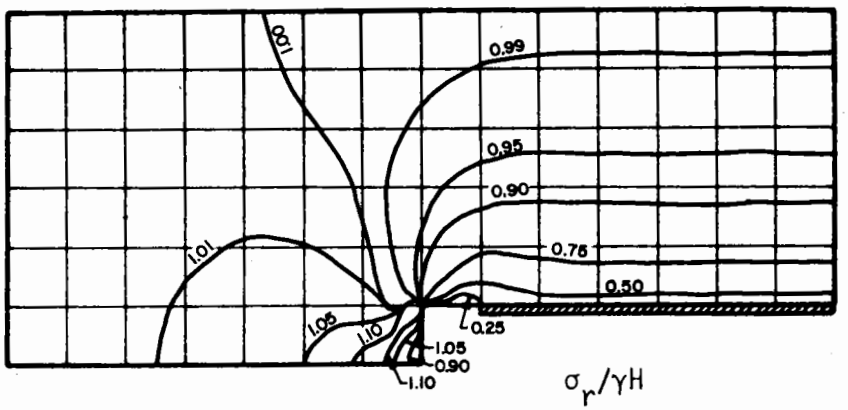

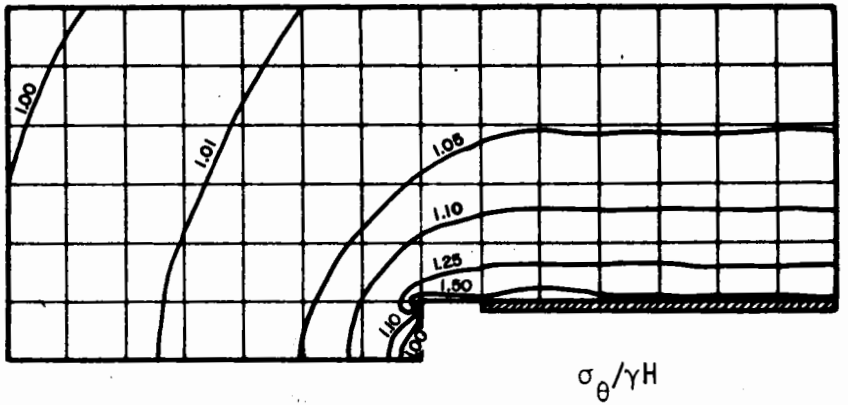

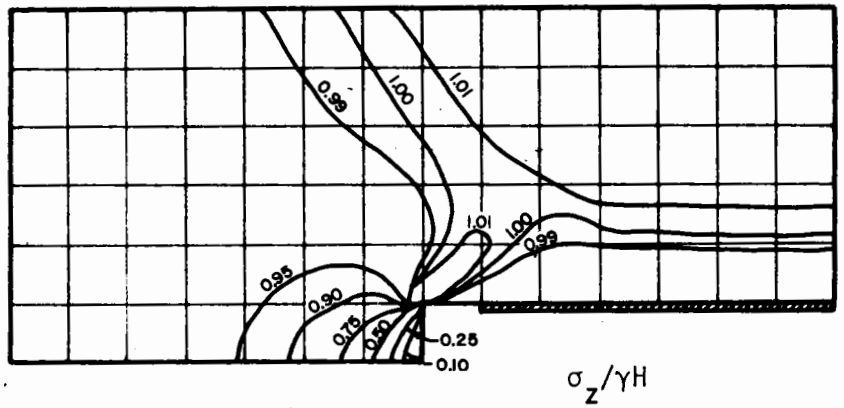

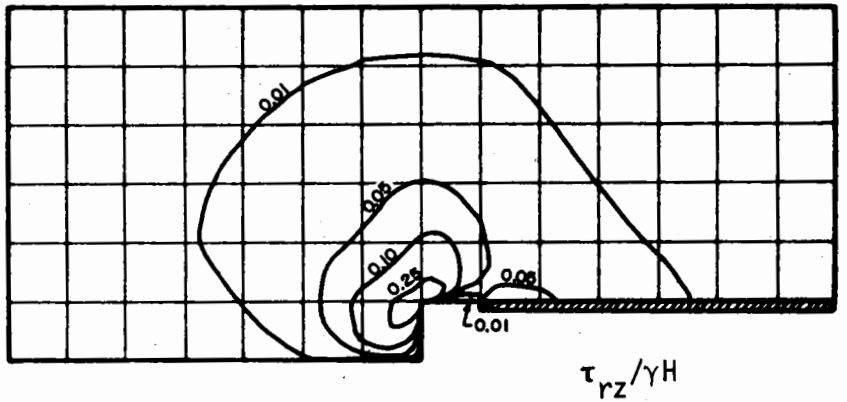

FIGURE 3.24 DISTRIBUTION OF STRESSES AROUND A PARTIALLY LINED TUNNEL IN A LINEAR-ELASTIC MEDIUM (CASE LLE 2)

longitudinal distances greater than one radius behind the face over 85 percent of the radial displacements have already occurred and that there is little longitudinal variation of stress magnitude beyond this distance. Since the majority of the displacements have occurred before the liner is installed, the amount of soil-liner interaction that will occur is not great. Thus, the liner has little effect on the stresses in the soil either around or ahead of it.

SOIL DISPLACEMENTS

Displacements of the surrounding soil due to the advancement of a completely lined tunnel (LLE1) are given in Fig. 3.25. The displacements that the soil mass experiences when the tunnel is advanced through only a short distance are given in part b of this figure. These incremental displacements are very small at most points throughout the medium. It is only in one small region, just ahead of the tunnel face, that these movements attain significant magnitudes. The directions of the arrows in Fig. 3.25b indicate that movement is toward the tunnel face, the only unsupported portion of the tunnel opening. The large radial displacements that were observed behind the face of the unlined tunnel (Fig. 3.6b) were, in this case, prevented by the liner.

Although the majority of the incremental displacements are so small that they do not show up in Fig. 3.25b, they cannot be ignored. A tunnel is driven in a series of short advances, and it is the small displacements from each advance that are superimposed such that they combine to give the displacements shown in Fig. 3.25a. When this total displacement distribution is compared to its counterpart in Fig. 3.6, two obvious differences stand out.

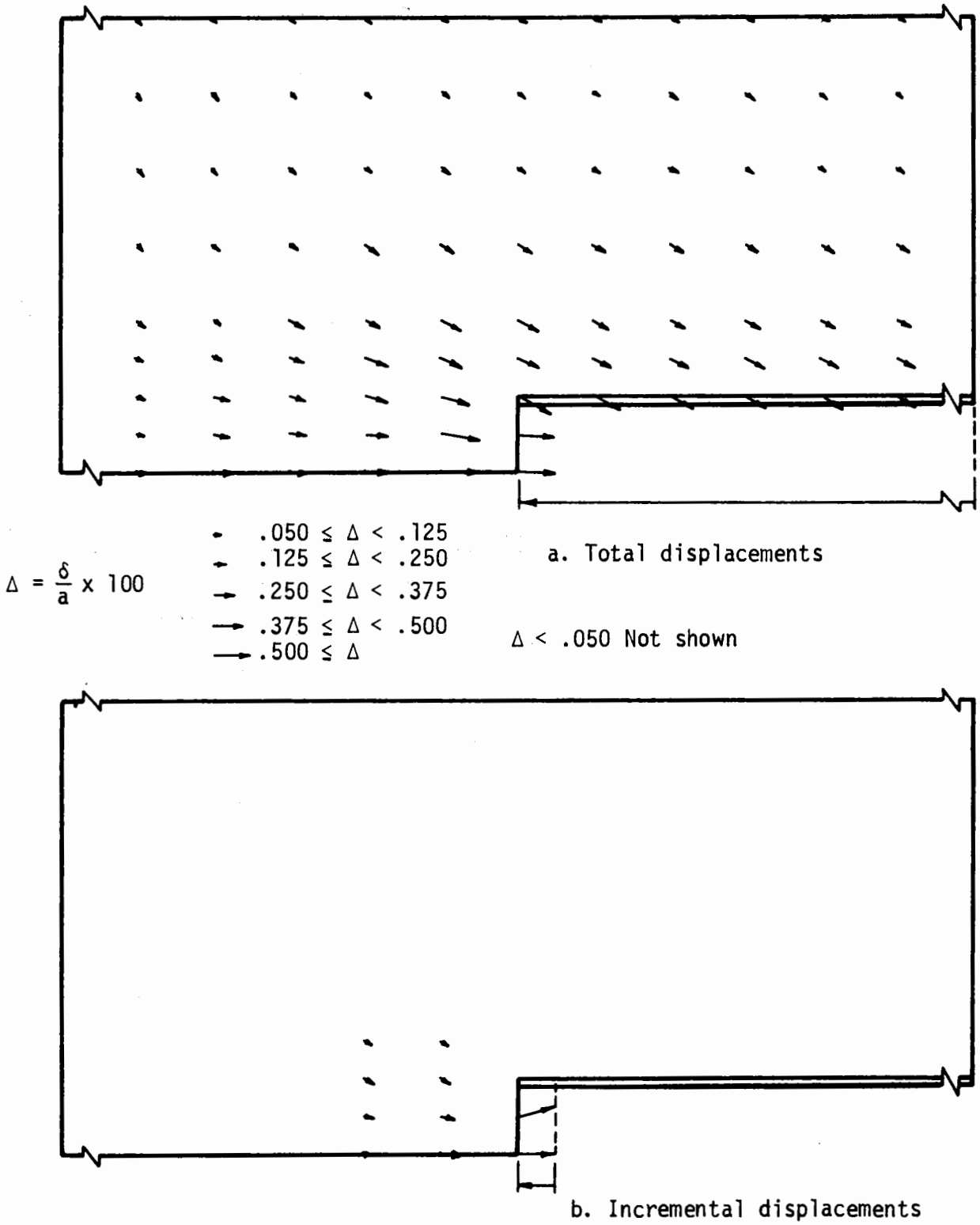

FIGURE 3.25 DISTRIBUTION OF DISPLACEMENTS AROUND A FULLY LINED TUNNEL IN A LINEAR-ELASTIC MEDIUM

First, there is much less radial displacement toward the completely lined tunnel than there is toward the unlined tunnel. Soil displacements at points behind the face of the unlined tunnel have very large radial components, but very small longitudinal components. Figure 3.6a shows that the majority of this radial displacement occurred after the face had passed. From Fig. 3.25a it can be seen that when a stiff liner is installed up to the face, it acts to "freeze" soil displacements (at a given cross section) at the values they had just before the face passed. This is illustrated by the uniformity of displacement magnitudes and directions to the right of a cross section about one radius ahead of the face.

A second difference between the two displacement distributions is in the amount of displacement that has occurred ahead of the two tunnels. Although the completely lined tunnel exhibited less radial displacement behind the face than did the unlined tunnel, it compensates for this by exhibiting significantly greater longitudinal displacements ahead of the face. This is reasonable since it should be expected that the displacements would be concentrated around the path of least resistance, which in this case is toward the unsupported tunnel face.

The distributions of total and incremental displacements for the partially lined tunnel (LLE2) are given in Fig. 3.26. Because the amount of unsupported tunnel surface area is greater, the soil displacements in the vicinity of this tunnel are larger than those obtained for the completely lined tunnel. This is true for both the incremental and total displacements.

Part a of Fig. 3.26 shows again that the stiff liner halts further displacements of the soil behind its leading edge. In this case, however,

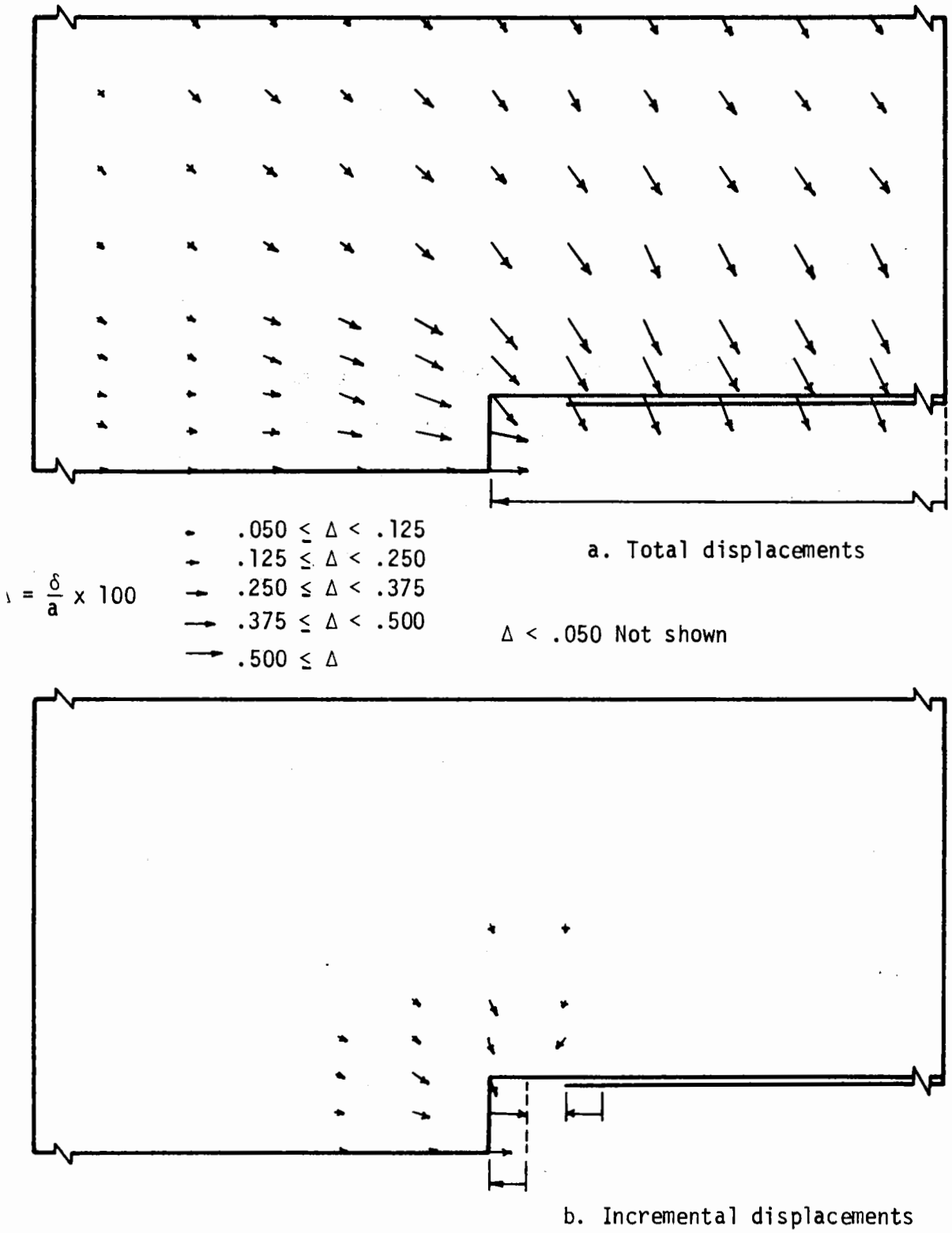

FIGURE 3.26 DISTRIBUTION OF DISPLACEMENTS AROUND A PARTIALLY LINED TUNNEL IN A LINEAR-ELASTIC MEDIUM (CASE LLE 2)

because of the unsupported length of tunnel wall more radial displacement occurs ahead of the liner than occurred in the completely lined tunnel case. Thus, the radial components of the displacements at locations far behind the face for this case are intermediate between those for the completely lined and unlined tunnels.

The position of the liner, relative to the tunnel face, also affects the longitudinal displacements ahead of the tunnel. In a zone extending approximately one to one and a half tunnel diameters ahead of the face the longitudinal displacements for the partially lined tunnel are larger than those for the completely lined tunnel. At distances farther ahead of the face than this, just the opposite is true. It appears that the liner extending all the way up to the face has two, counter-acting, effects on longitudinal displacements. As mentioned above, it inhibits radial displacements and thereby contributes to an increase in longitudinal displacements toward the face. However, by confining the displacements to a small region the liner also restricts the magnitude of these displacements. By keeping the liner a short distance behind the face, most of the soil movement is still confined to a zone around the tunnel face and thus, the displacements are still primarily longitudinal. Now, however, there is a larger opening into which the soil can move and so the displacements are larger. Since displacements ahead of the completely lined tunnel were almost totally longitudinal, the largest displacements were confined to a cylindrical zone the radius of which was only slightly larger than that of the tunnel. As soil moved into the tunnel face it was replaced by soil further ahead of the tunnel. Thus, large displacements extended far out

ahead of the face. In the partially lined case, soil moving into the tunnel opening was replaced by soil located both ahead and "above" the tunnel (upper left-hand quarter of the mesh). Since there was less demand on the soil ahead and on the axis of the tunnel, there was less displacement there than in the fully lined case.

RADIAL DISPLACEMENTS

The radial displacements of the fully lined and partially lined tunnel openings are shown in Figs. 3.27 and 3.28, respectively. Three curves are given in each figure. The dashed curve represents the displacements of the unlined tunnel. The two solid curves, A and B, give the total displacement of the soil and liner and the displacement of the liner only, respectively. Also, shown at the far right-hand side of each figure are the liner displacements predicted by the two-dimensional, finite element solution and the closed form solution. All displacements have been normalized with respect to the tunnel radius.

Figure 3.27 shows that the radial displacements of the fully lined tunnel are considerably smaller than the displacements of the unlined tunnel. Also, it is clear that most of the displacements occur ahead of the tunnel face and the liner. The actual displacement of the liner is very small and there is little variation with position along the tunnel axis. This is primarily due to the great stiffness of the liner. The two-dimensional finite element solution gives a displacement value only seven percent larger than that from this analysis, while the closed-form solution over estimates the displacement by 36 percent. The reasons for these differences are discussed in Chapter 4.

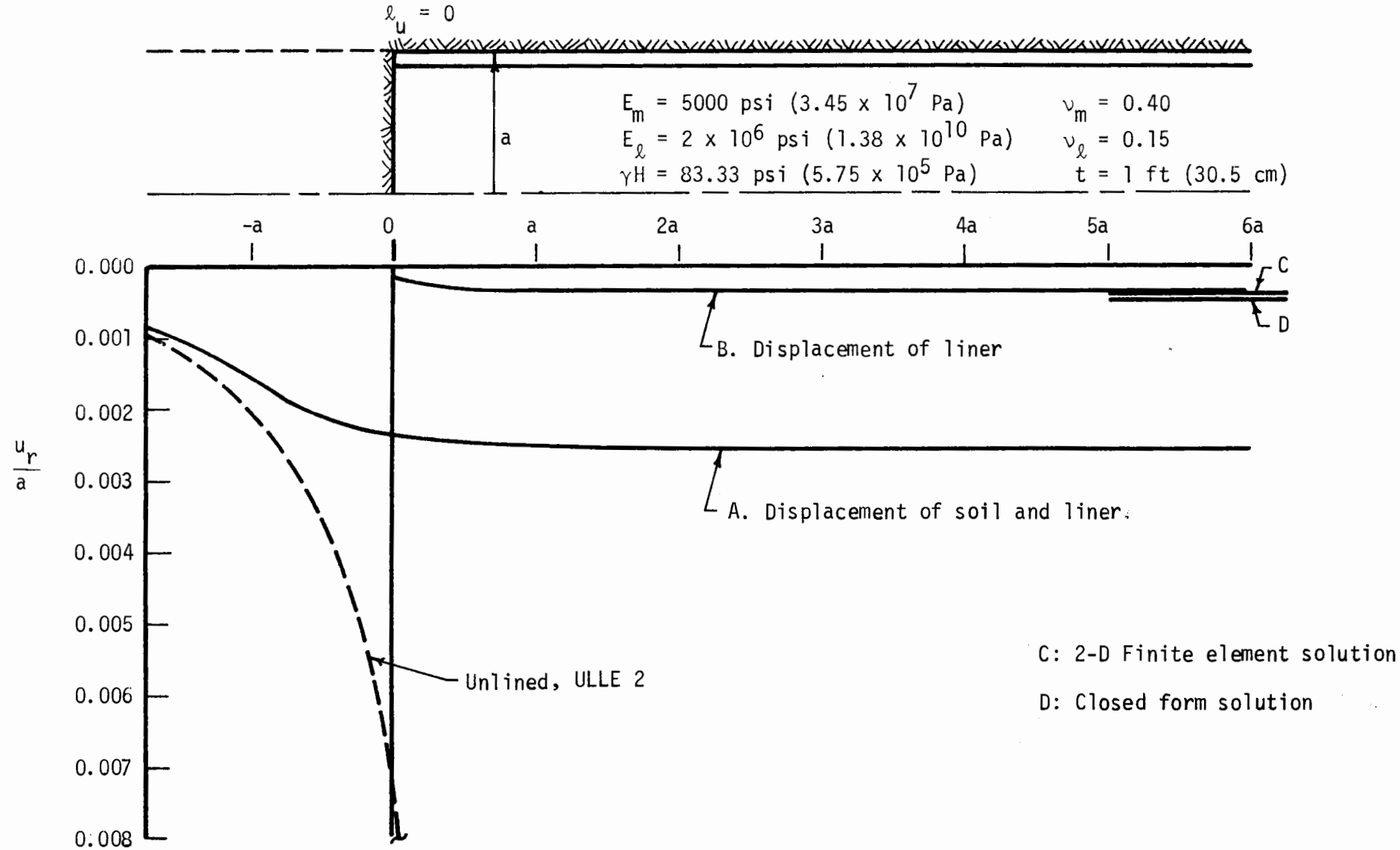

FIGURE 3.27 RADIAL DISPLACEMENTS FOR A FULLY LINED TUNNEL IN A LINEAR-ELASTIC MEDIUM (CASE LLE 1)

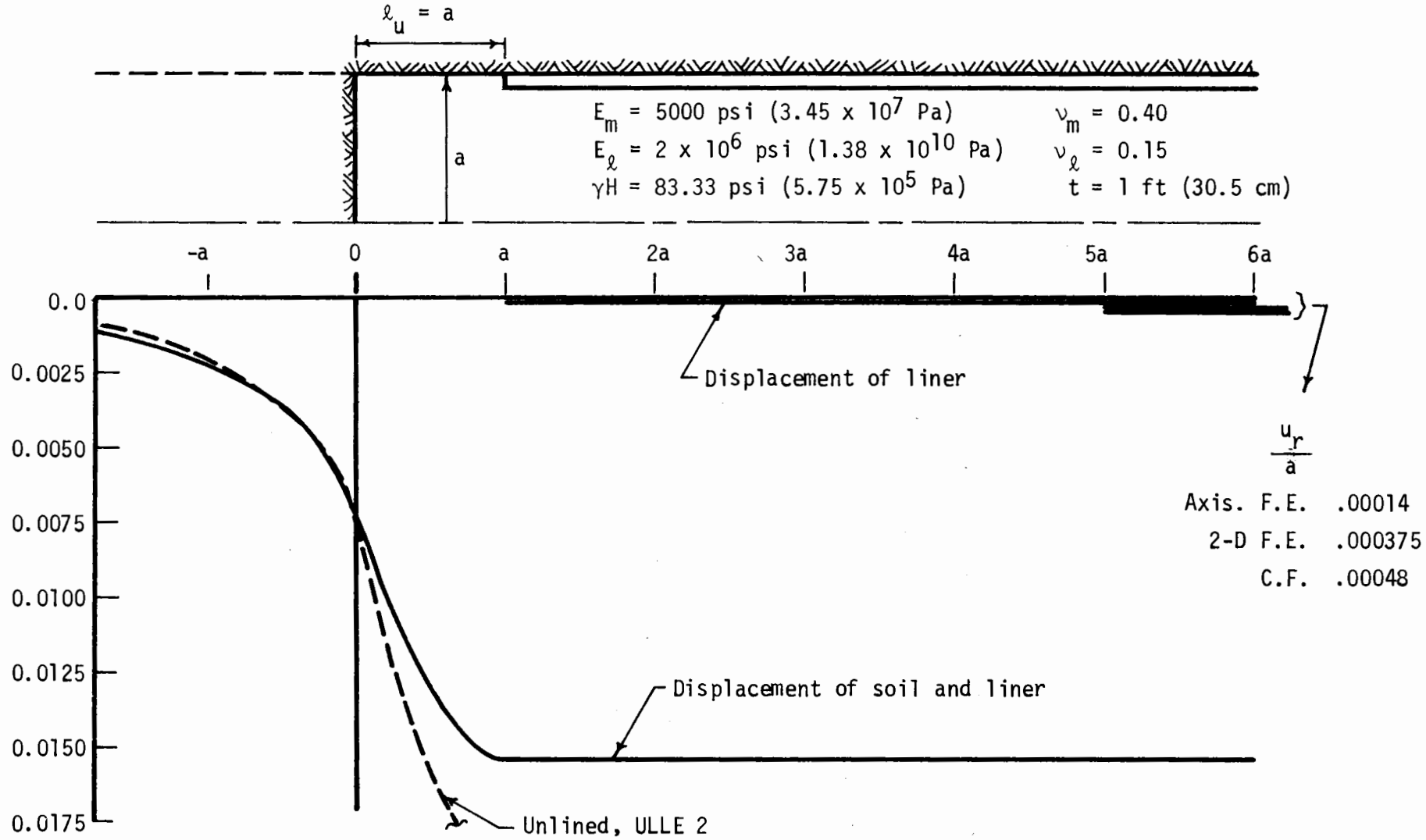

FIGURE 3.28 RADIAL DISPLACEMENTS FOR A PARTIALLY LINED TUNNEL IN A LINEAR-ELASTIC MEDIUM (CASE LLE 2)

The corresponding displacement for the partially lined tunnel are given in Fig. 3.28. Here the radial displacements are much larger, indicating that an unlined gap of only one radius length can significantly affect these displacements. Again, almost all of the displacement occurs ahead of the liner. In front of the tunnel face there is very little difference between the displacement for this and the unlined tunnel case. The two-dimensional finite element solution overestimated the liner displacement, in this case, by 168 percent, while the closed form solution exceeded the value by 243 percent.

These analyses indicate that the liner displacements are reduced to zero as the ratio u^*/u_e approaches one($u_\ell \rightarrow 0$ as $u^* \rightarrow u_e$), where u^* is the radial displacement of the soil just ahead of the liner, u_e is the maximum radial displacement of the unlined tunnel, and u_ℓ is the radial displacement of the liner. If no radial displacement is allowed ahead of the liner, the liner displacement should correspond to the value given by the two-dimensional finite element solution. If complete radial displacement of the soil occurs ahead of the liner there should be no liner displacement.

LONGITUDINAL DISPLACEMENTS

Normalized longitudinal displacements for the lined tunnels in a linear-elastic medium are shown in Fig. 3.29. Also given are the displacements for the corresponding unlined tunnel (ULLE2).

Longitudinal displacements for both lined tunnels exceeded those for the unlined tunnel, with the greatest displacement occurring ahead of the partially lined tunnel ($\ell_u = a$). As discussed in the section on soil

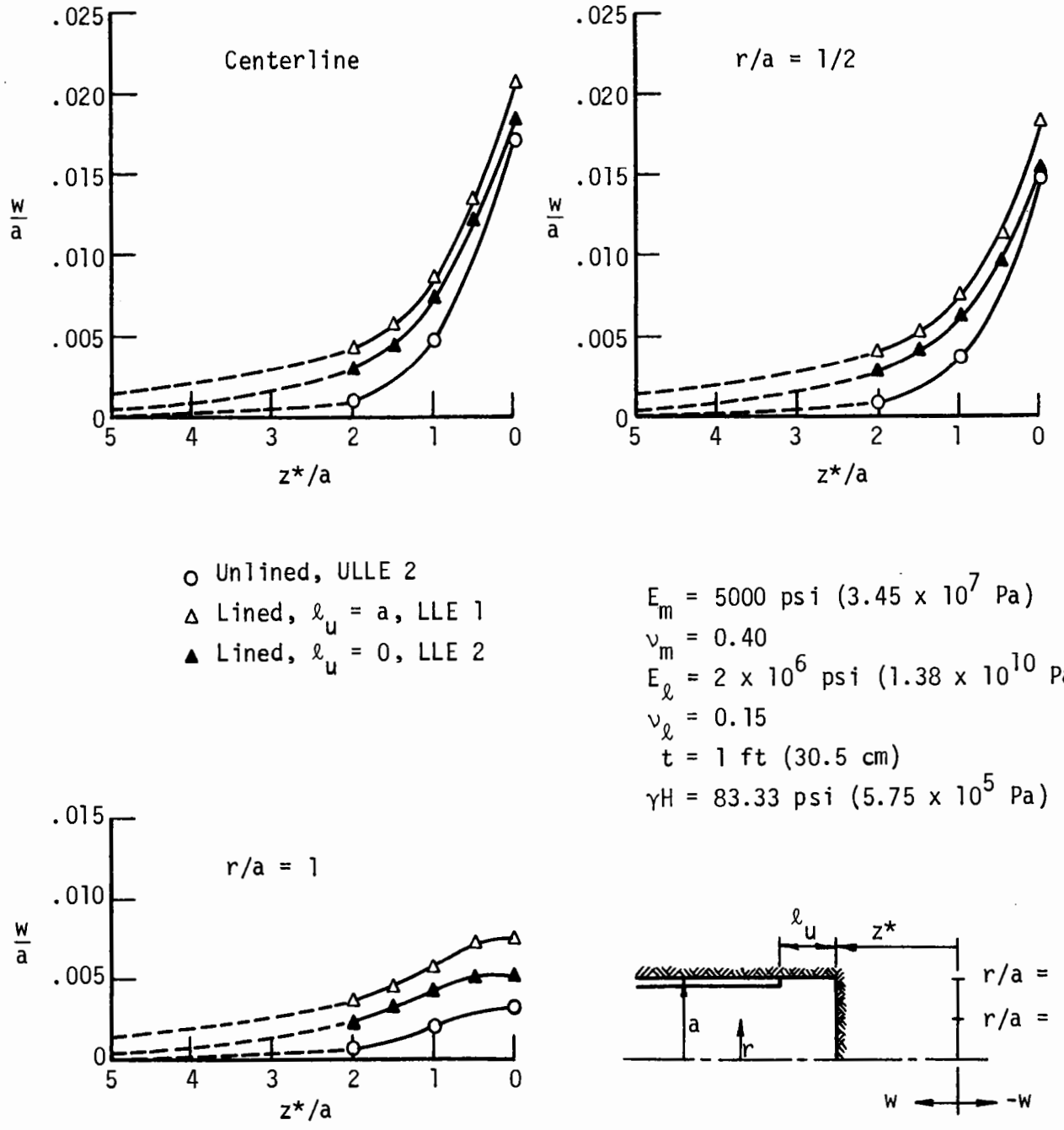

FIGURE 3.29 LONDITUDINAL DISPLACEMENTS ASSOCIATED WITH FULLY AND PARTIALLY LINED TUNNELS IN A LINEAR-ELASTIC MEDIUM

displacements, the liner restricts radial displacements behind it thereby resulting in increased displacements into the opening ahead of the liner. The displacements are larger for the partially lined tunnel because the opening into which the soil is allowed to move is larger than that for the fully lined tunnel.

The displacement curves in Fig. 3.29 indicate that at large z*/a values the partially lined tunnel displacements exceed those for the fully lined tunnel. Even though these small displacements may not be of much significance, this trend is not in agreement with Figs. 3.25 and 3.26 which give the general soil displacement distributions. It is likely that the general soil displacements are too small at points three to five radii ahead of the tunnel due to end effects from the left boundary of the mesh. It is also believed that the displacements shown by the dashed curves in Fig. 3.29 are probably too large because of end effects at the right boundary occurring when the tunnel was first advanced into the medium. The true displacements for this zone probably lie somewhere between the values given by Figs. 3.25 and 3.26 and those given by Fig. 3.29.

LINER THRUST

The longitudinal distributions of liner thrust for both the fully and partially lined tunnels are given in Fig. 3.30. In addition, the thrusts predicted by the two two-dimensional solutions are shown at the far right in this figure.

In the fully lined case, support provided by the soil ahead of the tunnel face reduces the external load and thus the thrust in the liner near

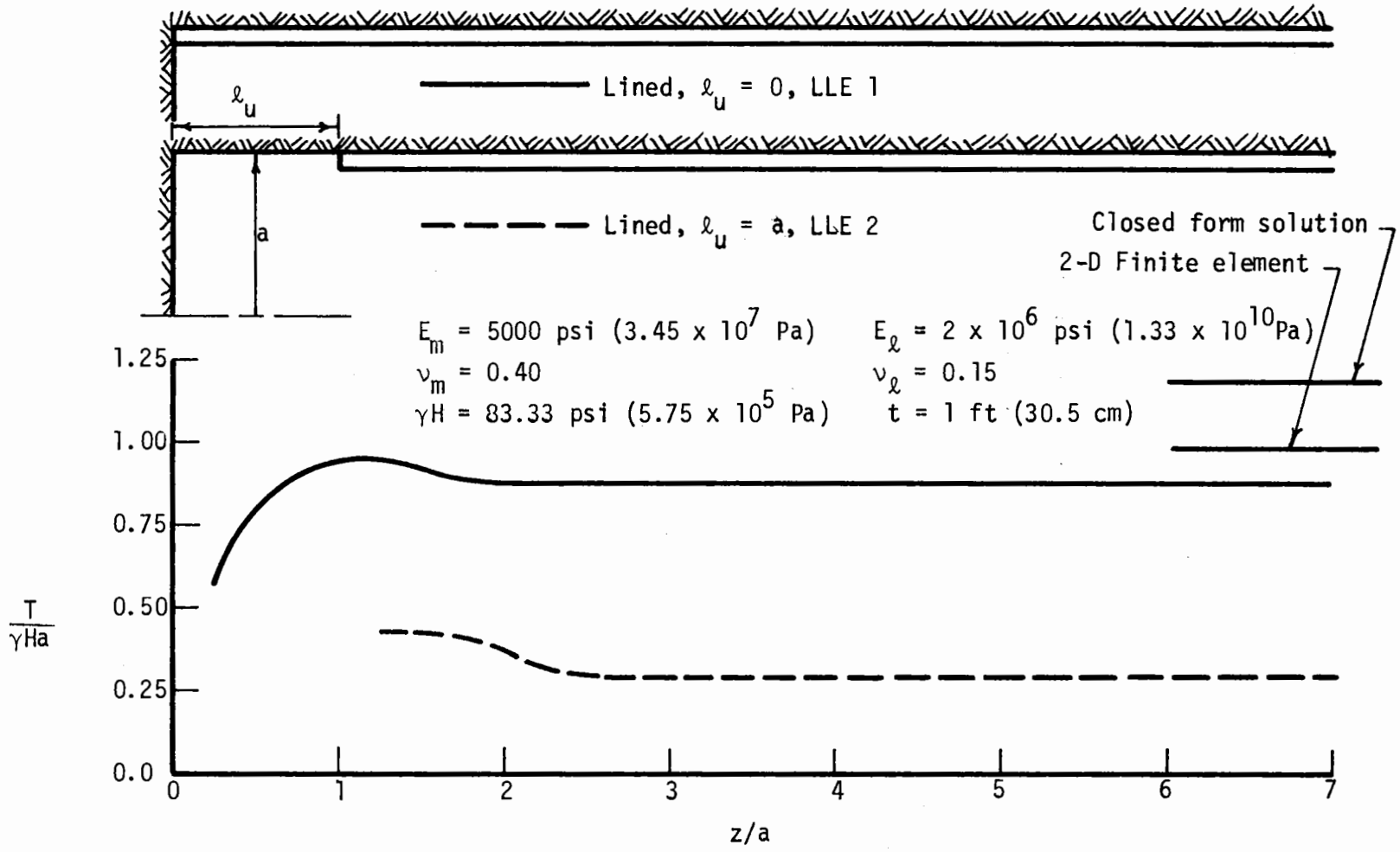

FIGURE 3.30 LINER THRUST FOR FULLY AND PARTIALLY LINED TUNNELS IN A LINEAR-ELASTIC MEDIUM

the face. This natural support rapidly decreases with distance behind the face resulting in an increase of liner thrust. At distances greater than approximately one tunnel diameter behind the face liner thrust is independent of longitudinal position.

For the partially lined tunnel the weight of the unsupported soil is transmitted by arching to both the ground ahead of the face and the forward end of the liner. Thus, that portion of the liner installed last carries the greatest load. With increasing distance behind the end of the liner, the thrust decreases to a minimum value.

Figure 3.30 shows that after the face and liner have advanced one or two diameters beyond a given point the liner thrust at that point has stabilized and is no longer influenced by what takes place ahead of the liner.

The magnitude of the thrust that remains in the liner is a function of the amount of radial displacement that has occurred both before and after the liner was installed. If no displacements whatsoever are allowed, the liner thrust should correspond to that due to the full overburden pressure, $T = \gamma Ha$.

The two-dimensional solutions cannot account for displacements occurring ahead of the liner and so they give high thrust values. In fact, because of the assumptions on which it is based, (Chapter 4), the closed form solution gives a thrust magnitude for this soil-liner combination that is greater than that which would result from the full overburden pressure. The thrust obtained from the two-dimensional finite element solution is slightly less than $T = \gamma Ha$ as a result of the small liner displacements that

occur. Thrust in the fully lined tunnel's liner is less than that given by the two-dimensional finite element solution because of the radial displacements that occur ahead of the face. Of the four thrust values given at the right in Fig. 3.30 the lowest one corresponds to the partially lined tunnel case for which the displacements occurring ahead of the liner were very large.

3.3.3 ELASTO-PLASTIC ANALYSES, $\phi = 0$

For cases LEP1 and LEP2 the soil surrounding the tunnel is assumed to behave as an elasto-plastic material whose shear strength is independent of the mean stress and angle of shearing resistance ($\phi = 0$). This is the same assumption that was made for the unlined tunnel analyses of Section 3.2.3. For these two cases, however, the position of the liner with respect to the face is the only variable. Soil properties are the same for both cases, and correspond to those used in unlined tunnel case ULEP1.

PLASTIC ZONE

To obtain an estimate of how much yielding would occur around these tunnels, the distribution of $\sqrt{J_2'}$ were plotted for the linear-elastic analyses. The resulting contours of $\sqrt{J_2'}/\gamma H$ are shown in Fig. 3.31. The value of c_u selected for the elasto-plastic analyses corresponds to $\sqrt{J_2'}/\gamma H = 0.168$. Thus, this contour should approximate the boundary between the elastic and plastic zones. The relationship will not be exact because of the stress redistribution that occurs as yielding progresses, and because there is a difference between the Poisson's ratio values for the linear-elastic and elasto-plastic analyses.

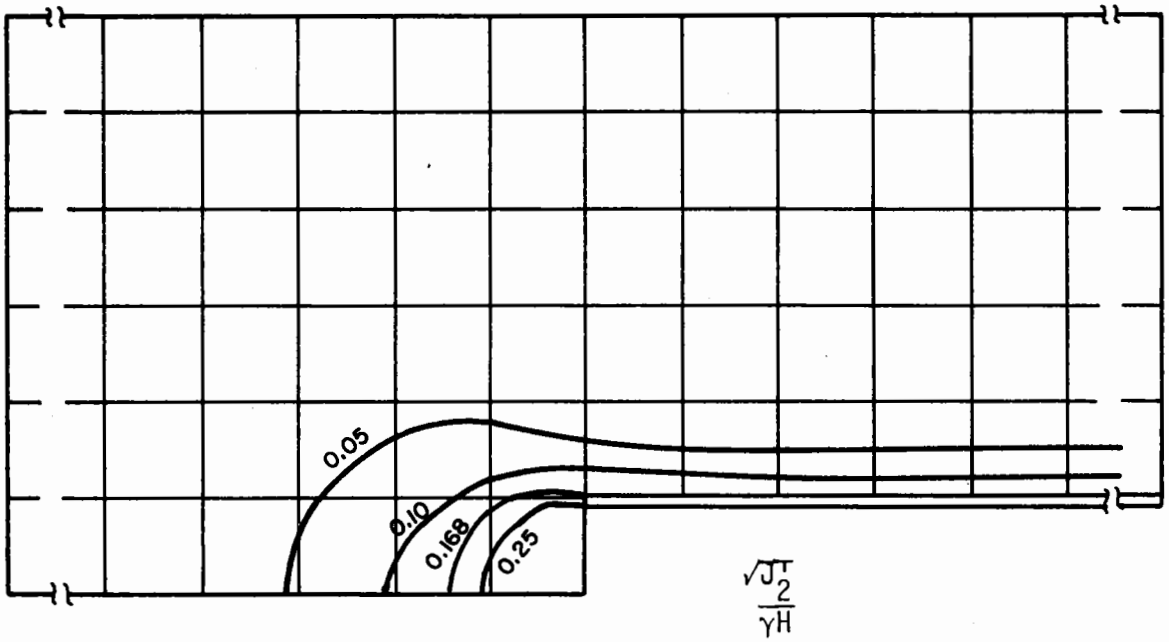

a. Case LLE 1

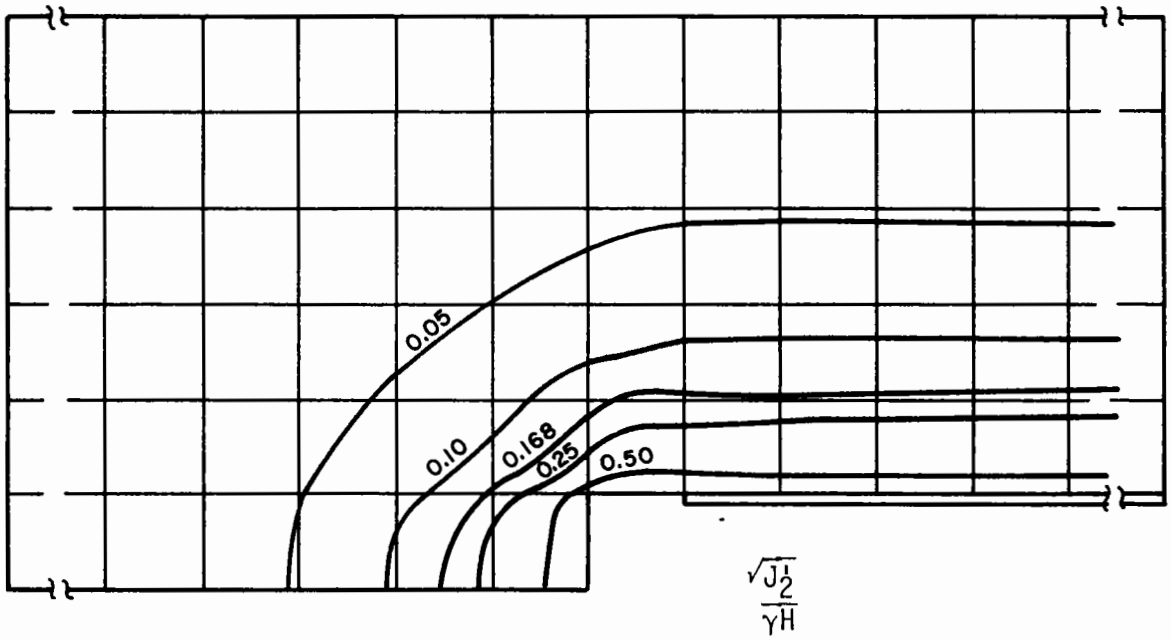

b. Case LLE 2

FIGURE 3.31 DISTRIBUTION OF $\sqrt{J_2'}$ AROUND FULLY AND PARTIALLY LINED TUNNELS IN A LINEAR-ELASTIC MEDIUM

Figure 3.32 gives the actual plastic zones that were obtained. It can be seen that the estimate provided by the 0.168 contour in Fig. 3.31 is very good.

The plastic zone for the fully lined tunnel is confined to a relatively small region just ahead of the face. Behind the face the liner provides enough support to the soil so that the stresses do not change very much from their free-field values. The changes that do occur are not great enough for the resulting stress difference or shear stress to exceed the shear strength of the soil.

A considerably larger plastic zone is obtained for the partially lined tunnel. For this case the unsupported length of tunnel just behind the face allows sufficient stress redistribution in the soil to cause yielding out beyond the tunnel perimeter. The effect of the liner in this case is to halt further yielding beyond what has already taken place ahead of it. Very little, if any yielding occurs behind the liner.

The plastic zones shown in Fig. 3.32, to the extent they exist, are similar in shape to those obtained for the unlined tunnels. The effect of the liner is to reduce the size of the plastic zone that forms behind its leading end and to increase the longitudinal extent of the plastic zone ahead of the face (see curve A in Fig. 3.12).

DISTRIBUTION OF STRESSES

Stresses in the soil surrounding the fully and partially lined tunnels are indicated by the normalized stress contours of Fig. 3.33 and 3.34, respectively. These distributions can be compared to those for cases LLE1

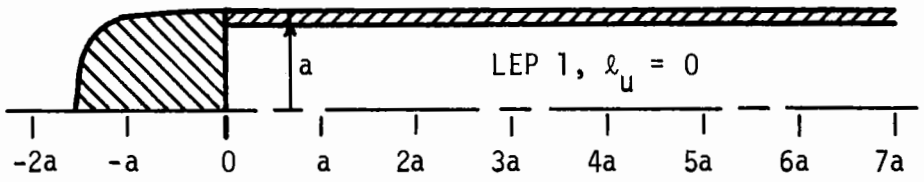

E_m = 5000 psi (3.45×10^7 Pa) $\quad \nu_m = 0.49$

$E_\ell = 2 \times 10^6$ psi (1.38×10^{10} Pa) $\quad \nu_\ell = 0.15$

γH = 83.33 psi (5.75×10^5 Pa) $\quad t$ = 1 ft (30.5 cm)

c_u = 14 psi (9.65×10^4 Pa)

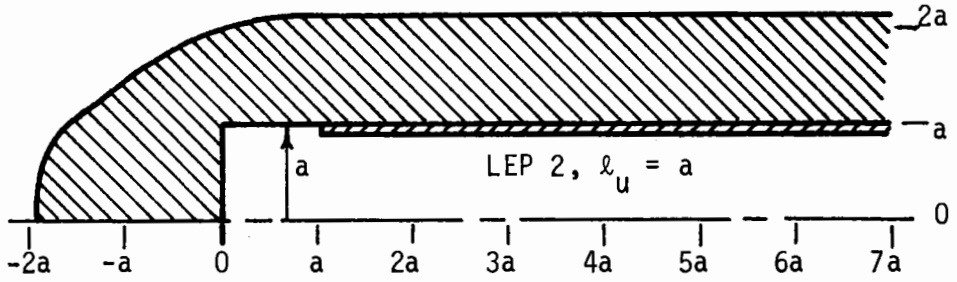

FIGURE 3.32 PLASTIC ZONES AROUND FULLY AND PARTIALLY LINED TUNNELS IN AN ELASTO-PLASTIC MEDIUM - $\phi = 0$

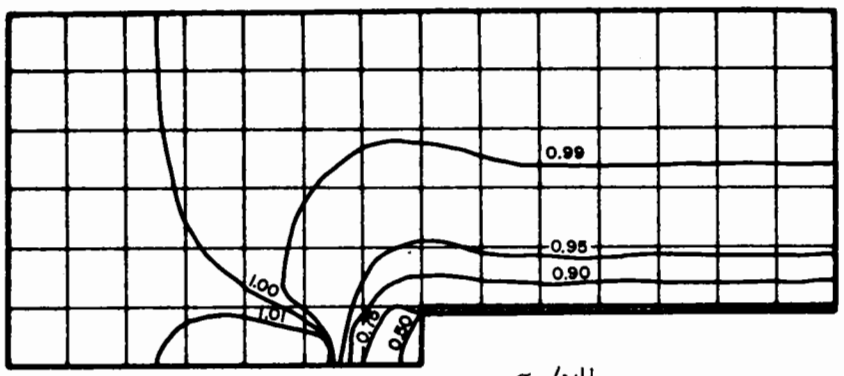

$\sigma_r/\gamma H$

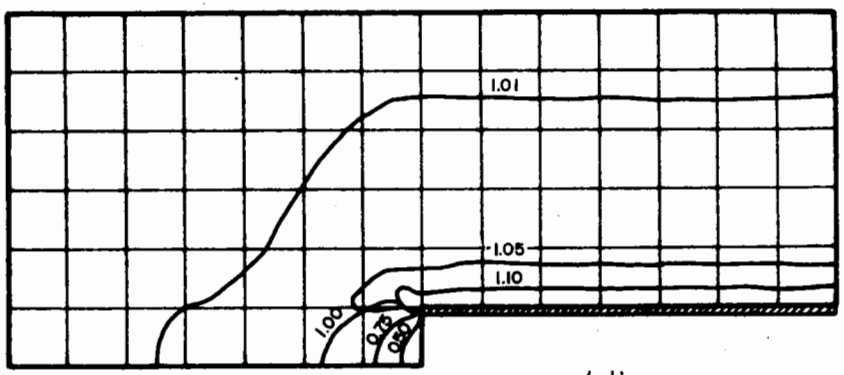

$\sigma_\theta/\gamma H$

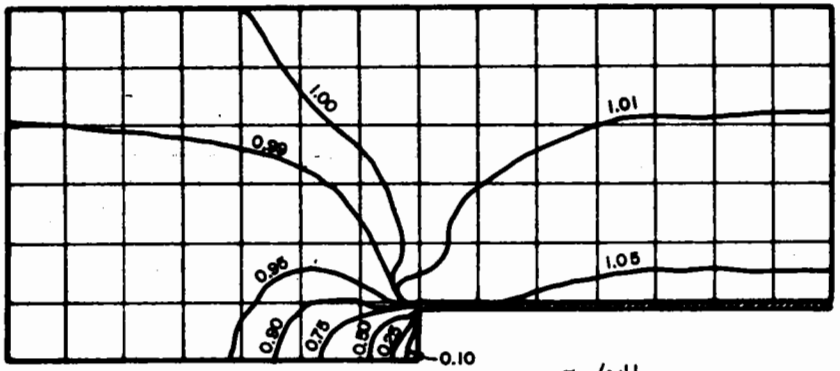

$\sigma_z/\gamma H$

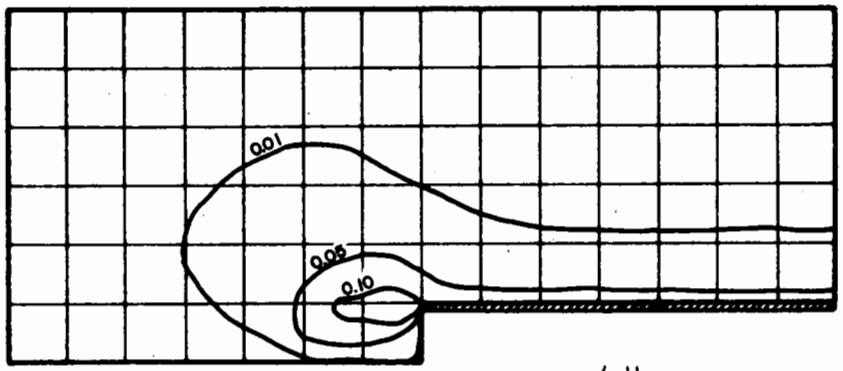

$\tau_{rz}/\gamma H$

FIGURE 3.33 DISTRIBUTION OF STRESSES AROUND A FULLY LINED TUNNEL IN AN ELASTO-PLASTIC MEDIUM - ϕ = 0 (CASE LEP 1)

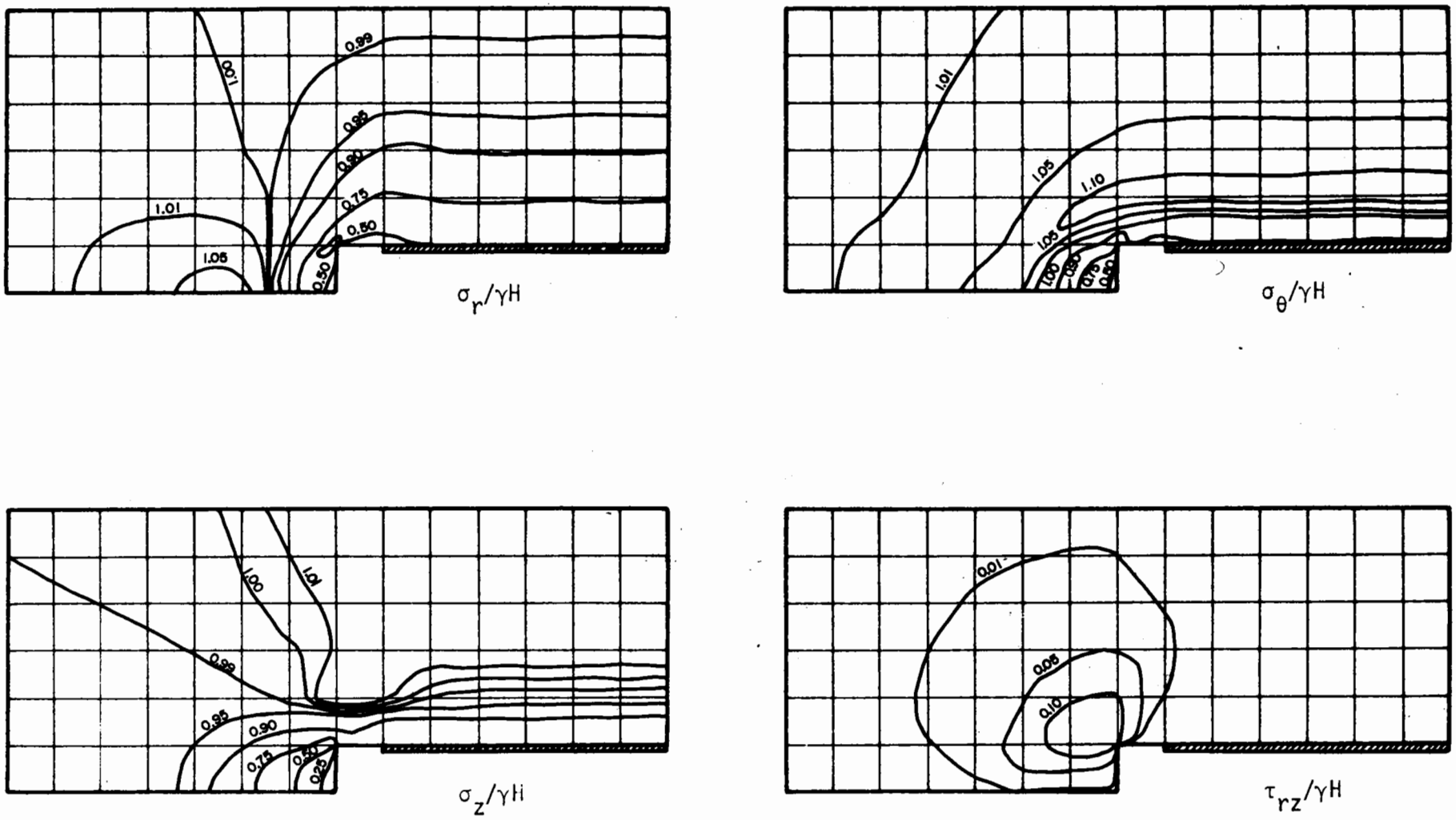

FIGURE 3.34 DISTRIBUTION OF STRESSES AROUND A PARTIALLY LINED TUNNEL IN AN ELASTO-PLASTIC MEDIUM - $\phi = 0$ (CASE LEP 2)

and LLE2 in which the soil was assumed to be linear-elastic. It must be kept in mind, however, that the value of Poisson's ratio is not the same for the linear-elastic and elasto-plastic analyses and that this may account for some of the differences and/or similarities between the stress distributions for the two types of analysis.

The stress distributions for the fully lined tunnel in an elasto-plastic medium (Fig. 3.33) are remarkably similar to those obtained from the linear-elastic analysis (Fig. 3.23). The differences that do exist can seemingly be explained solely on the basis of the plastic yielding, indicating the Poisson's ratio may have little affect on soil stresses when the tunnel is completely lined. Relative to those from the linear-elastic analysis, the radial and circumferential stress contours in Fig. 3.33 are slightly farther away from the tunnel boundary. Thus, in the soil just outside of the liner the radial stress has decreased slightly and the circumferential stress has increased slightly from the values obtained from the linear-elastic analysis. Ahead of the face, in the area of the plastic zone, there has been a reduction of both radial and circumferential stresses. The $\sigma/\gamma H = 1.00$ contour of both stresses intersected the tunnel axis at a point approximately three quarters of a radius ahead of the face in the linear-elastic analysis, but for the elasto-plastic analysis this point has moved out to about one and three quarters radii ahead of the face.

There is no significant difference between the longitudinal stress distributions obtained from the elasto-plastic and linear-elastic analyses of the fully lined tunnel.

The shear stresses in Fig. 3.33 are slightly lower than those in Fig. 3.23. In the elasto-plastic case no shear stresses (τ_{rz}) in excess of

0.14 γH occurred. Taking $\sqrt{J_2'}$ as a measure of the shear stress, it can be seen in Fig. 3.31a that "shear stresses" greater than 0.25 γH existed ahead of the tunnel in the linear-elastic case. Due to the plastic yielding in case LEP1 these "shear stresses" were everywhere reduced to less than 0.168 γH.

Figure 3.34 gives the soil stress distributions for the elasto-plastic analysis of the partially lined tunnel. When these stresses are compared to those from the linear-elastic analysis (Fig. 3.24), several significant differences are apparent.

Both σ_r and σ_θ stresses have been reduced in the area of the plastic zone ahead of the tunnel. Behind the liner there has been a slight general reduction of radial stresses except right next to the liner where there has been a small increase. As would be expected, the magnitudes of the circumferential stresses in the plastic zone have been reduced. Just outside the liner the circumferential stresses have been reduced from $\sigma_\theta \simeq 1.5\ \gamma H$ in the linear-elastic to $\sigma_\theta \simeq 0.9\ \gamma H$ in the elasto-plastic analysis.

The greatest change in longitudinal stresses due to plastic yielding occurs behind the tunnel face where there has been a slight stress reduction.

The high rz-shear stresses observed around the tunnel face in the linear-elastic analysis are not present in the elasto-plastic case. In addition, no shear stresses in excess of one percent of the free-field stress occur behind the liner in the elasto-plastic analysis.

SOIL DISPLACEMENTS

Soil displacements around the fully and partially lined tunnels are shown in Figs. 3.35 and 3.36, respectively. They are very similar to those given by the corresponding distributions for the linear-elastic analysis. The primary difference is in the magnitude of the displacements, with those from the elasto-plastic analysis being generally somewhat larger than the displacements from the linear-elastic analyses. In addition, the displacements behind the tunnel face in Figs. 3.35 and 3.36 appear to have slightly larger radial components relative to their longitudinal components.

RADIAL DISPLACEMENTS

Radial displacements of the fully lined tunnel opening are shown in Fig. 3.37. As was found in the linear-elastic analysis, most of the displacements occur ahead of the face and liner. The stiff liner resists inward movement, thereby affecting not only the displacements of the soil around it, but also the displacements of the soil ahead of it. Within a distance of about one diameter ahead of the face, the radial soil displacements for the completely lined tunnel are less than those of the unlined tunnel. However, at points farther ahead of the face the relationship is reversed. By restraining displacement of the soil immediately around it the liner contributes to increased displacements far ahead of it. In the region where the liner tends to prevent displacements its influence is greatest right at the tunnel face. This is clearly demonstrated by the downward bulge in curve A just ahead of the face in Fig. 3.37. In this case the restraining action of the liner, in combination with the increased tendency for displacement because

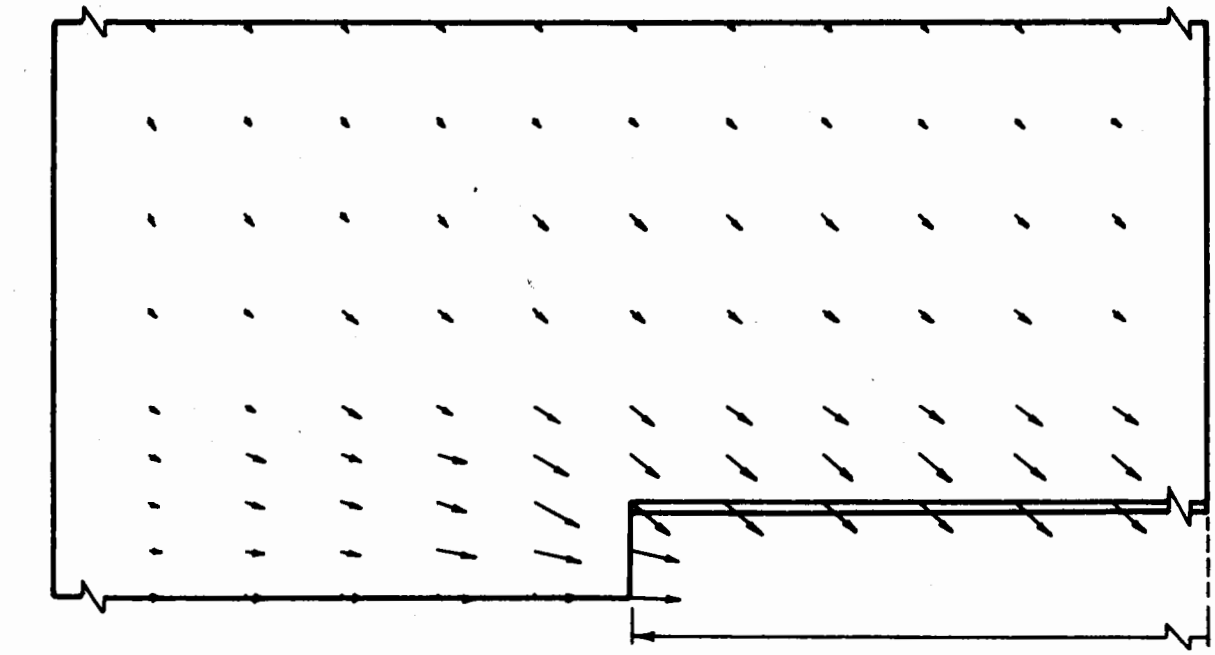

$\Delta = \frac{\delta}{a} \times 100$

$.050 \leq \Delta < .125$

$.125 \leq \Delta < .250$

$.250 \leq \Delta < .375$

$.375 \leq \Delta < .500$

$.500 \leq \Delta$

a. Total displacements

$\Delta < .050$ Not shown

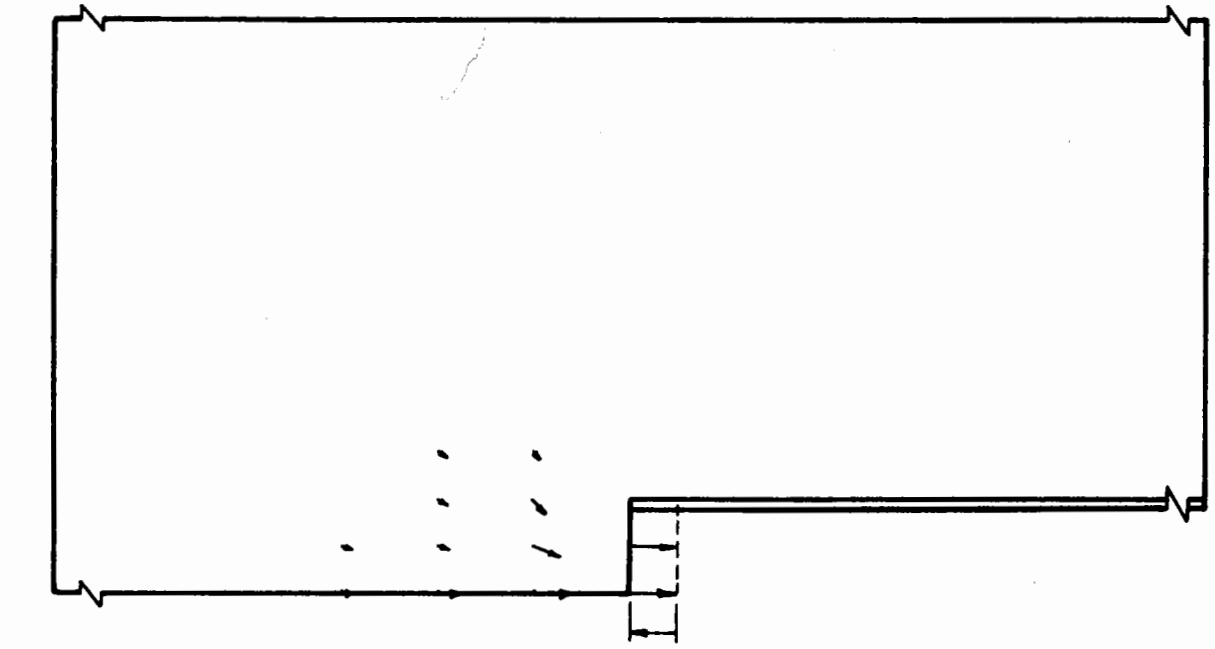

b. Incremental displacements

FIGURE 3.35 DISTRIBUTION OF DISPLACEMENTS AROUND A FULLY LINED TUNNEL IN AN ELASTO-PLASTIC MEDIUM - $\phi = 0$ (CASE LEP 1)

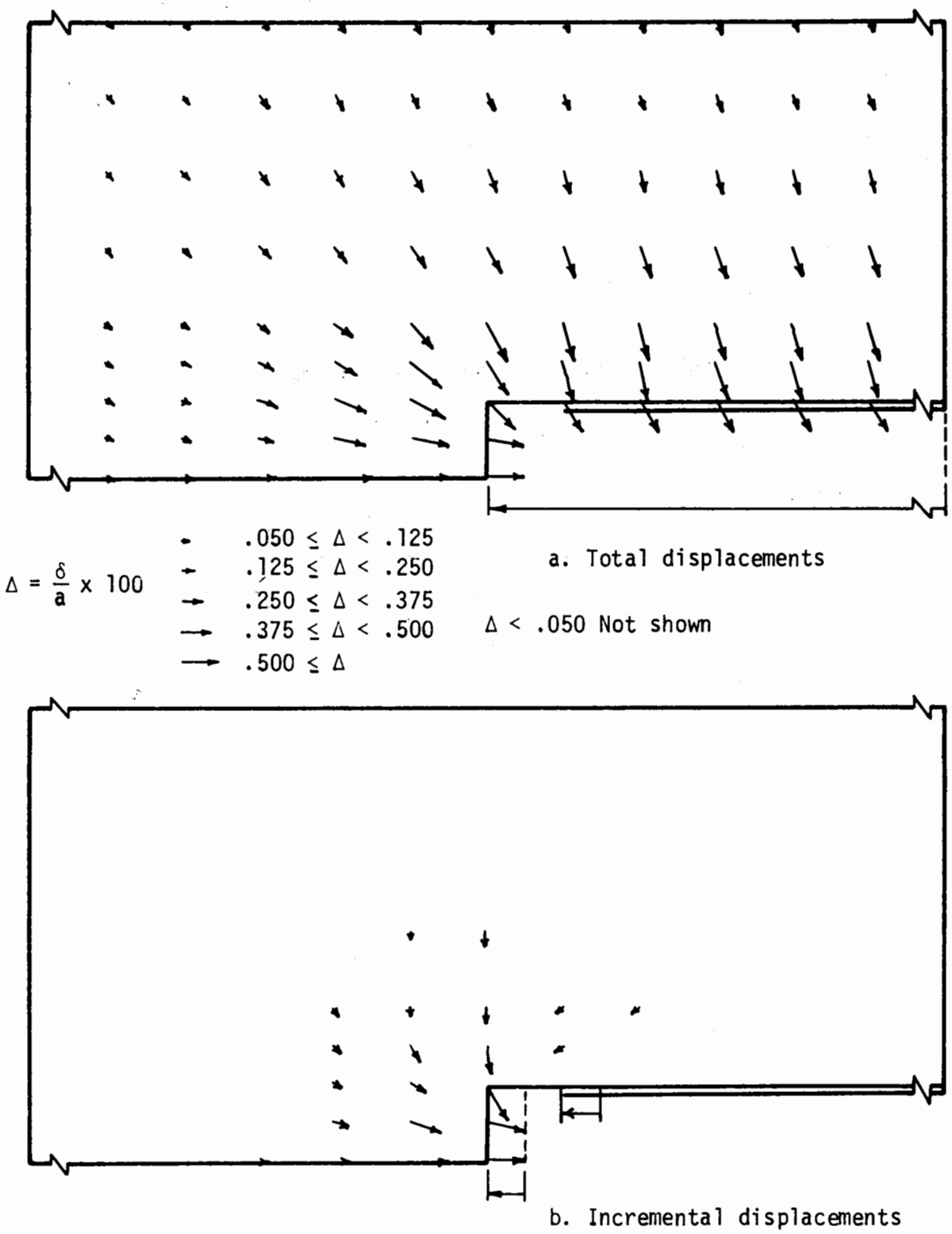

FIGURE 3.36 DISTRIBUTION OF DISPLACEMENTS AROUND A PARTIALLY LINED TUNNEL IN AN ELASTO-PLASTIC MEDIUM - $\phi = 0$ (CASE LEP 2)

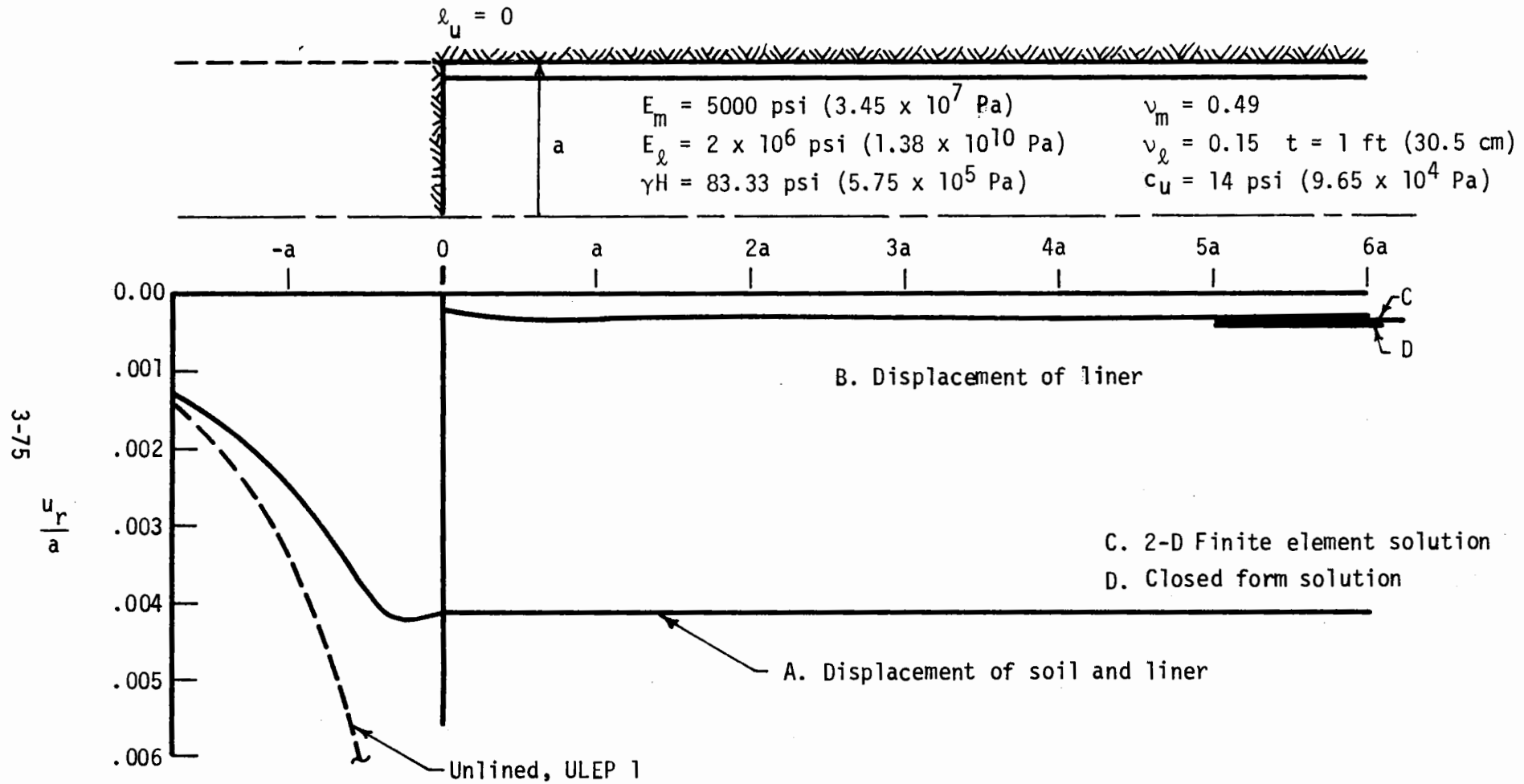

FIGURE 3.37 RADIAL DISPLACEMENTS FOR A FULLY LINED TUNNEL IN AN ELASTO-PLASTIC MEDIUM, ϕ = 0 (CASE LEP 1)

of plastic yielding, has resulted in the occurrence of greater displacements just ahead of the face (- a/4) than right at the face.

A comparison of the displacement curves A in Figs. 3.37 and 3.27 shows that radial displacements of the soil at the tunnel face from the elasto-plastic analysis are approximately 75 percent greater than those from the linear-elastic analysis. At the same time the liner displacements in the elasto-plastic case are ten percent less than those in the linear-elastic case.

The two-dimensional solutions, which assume the soil to be elastic, overestimate the liner displacement; the two-dimensional finite element solution by 18 percent and the closed form solution by 29 percent.

Figure 3.38 gives the radial displacements obtained from the partially lined tunnel analysis. Ahead of the face these displacements exceed those obtained from the unlined case. As mentioned above, this is a consequence of the combined effects of plastic yielding and the restraint provided by the liner to the soil immediately surrounding it.

Because yielding of the soil ahead of the tunnel causes greater displacements, the total displacements of the soil and liner (curve A) are greater for the elasto-plastic case than the linear-elastic case. This is similar to what was observed for the fully lined tunnel. For the partially lined tunnel, however, it was found that liner displacement is greater when a plastic zone forms around the tunnel than when such a zone does not form. Liner displacements from the elasto-plastic analysis are percent greater than those from the linear-elastic analysis.

The elastic, two-dimensional finite element solution gives a liner displacement that is 73 percent greater than the value obtained here.

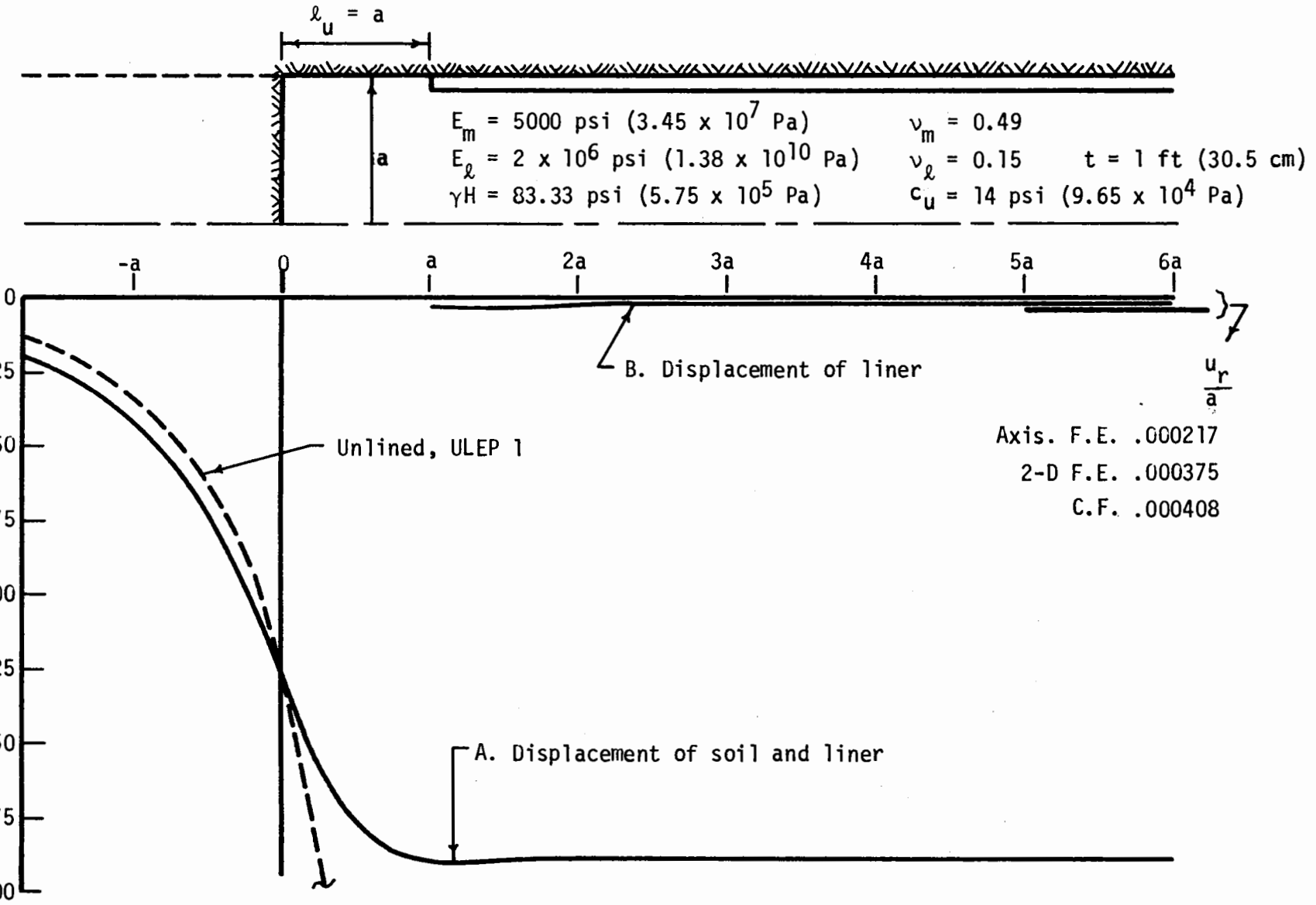

FIGURE 3.38 RADIAL DISPLACEMENTS FOR A PARTIALLY LINED TUNNEL IN AN ELASTO-PLASTIC MEDIUM - ϕ = 0 (CASE LEP 2)

Similarly, the closed form solution exceeds the displacement value by 88 percent.

LONGITUDINAL DISPLACEMENTS

The longitudinal displacements of a reference cross section as the tunnel approaches are given in Fig. 3.39 for the fully and partially lined tunnels in an elasto-plastic medium. Also shown are the displacements associated with the unlined tunnel in the same medium.

The trend indicated by the linear-elastic analyses is also observed here. Longitudinal displacements for the lined tunnels exceed those of the unlined tunnel. There is one exception here, however. Longitudinal displacements of the tunnel face ($z^* = o$) for the fully lined tunnel are less than those of the unlined tunnel. This indicates that the liner can have a restraining effect on longitudinal as well as radial displacements.

The maximum displacement occurred at the center line of the partially lined tunnel and was approximately four percent of the tunnel radius. This compares to a maximum of two percent of the radius obtained in the linear-elastic analysis, Fig. 3.29.

LINER THRUST

The longitudinal distributions of liner thrust for the fully and partially lined tunnels in an elasto-plastic medium are given in Fig. 3.40. The two curves are similar in shape to their counterparts in Fig. 3.30 for the linear-elastic analyses.

Plastic yielding of the soil ahead of the tunnel face has reduced the load carrying capacity of this soil, thereby shifting a greater

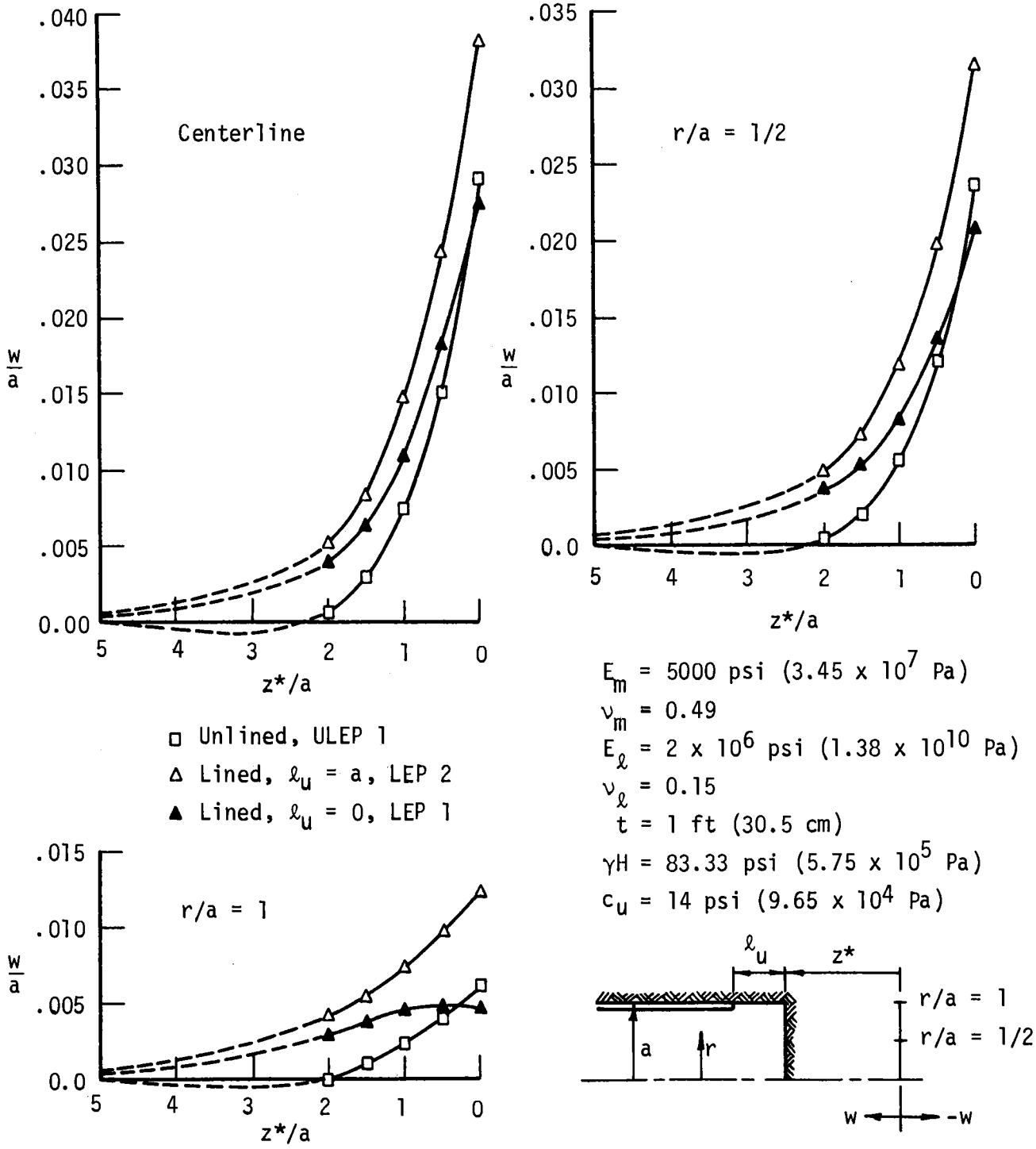

FIGURE 3.39 LONGITUDINAL DISPLACEMENTS ASSOCIATED WITH FULLY AND PARTIALLY LINED TUNNELS IN AN ELASTO-PLASTIC MEDIUM - $\phi = 0$

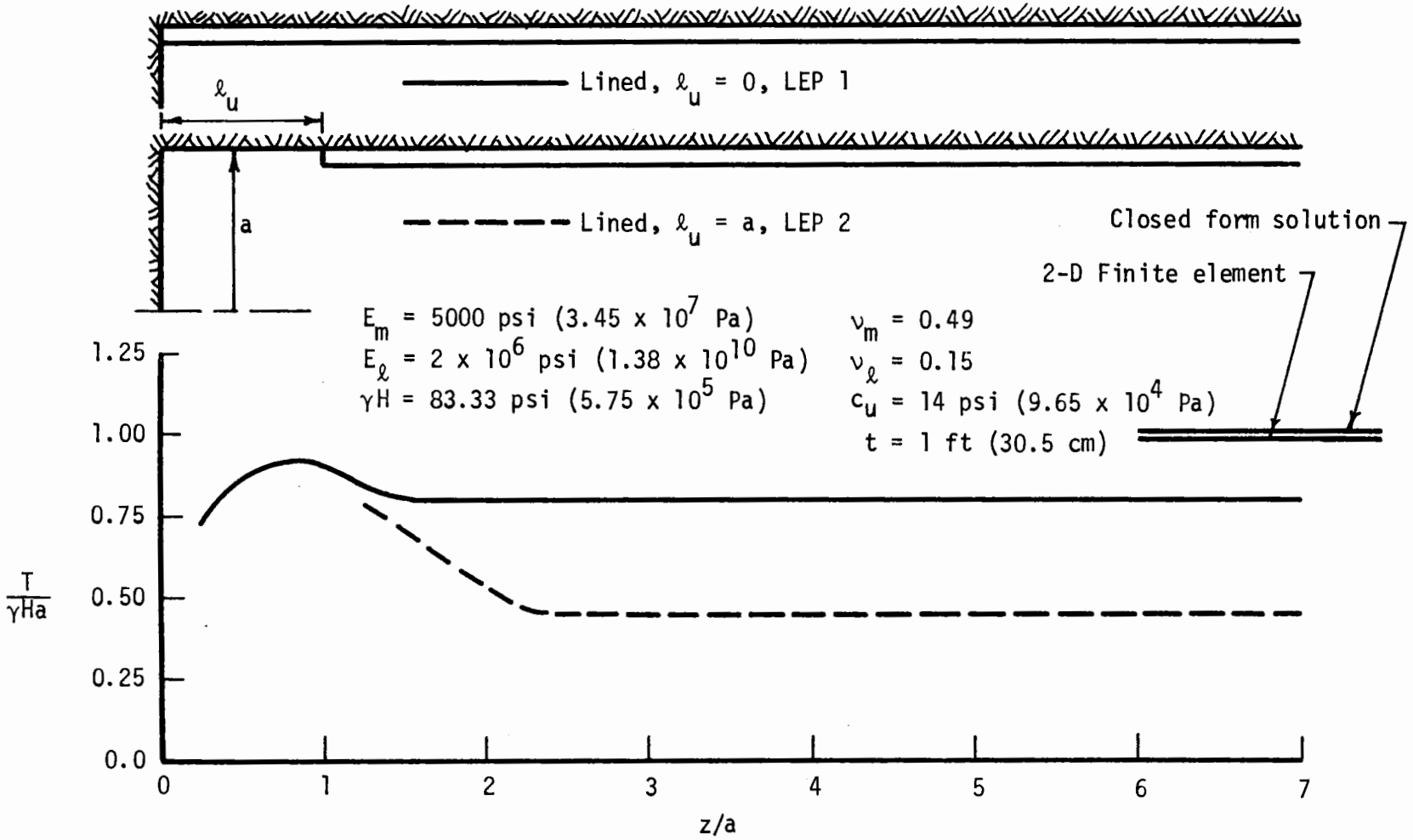

FIGURE 3.40 LINER THRUST FOR FULLY AND PARTIALLY LINED TUNNELS IN AN ELASTO-PLASTIC MEDIUM, ϕ = 0

proportion of the load to the leading end of the liner. Thus, for the fully lined tunnel the thrust in the liner right behind the face is increased from 0.57 γHa in the linear-elastic case to 0.72 γHa in the elasto-plastic case. Since the amount of plastic yielding is greater in the partially lined tunnel case, the thrust difference is also greater; increasing from 0.43 γHa in the linear-elastic case to 0.78 γHa in the elasto-plastic case.

At distances greater than one to two tunnel diameters behind the end of the liner, the thrust is independent of longitudinal position with respect to the face. Here again there is a difference between the results from the linear-elastic and elasto-plastic analyses. Figures 3.33 and 3.23 show that plastic yielding ahead of the fully lined tunnel reduces the mangitude of the radial stresses there. Thus, when the tunnel is advanced into this zone the radial stresses acting on the liner in the elastp-plastic case will be less than those in the linear-elastic case. The result is lower thrust in the liner for the elasto-plastic case. Around the partially lined tunnel the extent of plastic yielding and radial displacement is greater, resulting in a greater reduction of radial stresses around this tunnel than in the fully lined case. Thus, thrust in the partially lined tunnel is less than that in the fully lined tunnel. However, the amount of potential radial displacement is greater in the elasto-plastic case than in the linear-elastic case. Since the liners are installed at the same location behind the face in these two analyses, the liner in the elasto-plastic case must resist greater deformations than the liner in the linear-elastic case. Thus, the liner in the elasto-plastic medium is subjected to greater external pressures and as a consequence must carry a greater thrust than the same liner in the linear-elastic medium.

Again, the elastic, two-dimensional solutions overestimated the thruse in the liner. The two-dimensional finite element solution yielded a thrust magnitude of 0.98 γHa, exactly the same value as obtained for the soil liner combination of the linear-elastic case (Fig. 3.30). The closed form solution gave a thrust of 1.004 γHa. The only difference between the elastic properties of the medium in the linear-elastic and elasto-plastic analyses is the value of Poisson's ratio. It appears that for the liner properties considered the closed-form solution is significantly influenced by Poisson's ratio of the medium whereas the two-dimensional finite element solution is not. This would tend to indicate that while Poisson's ratio of the soil is different for the linear-elastic and elasto-plastic analyses, the differences in results obtained is due primarily to the effect of plastic yielding.

3.3.4 ELASTO-PLASTIC ANALYSES, $\phi \neq 0$

For the lined tunnel analyses LEP3 and LEP4 the soil surrounding the tunnel was assumed to be an elasto-plastic material whose shear strength is a function of the mean stress and the angle of shearing resistance, as well as cohesion ($c \neq 0$, $\phi \neq 0$). For case LEP3 the tunnel was assumed to be lined all the way up to the face, while for case LEP4 it was assumed that the liner extended up to a point one tunnel radius behind the face. Except for this difference the two analyses were identical, both considering the same soil properties used in unlined tunnel case ULEP6 (c = 14 psi = 9.65 x 10^4 Pa, $\phi = 30°$).

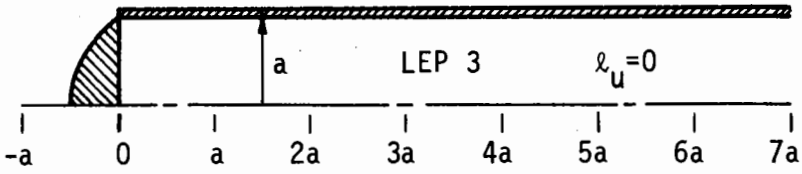

E_m = 5000 psi (3.45×10^7 Pa) $\quad \nu_m = 0.40$

$E_\ell = 2 \times 10^6$ psi (1.38×10^{10} Pa) $\quad \nu_\ell = 0.15$

$\gamma H = 83.33$ psi (5.75×10^5 Pa) $\quad t = 1$ ft (30.5 cm)

$c = 14$ psi (9.65×10^4 Pa) $\quad \phi = 30°$

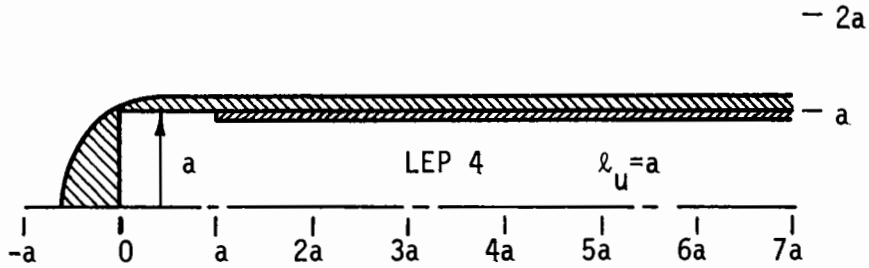

FIGURE 3.41 PLASTIC ZONES AROUND FULLY AND PARTIALLY LINED TUNNELS IN AN ELASTO-PLASTIC MEDIUM - $\phi \neq 0$.

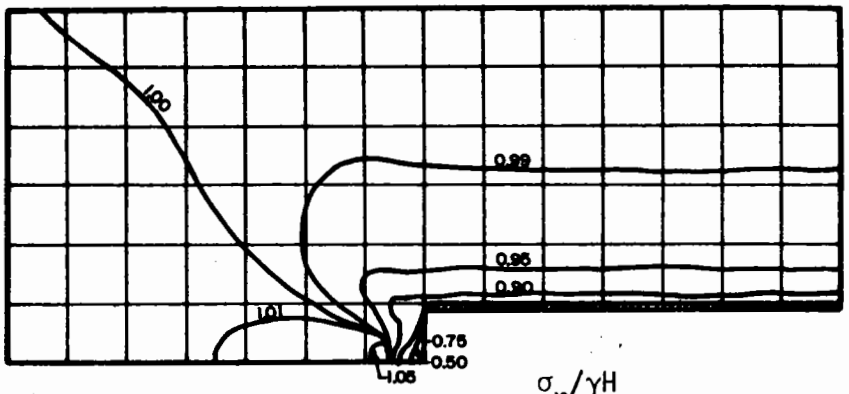

$\sigma_r/\gamma H$

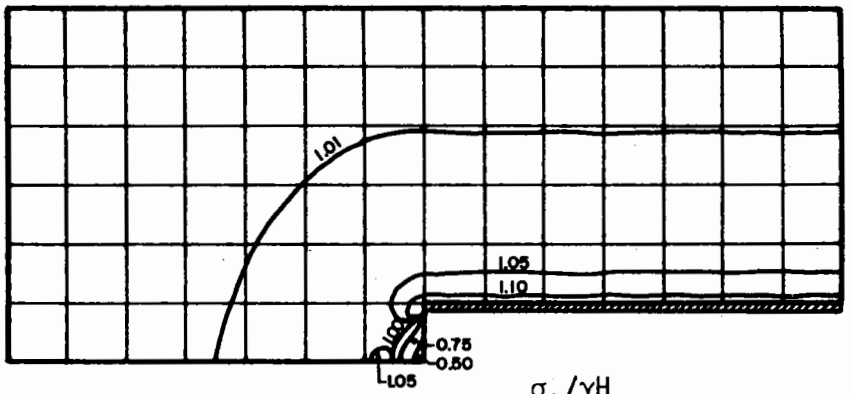

$\sigma_\theta/\gamma H$

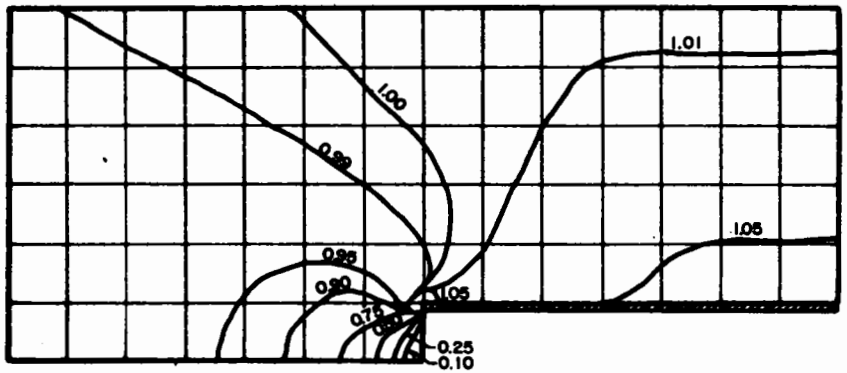

$\sigma_z/\gamma H$

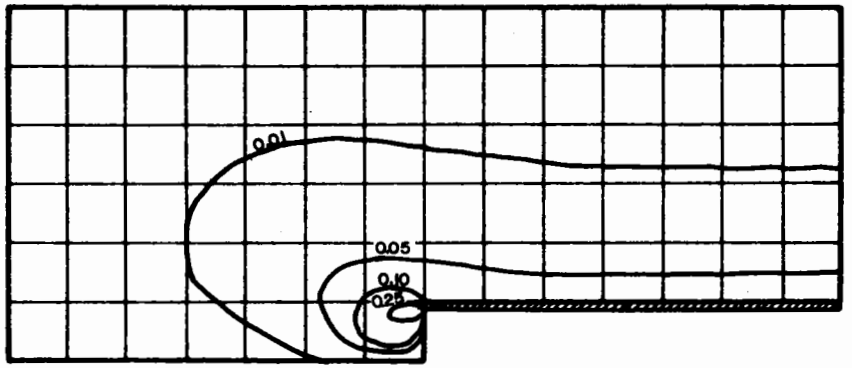

$\tau_{rz}/\gamma H$

FIGURE 3.42 DISTRIBUTION OF STRESSES AROUND A FULLY LINED TUNNEL IN AN ELASTO-PLASTIC MEDIUM - $\phi \neq 0$ (CASE LEP 3).

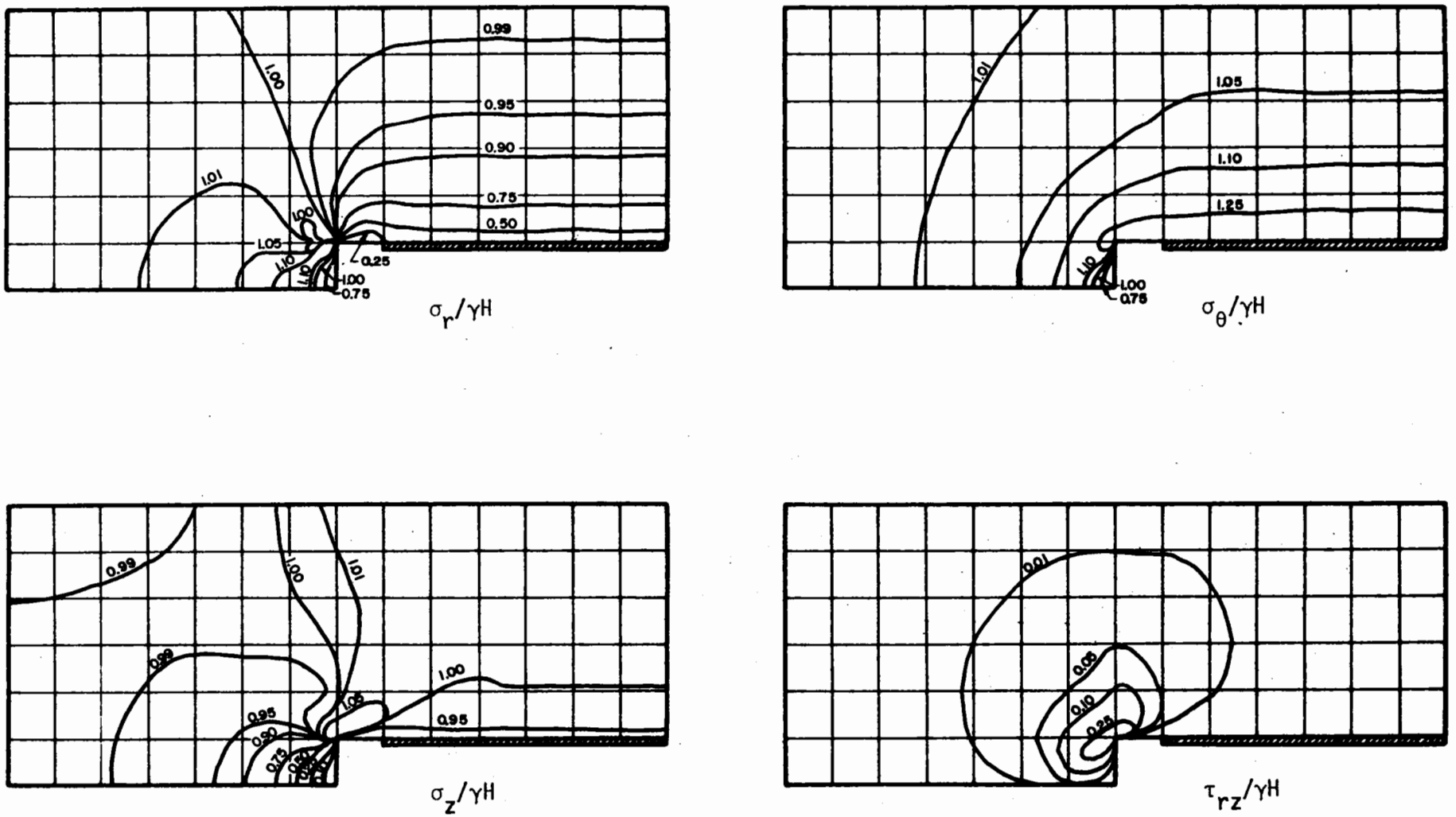

FIGURE 3.43 DISTRIBUTION OF STRESSES AROUND A PARTIALLY LINED TUNNEL IN AN ELASTO-PLASTIC MEDIUM - $\phi \neq 0$ (CASE LEP 4)

PLASTIC ZONE

The plastic zones that were obtained in these two analyses are shown in Fig. 3.41. For the fully lined tunnel only the soil in a small zone just ahead of the tunnel has yielded. The longitudinal extent of this zone does not exceed that observed for the unlined case. This is a departure from the trend indicated by the $\phi = 0$ elasto-plastic analyses. In those analyses the effect of the liner was to increase the magnitude of the stress difference ahead of the face such that the plastic zone extended farther ahead of the liner in the fully lined case than in the unlined case. Here the mean stress, in conjunction with the high angle of shearing resistance, has increased the shear strength of the soil ahead of the tunnel to such a degree that no additional plastic yielding occurs there.

When the liner was kept one radius behind the tunnel face the size of the plastic zone that developed was intermediate between those observed for the unlined and fully lined cases. Compare Figs. 3.41 and 3.18. Although plastic yielding occurred in a radial direction around the liner, it was confined to a relatively small region and had very little effect on the behavior of the tunnel.

SOIL STRESSES

Stresses in the soil surrounding the fully and partially lined tunnels are illustrated in Figs. 3.42 and 3.43, respectively, by normalized stress contours. It is apparent that these stress distributions are intermediate between those of the linear-elastic analyses (cases LLE1 and LLE2, Figs. 3.23 and 3.24) and the elasto-plastic, $\phi = 0$ analyses (cases LEP1 and LEP2, Figs. 3.33 and 3.34). The differences are due to the different amount

of plastic yielding that occurred in each case. Because there was very little plastic yielding in these last two analyses the resulting stress distributions resemble those from the elastic cases more closely than those from the elasto-plastic, $\phi = 0$ analyses.

Again, it should be recalled that the liner is so rigid with respect to the soil that once it is installed little, if any, further stress changes can occur in the soil around it. Thus, the differences in stresses behind the leading end of the liner in the linear-elastic and elasto-plastic, $\phi \neq 0$ analyses are due to the small amount of yielding that has occurred ahead of the liner in the latter analyses. These differences are not great.

SOIL DISPLACEMENTS

Soil displacements around the fully and partially lined tunnels are shown in Figs. 3.44 and 3.45, respectively. Figure 3.44 shows that for the fully lined tunnel the magnitudes of the net displacements and the radial components of displacement are larger than those observed in the linear-elastic analysis (Fig. 3.25), but smaller than those observed for the elasto-plastic, $\phi = 0$ analysis (Fig. 3.35) where the extent of plastic yielding was greater. A similar trend is indicated by the displacement distributions for the partially lined tunnel case, although here the displacement magnitudes are much closer to those of the linear-elastic case.

RADIAL DISPLACEMENTS

Radial displacements of the fully and partially lined tunnel openings are given in Figs. 3.46 and 3.47, respectively. In both cases the

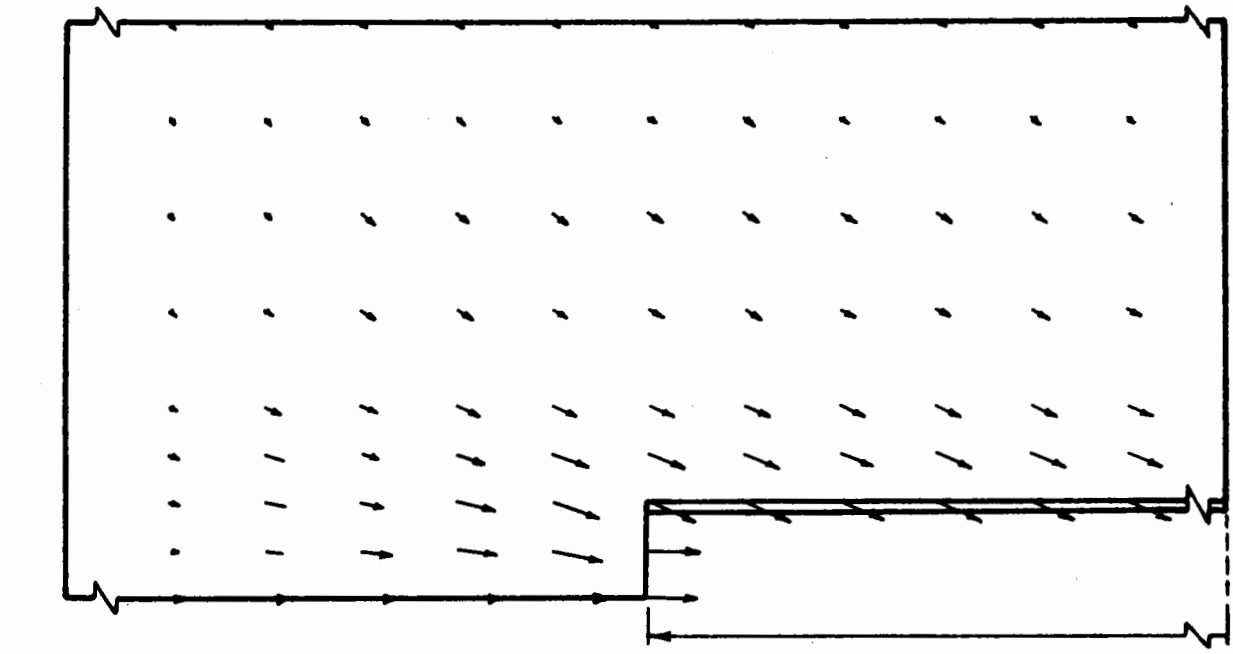

$\Delta = \frac{\delta}{a} \times 100$

$.050 \leq \Delta < .125$

$.125 \leq \Delta < .250$

$.250 \leq \Delta < .375$

$.375 \leq \Delta < .500$

$.500 \leq \Delta$

a) Total displacements

$\Delta < .050$ Not shown

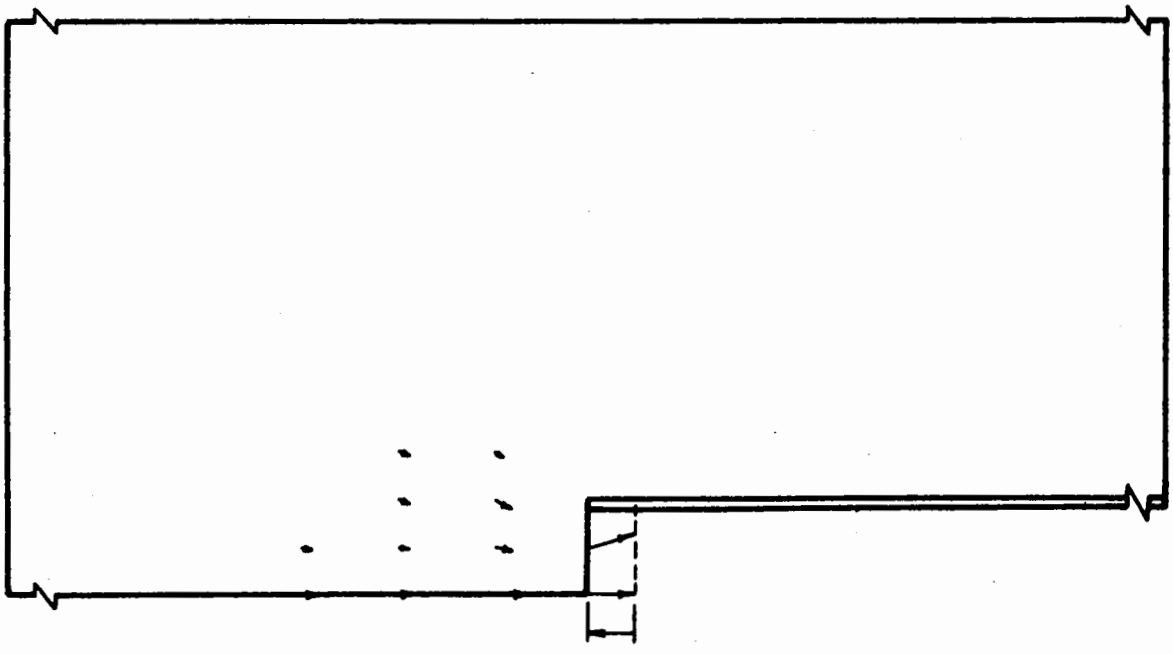

b) Incremental displacements

FIGURE 3.44 DISTRIBUTION OF DISPLACEMENTS AROUND A FULLY LINED TUNNEL IN AN ELASTO-PLASTIC MEDIUM - $\phi \neq 0$ (CASE LEP 3).

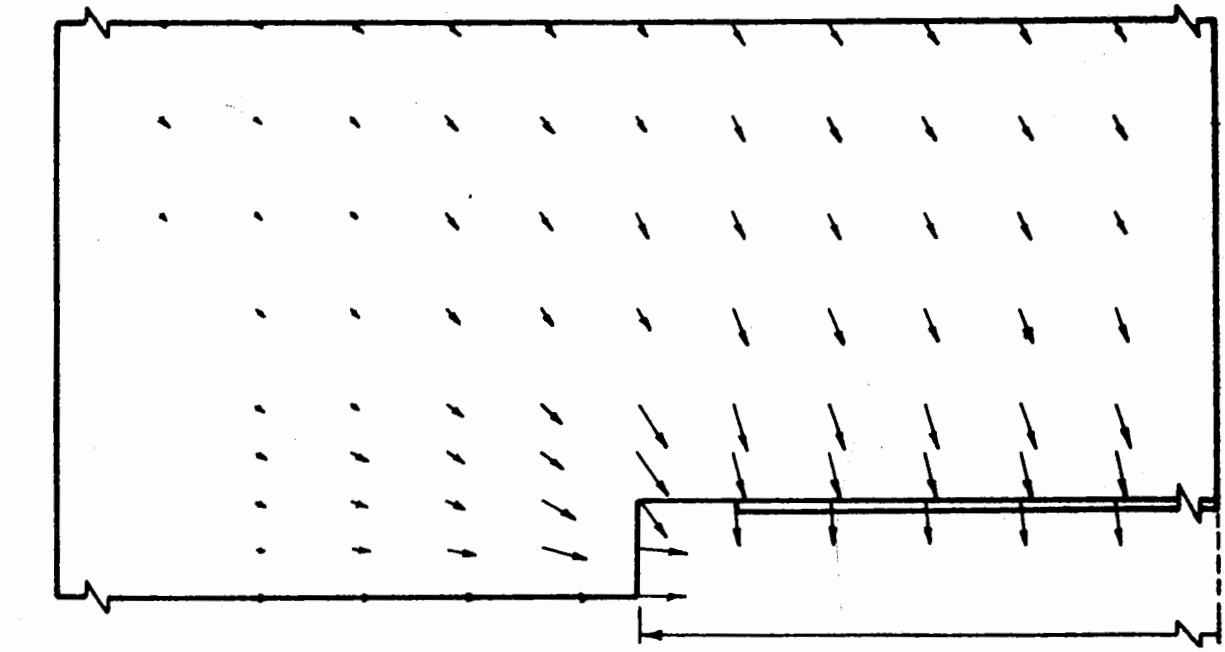

$\Delta = \frac{\delta}{a} \times 100$

- .050 ≤ Δ < .125
- .125 ≤ Δ < .250
- .250 ≤ Δ < .375
- .375 ≤ Δ < .500
- .500 ≤ Δ

a) Total displacements

Δ < .050 Not shown

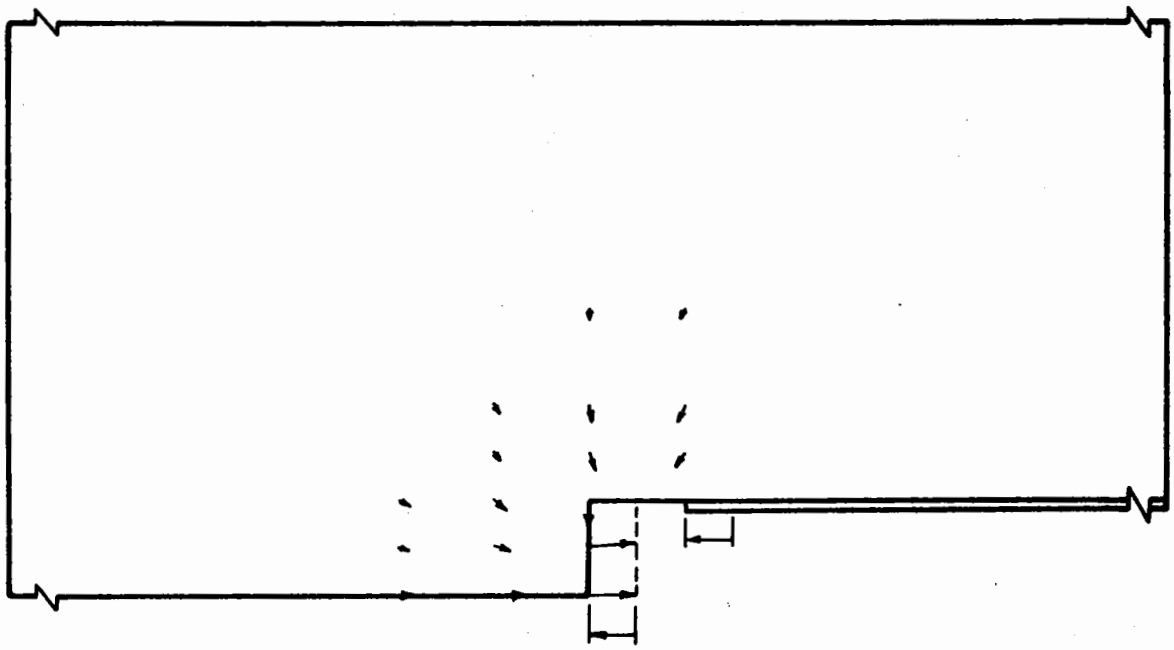

b) Incremental displacements

FIGURE 3.45 DISTRIBUTION OF DISPLACEMENTS AROUND A PARTIALLY LINED TUNNEL IN AN ELASTO-PLASTIC MEDIUM - $\phi \neq 0$ (CASE LEP 4).

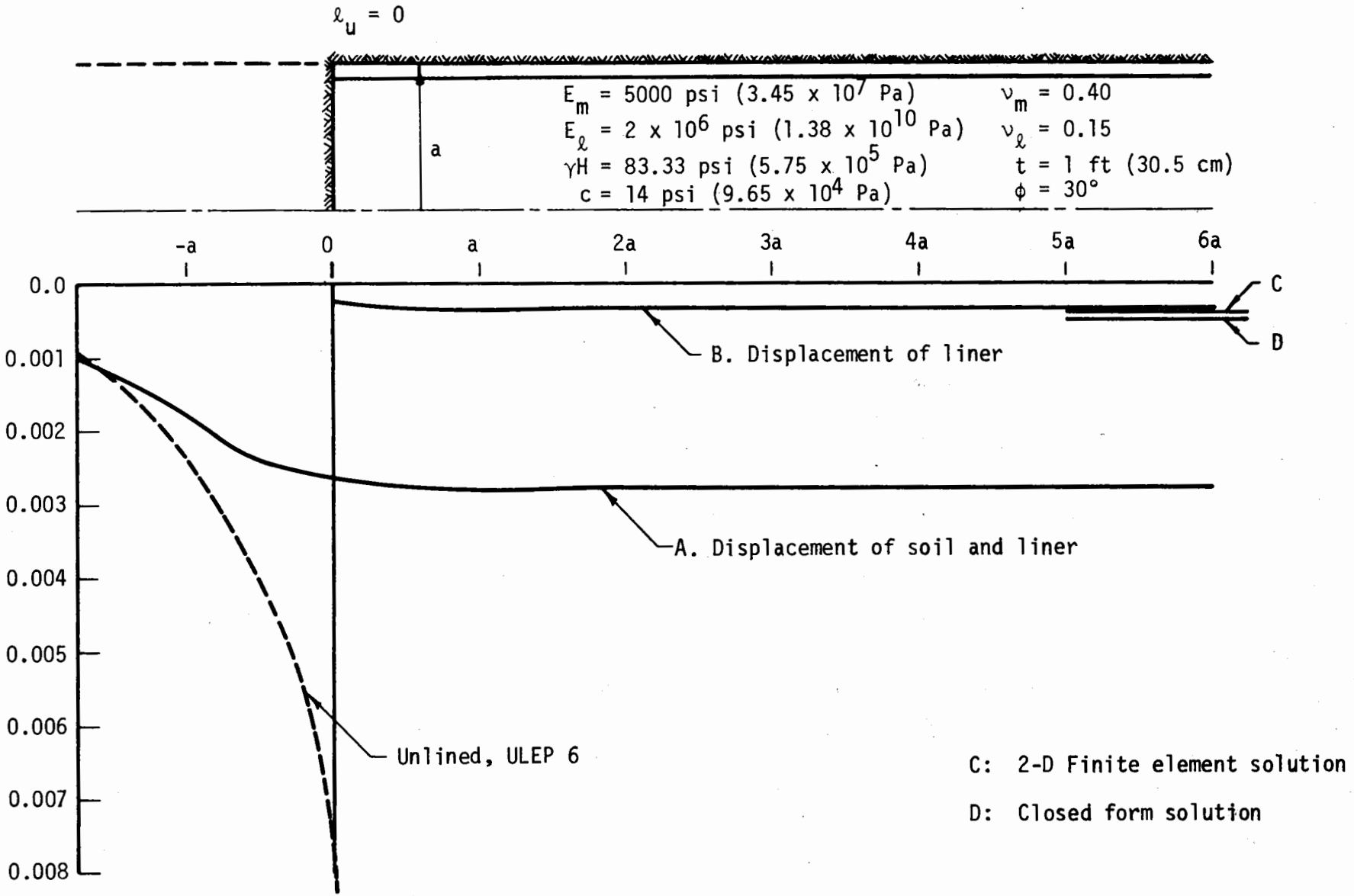

FIGURE 3.46 RADIAL DISPLACEMENTS FOR A FULLY LINED TUNNEL IN AN ELASTO-PLASTIC MEDIUM - $\phi \neq 0$ (CASE LEP 3).

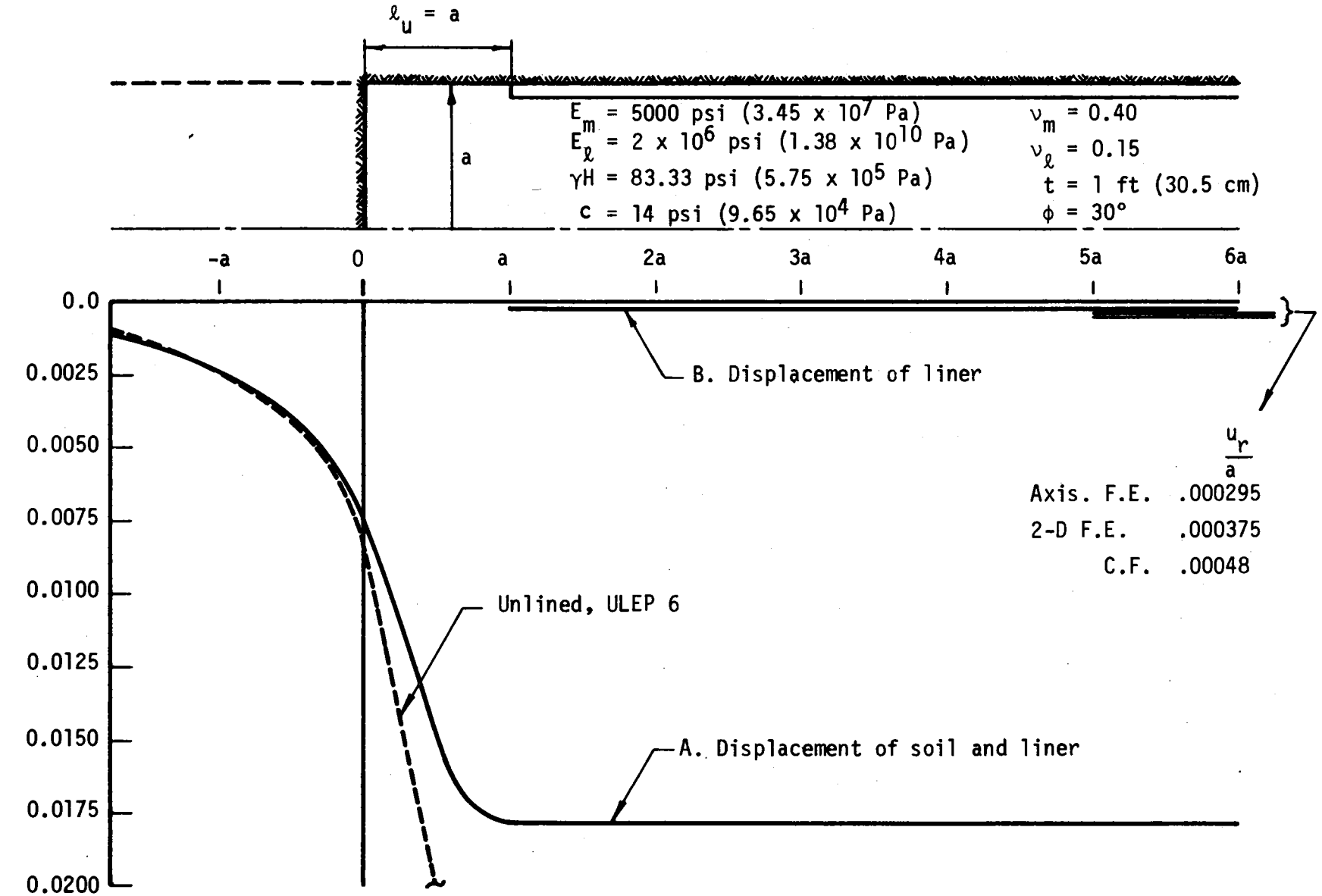

FIGURE 3.47 RADIAL DISPLACEMENTS FOR A PARTIALLY LINED TUNNEL IN AN ELASTO-PLASTIC MEDIUM - $\phi \neq 0$ (CASE LEP 4).

total displacements of the tunnel wall are slightly larger than those for the linear-elastic cases due to the increased displacements ahead of the liner arising from the small plastic zones that developed. However, the radial displacements of the liner in both cases are almost identical to those observed in the linear-elastic analyses.

LONGITUDINAL DISPLACEMENTS

Longitudinal displacements of a reference cross section that occur as the tunnel approaches are given in Fig. 3.48 for the fully and partially lined tunnels. Also shown for comparison are the corresponding displacements associated with the unlined tunnel in the same soil.

Figure 3.48 shows that for $z^*/a > 0.5$ the longitudinal displacements for the partially lined tunnel are less than those for the fully lined tunnel. This is a departure from the trend indicated by the previous analyses. Figures 3.29 and 3.39 show that the partially lined tunnel displacements, w, are everywhere greater than the fully lined tunnel displacements.

When the longitudinal displacement curves for the three fully lined tunnel analyses (linear-elastic, elasto-plastic - $\phi = 0$, elasto-plastic - $\phi \neq 0$) are considered together (Fig. 3.49a) it is clear that as the size of the plastic zone ahead of the tunnel increases the displacements at all z^* increase. The longitudinal displacements for case LEP3 ($Z' \simeq a/2$) are everywhere greater than those for case LLE1 (no plastic zone) and the displacements for case LEP1 ($Z' \simeq 2a$) are everywhere greater than those for case LEP3. For the partially lined tunnels a similar relationship holds only within the plastic zones (see $z^*/a = 0$, Fig. 3.49b). In the elastic regions beyond the plastic zones the longitudinal displacements from the elasto-plastic analyses

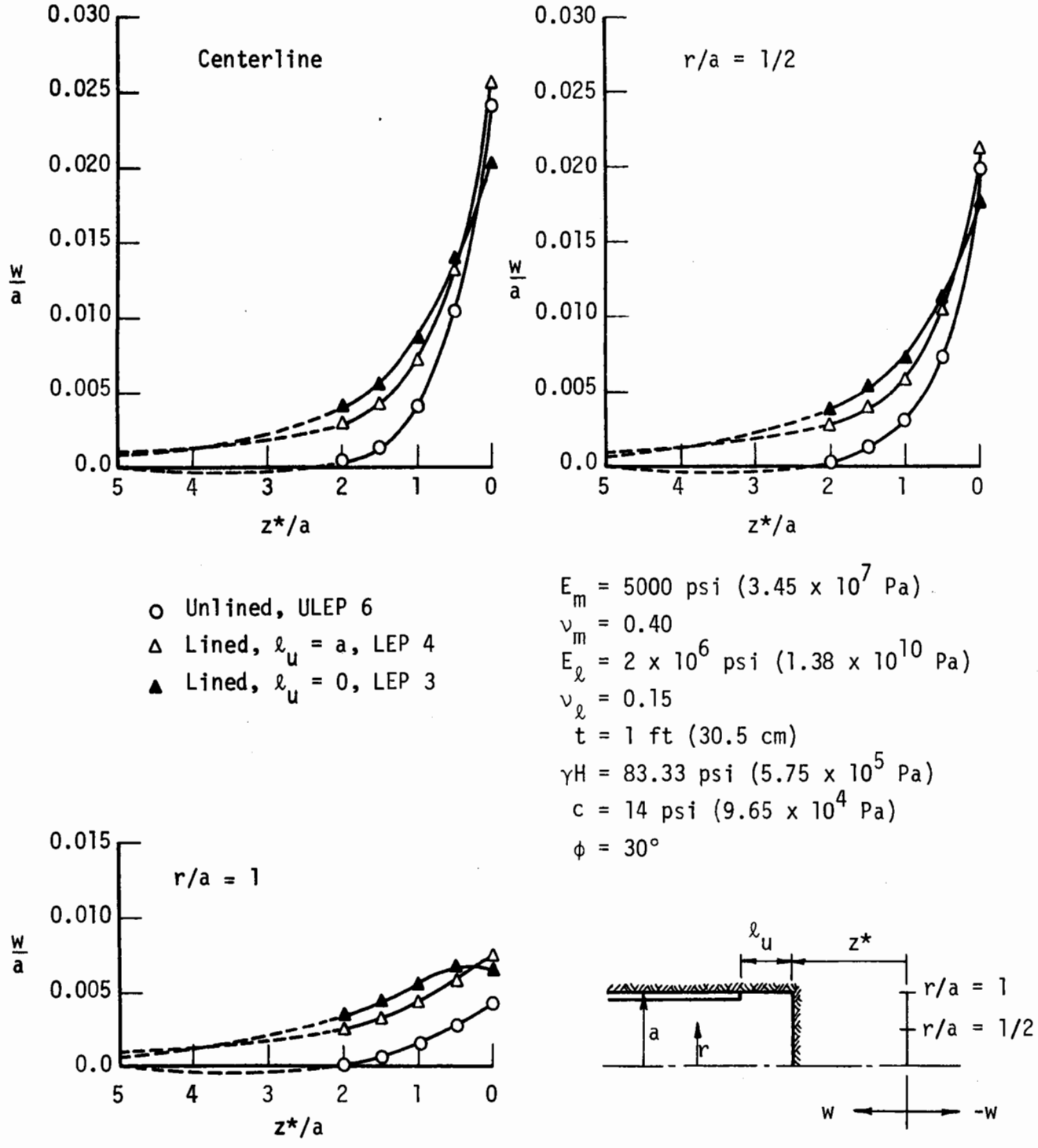

FIGURE 3.48 LONGITUDINAL DISPLACEMENTS ASSOCIATED WITH FULLY AND PARTIALLY LINED TUNNELS IN AN ELASTO-PLASTIC MEDIUM - $\phi \neq 0$.

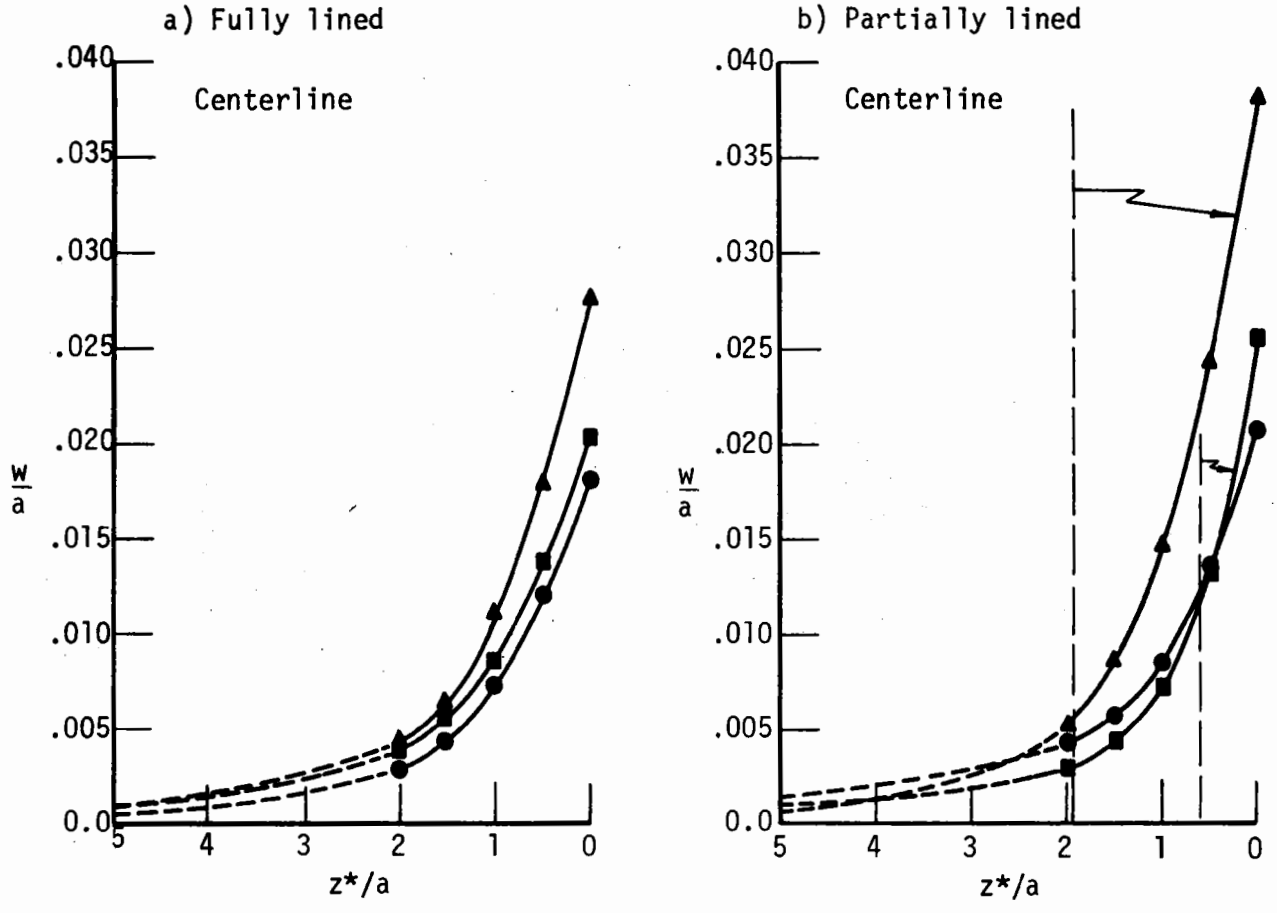

FIGURE 3.49 RELATIONSHIP BETWEEN LONGITUDINAL DISPLACEMENT CURVES FROM LINEAR-ELASTIC, ELASTO-PLASTIC - $\phi = 0$, AND ELASTO-PLASTIC - $\phi \neq 0$ ANALYSES

are smaller than the corresponding displacements from the linear-elastic analyses. In Fig. 3.48 the displacements, w, for the fully lined case are everywhere larger than in the linear-elastic analyses, whereas the displacements for the partially lined tunnel are smaller than in the linear-elastic analysis at all points $z^* \geq a/2$. Thus, the small plastic zones that resulted in these two cases contributed to a shift of the displacement curves such that for $z^* \geq a/2$ the longitudinal displacements for the fully lined tunnel are greater than those for the partially lined tunnel.

LINER THRUST

The longitudinal distributions of liner thrust for the fully and partially lined tunnels in an elasto-plastic, $\phi \neq 0$ medium are given in Fig. 3.50.

The thrust distributions in Fig. 3.50 are almost identical to those obtained from the linear-elastic analyses, Fig. 3.30. Apparently, the small amount of plastic yielding that occurred ahead of these liners was not sufficient to appreciably alter the liner forces.

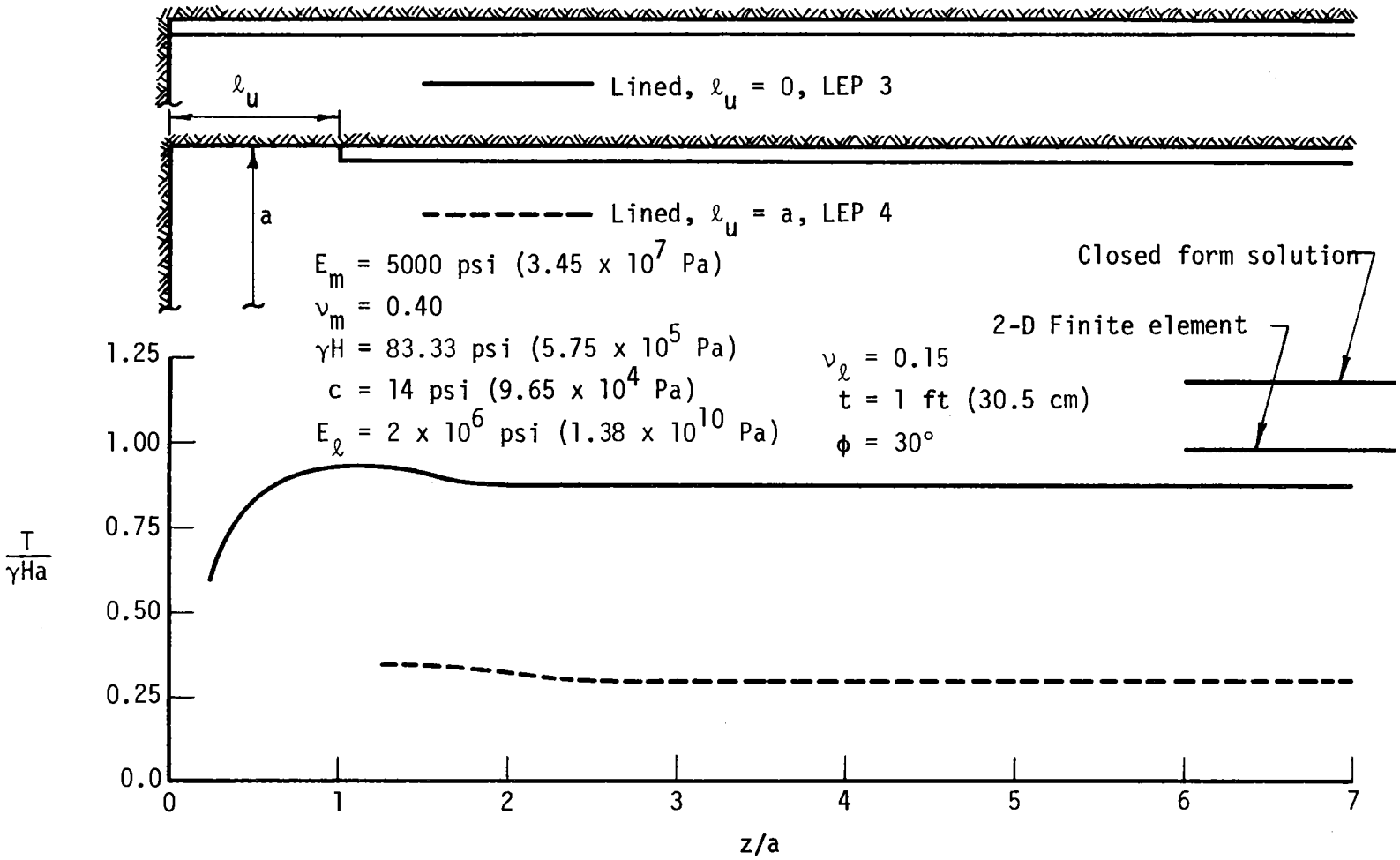

FIGURE 3.50 LINER THRUST FOR FULLY AND PARTIALLY LINED TUNNELS IN AN ELASTO-PLASTIC MEDIUM - $\phi \neq 0$.

CHAPTER 4

DISCUSSION OF RESULTS AND METHODS OF ANALYSIS

4.1 GENERAL

One of the most significant points illustrated by the analyses performed is the relationship between the ground displacements occurring ahead of a tunnel liner and the magnitude of the liner forces. It is evident from a comparison of the completely and partially lined tunnel analyses that such a relationship exists and that liner behavior is thus a function of position of liner installation as well as of the properties of the soil and liner. This relationship is further clarified in this chapter. In addition, certain two- and three-dimensional methods of tunnel analysis are examined with respect to the results presented in Chapter 3 and their applicability to the advancing tunnel problem is evaluated.

4.2 GROUND DISPLACEMENTS AND PRESSURES ACTING ON TUNNEL LINERS

In general, there are three main types of ground loading or ground pressure to which a tunnel lining may be subjected. These are the following:

a) Swelling pressure is the pressure that builds up due to swelling of the ground surrounding the liner. It is associated with an increase in water content of the ground and may or may not occur in conjunction with the formation of a plastic zone. The magnitude of this pressure depends on the properties of the ground mass, the time of liner installation and the stiffness of the liner. This

pressure may be several times the magnitude of the in situ stresses.

b) True ground pressure results when the liner is installed before all of the radial displacements of the tunnel opening at the point of installation have ceased. The magnitude of this pressure can range from the full mangitude of the in situ stresses, if a rigid liner is installed prior to any displacements of the ground, to zero, if the liner is installed after all displacements have occurred.

c) Loosening pressure is a local pressure on the roof (crown) of the tunnel due to the weight of material that has loosened and come to rest on the liner. The magnitude of this pressure is not directly related to the in situ stress field.

Thus far in this investigation only the true ground pressure has been considered. For a given ground mass and tunnel lining combination the magnitude of this pressure depends on the stress-strain-time properties of the ground mass, the in situ stress field, the properties of the liner (stiffness), and the method and details of construction.

Initial ground pressures (following construction) are strongly influenced by the construction procedures, whereas the long term or final pressures, if significantly different from the initial values, are more a function of the time-dependent behavior of the ground mass. This is illustrated in Figs. 4.1 and 4.2.

Consider first a continuous ground mass that does not exhibit

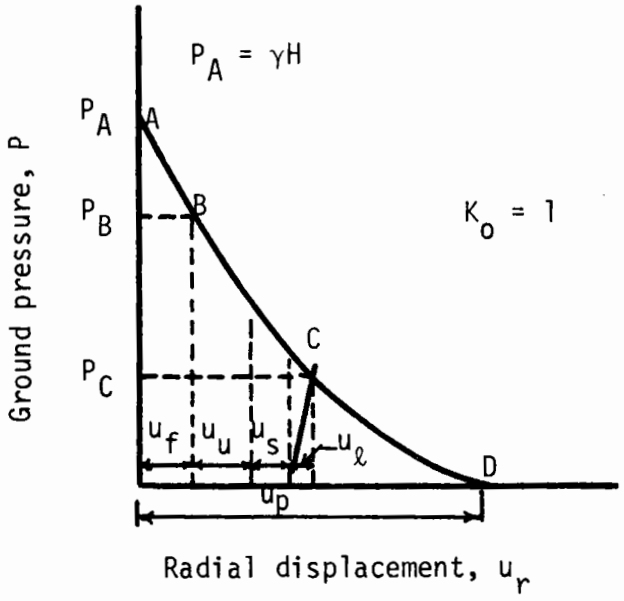

FIGURE 4.1 CONCEPTUAL GROUND REACTION CURVE FOR TIME-INDEPENDENT GROUND MASS

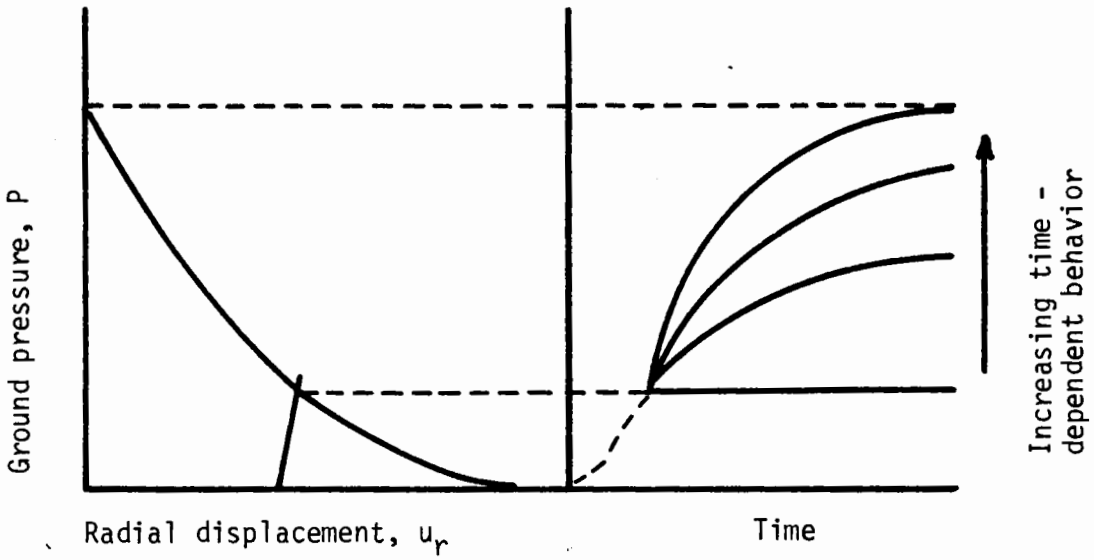

FIGURE 4.2 CONCEPTUAL GROUND REACTION CURVE AND EFFECT OF TIME - TIME-DEPENDENT GROUND MASS (Modified from Peck [16])

time-dependent behavior and that remains continuous after excavation. The ground reaction curve, AD, [5,16] in Fig. 4.1 illustrates the relationship between true ground pressure and radial ground displacement for a $K_o = 1$ in situ stress field. Curve AD, shown here for non-linear behavior, is a function of the stress-strain properties of the ground mass. This curve would be a straight line if the ground mass was linear-elastic. If no ground displacements are allowed before a perfectly rigid liner is placed in contact with the ground the resulting ground pressure is P_A, equal to the full magnitude of the in situ stresses (here taken as the weight of the overburden, γH). The condition of no prior displacements is rarely, if ever, satisfied because there is almost always some displacement that occurs ahead of the tunnel face. In Fig. 4.1 this displacement has been designated u_f. Thus, if a perfectly rigid liner is installed right at the face the ground pressure will be $P_B < P_A$. The general case is indicated by point C, the intersection of the ground reaction curve and the liner reaction curve. This corresponds to a less than perfectly rigid liner that is installed some distance behind the face such that a small gap is left between it and the ground. The total radial displacement that occurs before ground-liner equilibrium is reached is $u_f + u_u + u_g + u_\ell$, where

u_f = radial displacement occurring ahead of the face

u_u = radial displacement occurring between the face and the point of installation

u_g = radial displacement occurring at the point of installation before the gap is filled

u_ℓ = radial displacement of the liner under load.

The ground pressure decreases as the ratio $(u_f + u_u + u_g + u_\ell)/u_p$ increases from zero to one. If $u_f + u_u + u_g = u_p$ the liner carries no load.

If the ground mass exhibits time-dependent behavior the ground reaction curve will be of a similar form to that of Fig. 4.1, but the initial ground pressure will increase with time as illustrated in Fig. 4.2. For some soils the ground pressure may increase to a magnitude equal to the full overburden pressure, γH.

4.3 TWO DIMENSIONAL ANALYSES

It is clear from Fig. 4.1 and the results of the lined tunnel analyses in Chapter 3 that the methods and details of construction, principally the position of liner installation relative to the face, can strongly influence the magnitude of the initial true ground pressure. One of the primary advantages of the three-dimensional finite element analysis is its ability to account for these factors. Likewise, the primary disadvantage of certain two-dimensional solution methods is their inability to account for these factors.

4.3.1 FINITE ELEMENT METHOD

In Chapter 3 the liner thrusts and displacements obtained from the finite element analyses of an advancing tunnel were compared to the corresponding values predicted by finite element and closed-form two-dimensional solution methods. It was found that the two-dimensional methods consistently overestimated liner thrust and displacement. This resulted because these methods could not account for the ground displacements occurring prior to ground-liner contact (u_f, u_u, u_g).

The linear-elastic two-dimensional finite element solution method

yielded values that compared favorably with the fully lined tunnel cases because the two analyses differed only by the displacement, u_f, occurring ahead of the tunnel face. The same two-dimensional solution considerably overestimated liner thrust and displacement for the partially lined tunnel cases because the two methods differed by the increased radial displacement, $u_f + u_u$. This is illustrated in Fig. 4.3. It is clear that, while it may be only slightly in error for the special case of a tunnel lined right up to the face, the standard two-dimensional finite element solution cannot yield correct results. This is especially true if elasto-plastic behavior of the ground mass is to be considered since the liner, in initial contact with the ground, will inhibit formation of the plastic zone.

It should be noted that the potential exists for modifying the standard two-dimensional finite element analysis to at least partially account for the displacements occurring before ground-liner contact. Special finite elements, known as joint elements [2,9], could be inserted in the mesh between the liner and ground elements as shown in Fig. 4.4. By correctly specifying joint element behavior--little or no resistance to a predetermined amount of radial displacement--the displacements u_f, u_u and u_g could be included in the analysis. The difficulty with this procedure is, of course, determining the magnitude of the u_f and u_u displacements without the aid of a three-dimensional analysis.

4.3.2 CLOSED FORM SOLUTION

The Burns and Richard [4] closed form solution when applied to a lined tunnel, while suffering from the same shortcomings as the

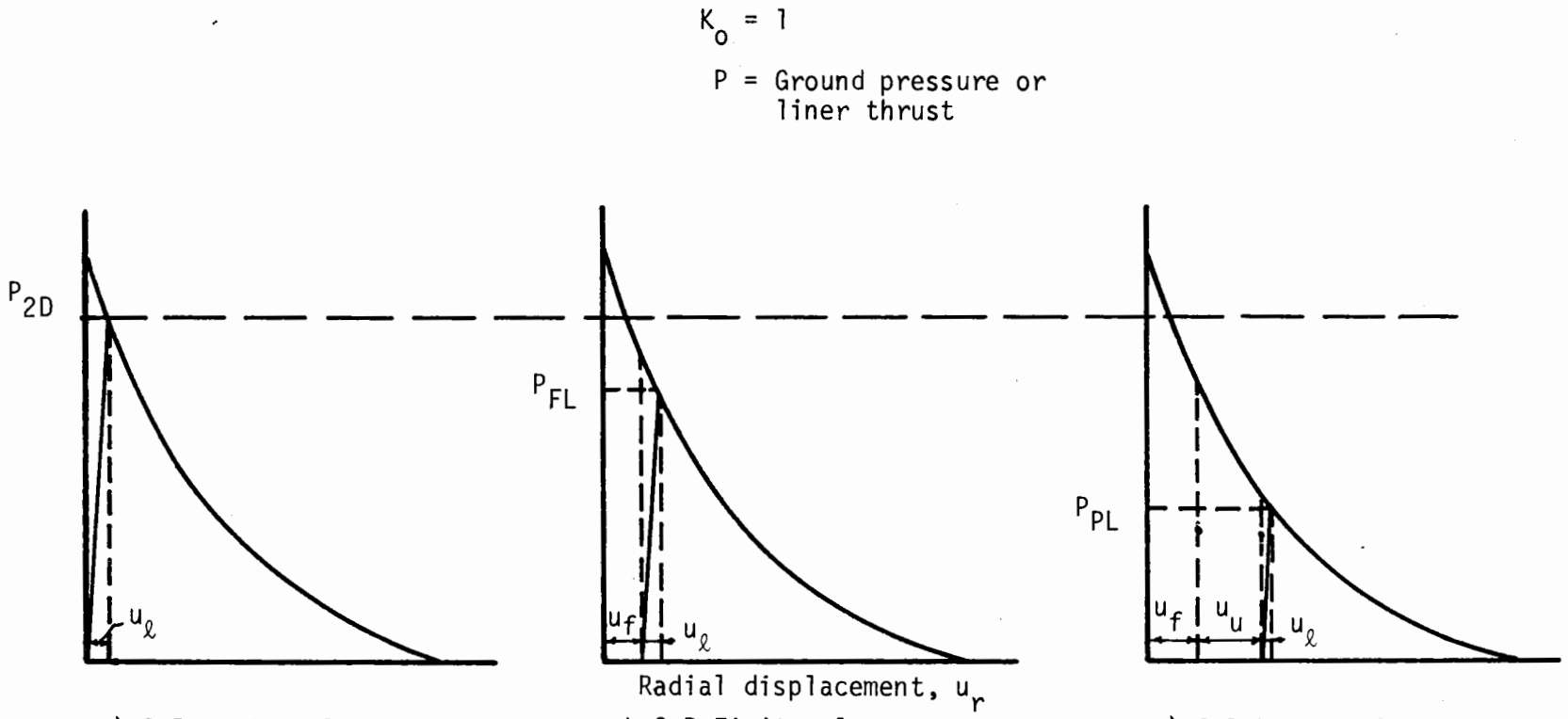

FIGURE 4.3 RADIAL DISPLACEMENTS CONSIDERED BY TWO- AND THREE-DIMENSIONAL FINITE ELEMENT ANALYSES AND RESULTING GROUND PRESSURES

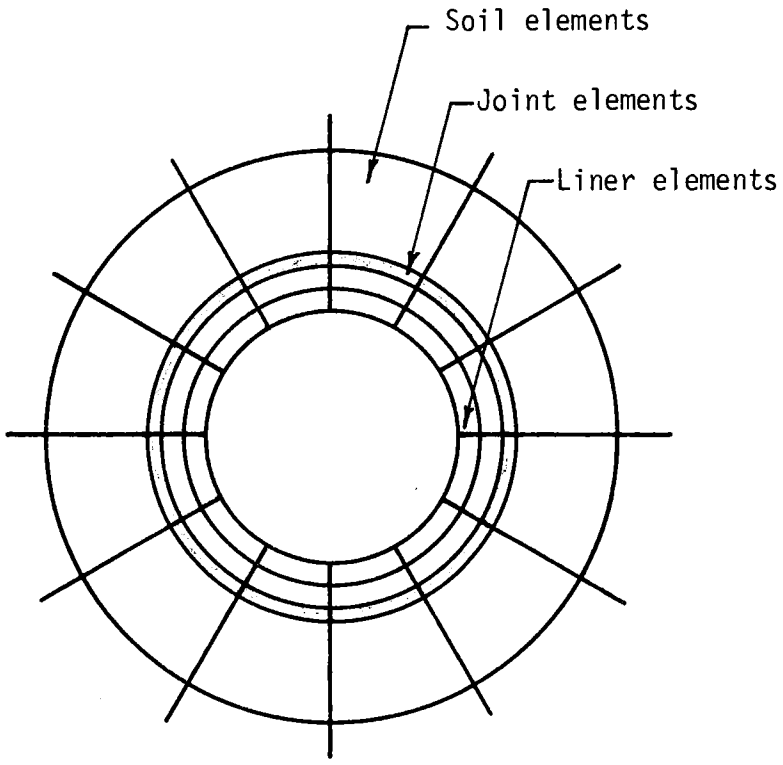

FIGURE 4.4 TWO-DIMENSIONAL FINITE ELEMENT MESH WITH JOINT ELEMENTS

two-dimensional finite element solution, is even less applicable to the problem of an advancing tunnel because the boundary conditions apply to a different problem. This two-dimensional, linear-elastic solution was derived in order to investigate the problem of a tunnel liner (underground protective structure) buried in a ground mass which is subsequently loaded by a vertical surface pressure such as from a nuclear blast. Stresses in the ground-liner system due to the in situ stress field were not considered. The boundary conditions assumed in the derivation of this solution are illustrated in Fig. 4.5 along with those for the standard two-dimensional analysis of a tunnel liner loaded by the natural ground stresses. It can be seen that whereas a tunnel under construction is advanced through an already stressed medium, the closed form solution assumes the tunnel to be in place before any stress is applied.

The Burns and Richard equations were later modified [12,15,17] to eliminate the one-dimensional loading restriction ($K = \nu_m/(1 - \nu_m)$) and applied to tunnel liners subjected to loading by the weight of the overburden ($\sigma_v = \gamma H$, $\sigma_h = K_o \gamma H$, K_o independent of ν_m). However, the problem with the boundary conditions still remains.

In the course of this investigation the modified Burns and Richard equations [15] were used to estimate liner thrust and displacements for $K_o = 1$ (see liner thrust and displacement plots in Chapter 3). The closed form solution consists of two sets of equations. One set applies to the conditions of no circumferential slippage at the ground liner contact, while the second set applies to the condition of full slippage at the contact. However, for $K_o = 1$ both sets of equations reduce to the same expressions.

a) Burns and Richard's boundary conditions

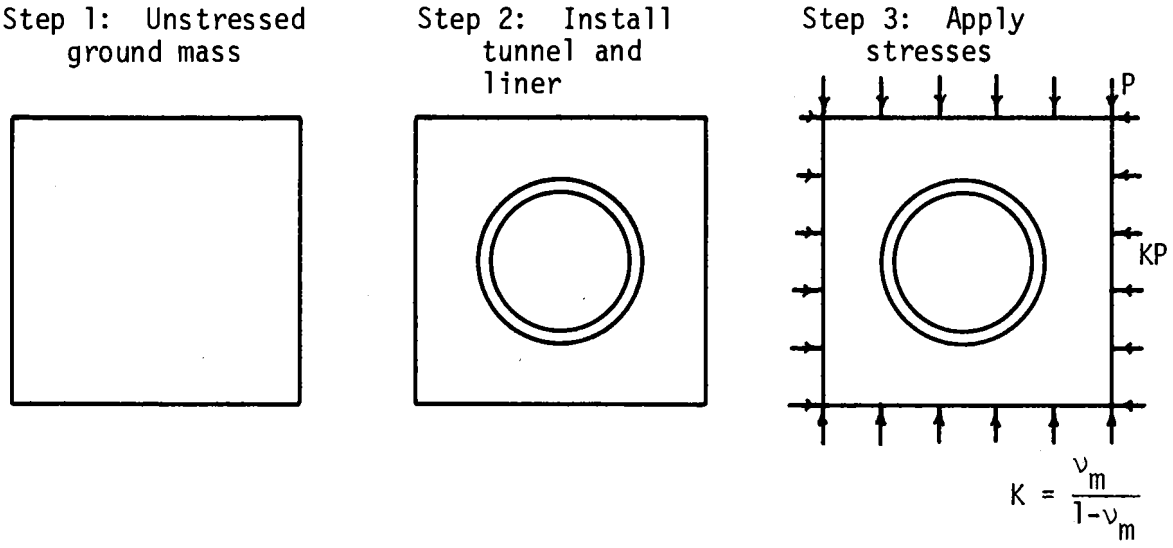

b) Correct boundary conditions for tunnel (finite element analysis)

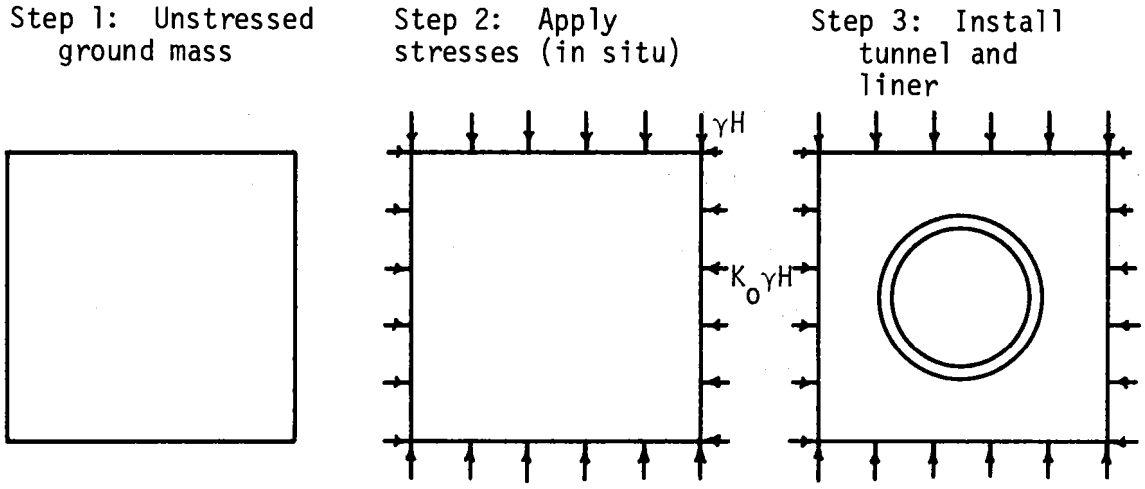

FIGURE 4.5 COMPARISON OF BOUNDARY CONDITIONS FOR THE a) BURNS AND RICHARD AND b) FINITE ELEMENT SOLUTIONS

Thrust coefficient:

$$T/\gamma Ha = 1 - b_1, \tag{4.1}$$

Radial displacement coefficient:

$$\frac{u_r/a}{\gamma H/M_c} = (1 - \nu_m)(1 - b_1)\, C \tag{4.2}$$

where,

$$b_1 = \frac{(1 - 2\nu_m)(C - 1)}{(1 - 2\nu_m)(C) + 1} \tag{4.3}$$

$$C = \frac{\dfrac{E_m}{(1 + \nu_m)(1 - 2\nu_m)}}{\dfrac{E_\ell}{(1-\nu_\ell^2)} \quad \dfrac{t}{a}} \tag{4.4}$$

To illustrate the effect that the difference in boundary conditions has, the thrust and displacement coefficients, as calculated by the closed form solution and the two-dimensional finite element method, have been plotted as functions of the compressibility ratio, C, and Poisson's ratio, ν_m, in Figs. 4.6 and 4.7, respectively. It is evident that the closed form solution consistently gives thrust and displacement values in excess of those predicted by the already conservative two-dimensional finite element solution.

4.4 THREE-DIMENSIONAL ANALYSES

Three-dimensional finite element analyses, of which the axi symmetric is a special case, allow a more complete treatment of the advancing tunnel

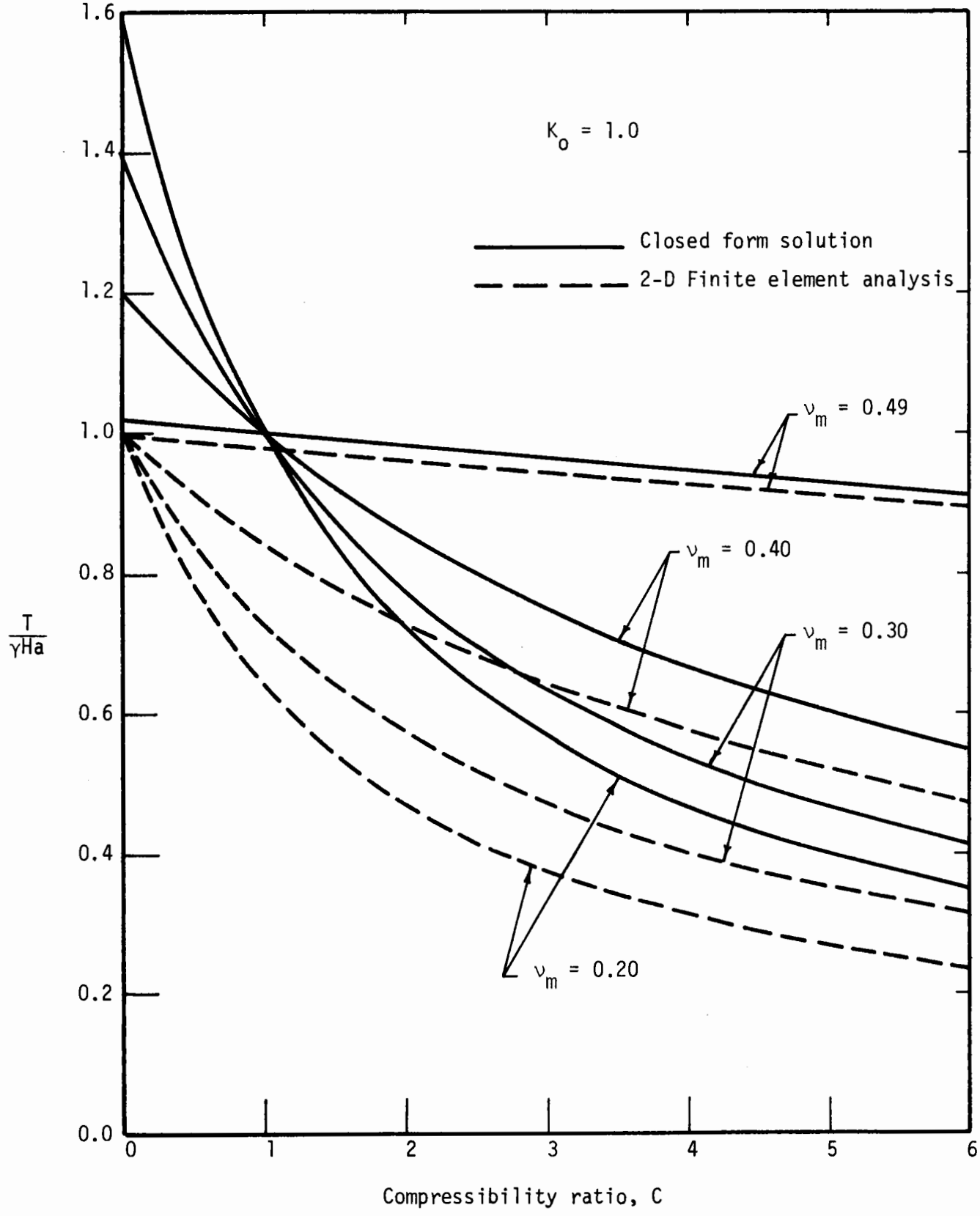

FIGURE 4.6 VALUES OF THRUST COEFFICIENT AS GIVEN BY CLOSED FORM AND FINITE ELEMENT TWO-DIMENSIONAL, LINEAR-ELASTIC SOLUTIONS

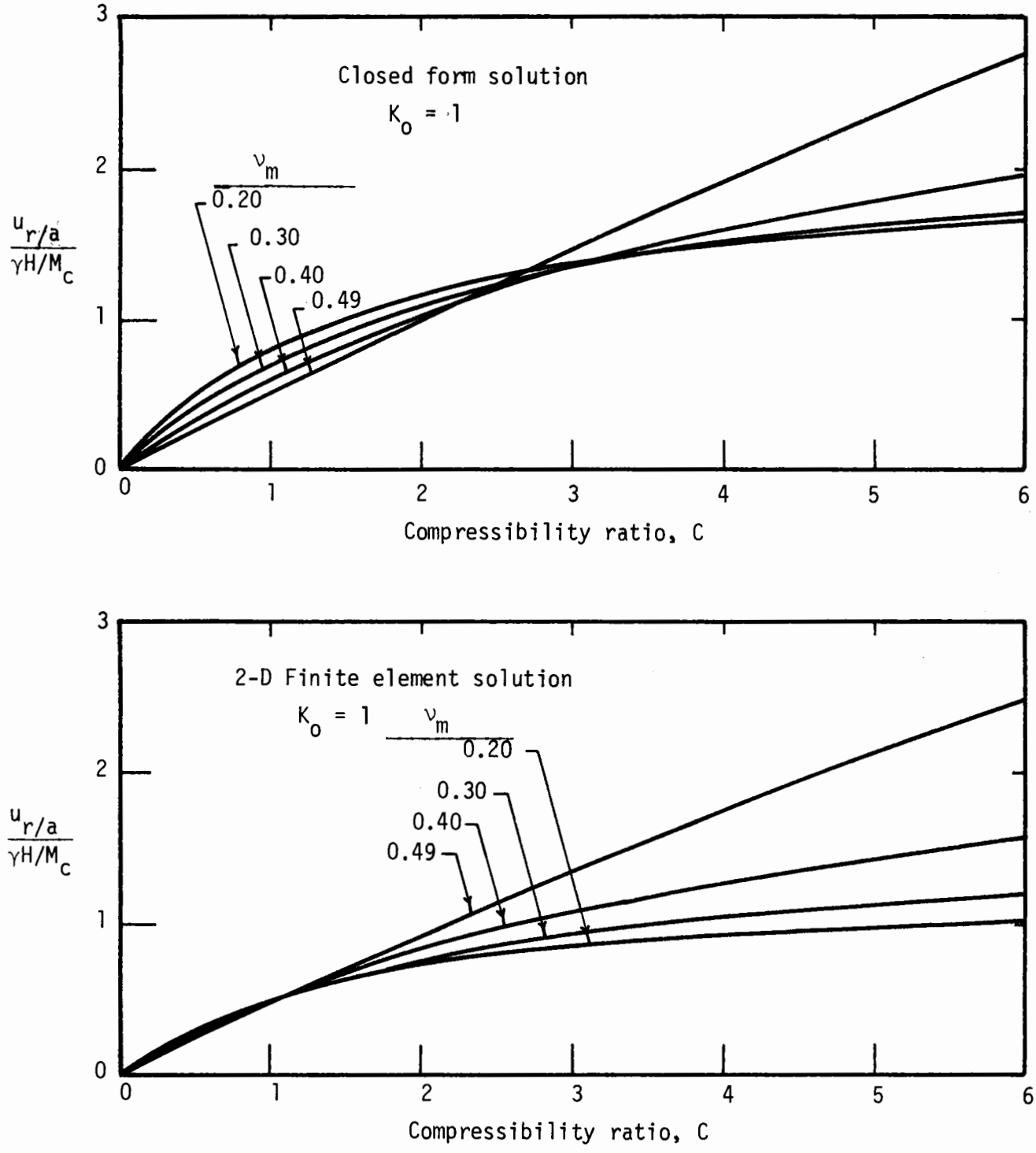

FIGURE 4.7 VALUES OF RADIAL DISPLACEMENT COEFFICIENT AS GIVEN BY CLOSED FORM AND FINITE ELEMENT TWO-DIMENSIONAL, LINEAR-ELASTIC SOLUTIONS

problem than is possible with the above two-dimensional methods. However, as was learned during the course of this investigation, simply expanding the analysis to three dimensions is not sufficient, especially if lined tunnels are to be considered. Also important are such factors as simulation of the advancement of the tunnel and, in certain cases, the details of excavation and liner installation (construction details).

4.4.1 EXCAVATION SEQUENCE

In the analysis of a lined tunnel simulation of the physical advancement of the tunnel through the ground mass is just as important as consideration of the three-dimensional geometry. This point was clearly demonstrated when two additional analyses of the lined tunnel case LLE2 (partially lined tunnel) were made without using the standard excavation sequence adopted for all other analyses. In the first such analysis, no excavation simulation was used at all. The finite element mesh was generated with the tunnel and liner in place before the boundary stresses were applied. In the second analysis the entire tunnel was "excavated" in one step and at the same time the full length of liner was inserted. This occurred after the boundary stresses had been applied to the mesh. The resulting distributions of liner thrust for these two analyses are given in Fig. 4.8 along with the distribution obtained when the full excavation sequence was used. This figure shows that while all three analyses give an indication of the longitudinal variation (3-D distribution for the general 3-D analysis) of liner thrust, none of the three is close to being in agreement with the other two in terms of thrust magnitude. The situation becomes

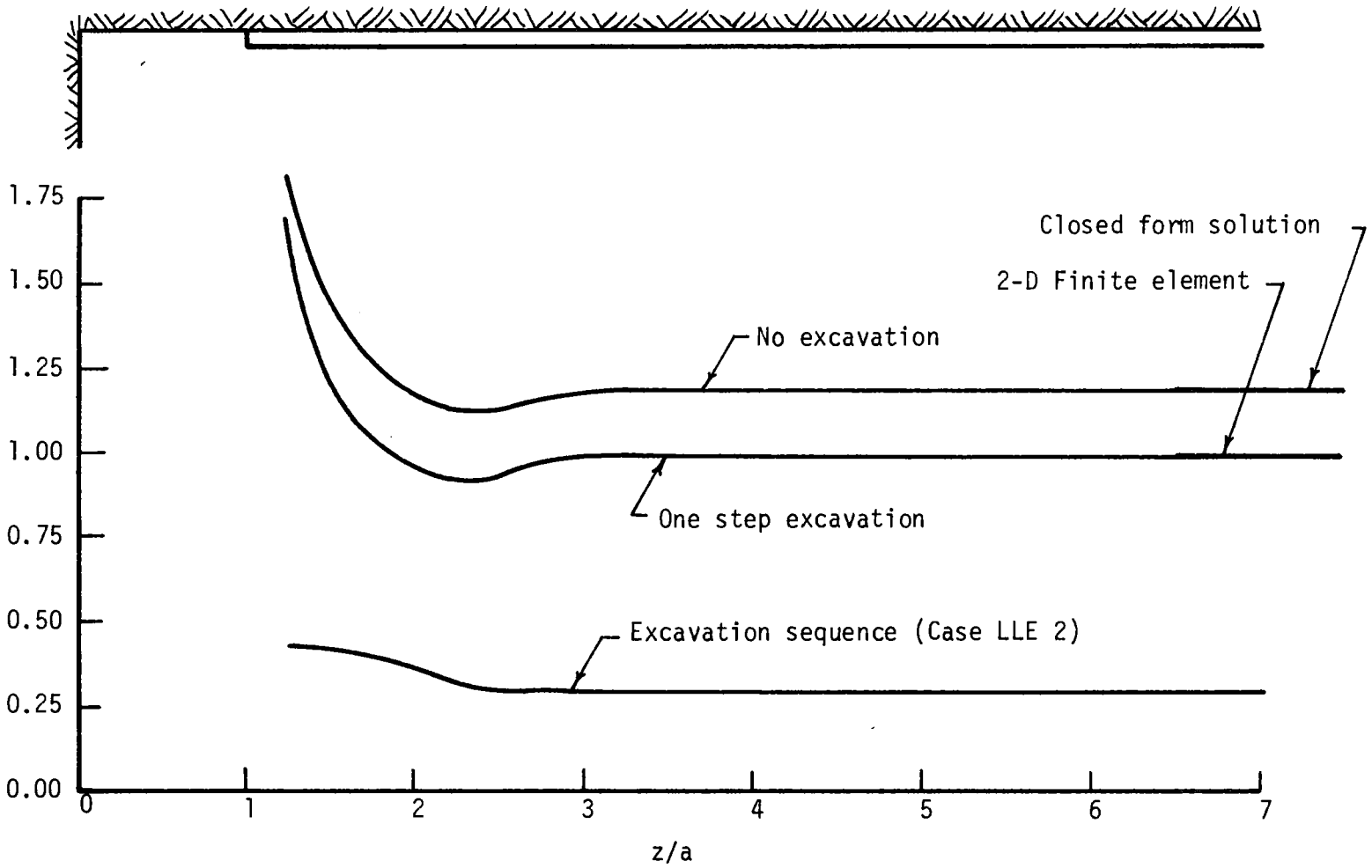

FIGURE 4.8 LINER THRUST DISTRIBUTIONS OBTAINED WHEN NO EXCAVATION, ONE STEP EXCAVATION AND FULL EXCAVATION SEQUENCE ARE USED

even worse if elasto-plastic behavior of the ground mass is to be considered because, as in the two-dimensional analyses, the full extent of plastic yielding is prevented by the liner.

It appears that the altered stress zone ahead of the tunnel is of major significance to tunnel behavior. It is only the analysis that correctly simulates the advancement of the tunnel through this zone that gives correct results.

By comparing thrust magnitudes at points far behind the face with the values given by the two-dimensional analysis it is seen that when no excavation sequence is used, the three-dimensional analysis corresponds to the two-dimensional closed form solution. Also, a three-dimensional analysis using one-step excavation corresponds to the two-dimensional finite element analysis. It seems clear that unless excavation simulation is used many of the advantages of the three-dimensional analysis are lost.

It should be pointed out that excavation simulation is less significant in the analysis of unlined tunnels. For such cases the analyses that simulate formation of the entire tunnel in one excavation step give results nearly identical to those obtained when the full excavation sequence is used. However, if the finite element mesh is generated with the tunnel already in place, the distribution of ground stresses obtained is correct, but the displacements are not. The displacement at a given point is off by an amount equal to the displacement that would occur at that point, due to application of the in situ stresses, had the tunnel not been present. These "initial" displacement values can be calculated or obtained from other parts of the mesh far from the tunnel and subtracted from the total displacements to get the correct results.

4.4.2 CONSTRUCTION DETAILS

Most soft ground tunnels are constructed with the aid of a tunneling shield behind or within which the lining is assembled and then installed. The following two examples indicate that the shield and the method of liner installation, in the way that they affect radial ground displacements, are important to liner performance.

As mentioned in Chapter 1, Ward [18] and Muir Wood [13] published displacement data for two tunnels in London Clay. Both tunnels were constructed in a similar manner, by assembling a segmented liner within the tail piece of a tunneling shield. To analyze these tunnels in order to estimate their short term behavior it might be assumed, as a first approximation, that the shield acts to support the ground between the face and the liner and that, in effect, the tunnel is lined all the way to the face. To determine if this was a reasonable assumption for these two tunnels the radial displacements obtained from the various finite element analyses were compared to those measured for the real tunnels. Rather than make additional analyses to specifically model these two cases, since all that was required was a comparison of the general trends of the radial displacement data, the finite element data already available was adjusted to correspond to the estimated ground conditions, depth and size of the real tunnels. Elastic modulus values (initial tangent modulus) were estimated on the basis of published data for London Clay [19]. The available data on the shear strength of the clay indicated that, at the depths considered, very little, if any, plastic yielding of the clay should have occurred. The scaling was not exact because

differences in K_o values and liner properties were not considered, but it was sufficient to indicate the important features of the measured data.

The comparison with Ward's data [18] is shown in Fig. 4.9. None of the displacement distributions from the lined tunnel analyses could be made to fit the measured data unless an unreasonably low modulus was assumed for the clay. Instead, it was found that the best agreement was obtained with the displacements from the unlined tunnel analyses (broken and dashed curves). this is not too surprising when the stiff nature of the London Clay, the details of the shield and the method of liner installation are considered. The shield was fabricated with a bead 9 in. long by 0.5 in. thick (23 cm x 1.3 cm) around the upper 300 degrees of its cutting edge. In addition, the cast iron liner was normally assembled within the shield, leaving a 1.5 in. (3.8 cm) gap between the lining and the clay when the shield advanced. This void was filled with cement grout soon after the shield advanced.

The measured displacements given in Fig. 4.9 are for a point 1.6 ft (49 cm) outside the tunnel springline, but they clearly show the effects of these construction details. The first radial displacements occur about one tunnel diameter ahead of the face, but they remain small (u_f) until the bead on the shield passes, whereupon they almost double as the clay moves into the void behind the bead. The restraining effect of the shield on the displacements is clearly indicated, but it is also apparent that the shield only delays and does not prevent further displacement (u_u). Figure 4.9 shows that as the tail of the shield passes, the clay begins to move again, this time into the gap left by the skin of the shield (u_g). It appears that these additional displacements occur either before the grout is injected or before it has had time to set. Once the grout does set the liner becomes effective

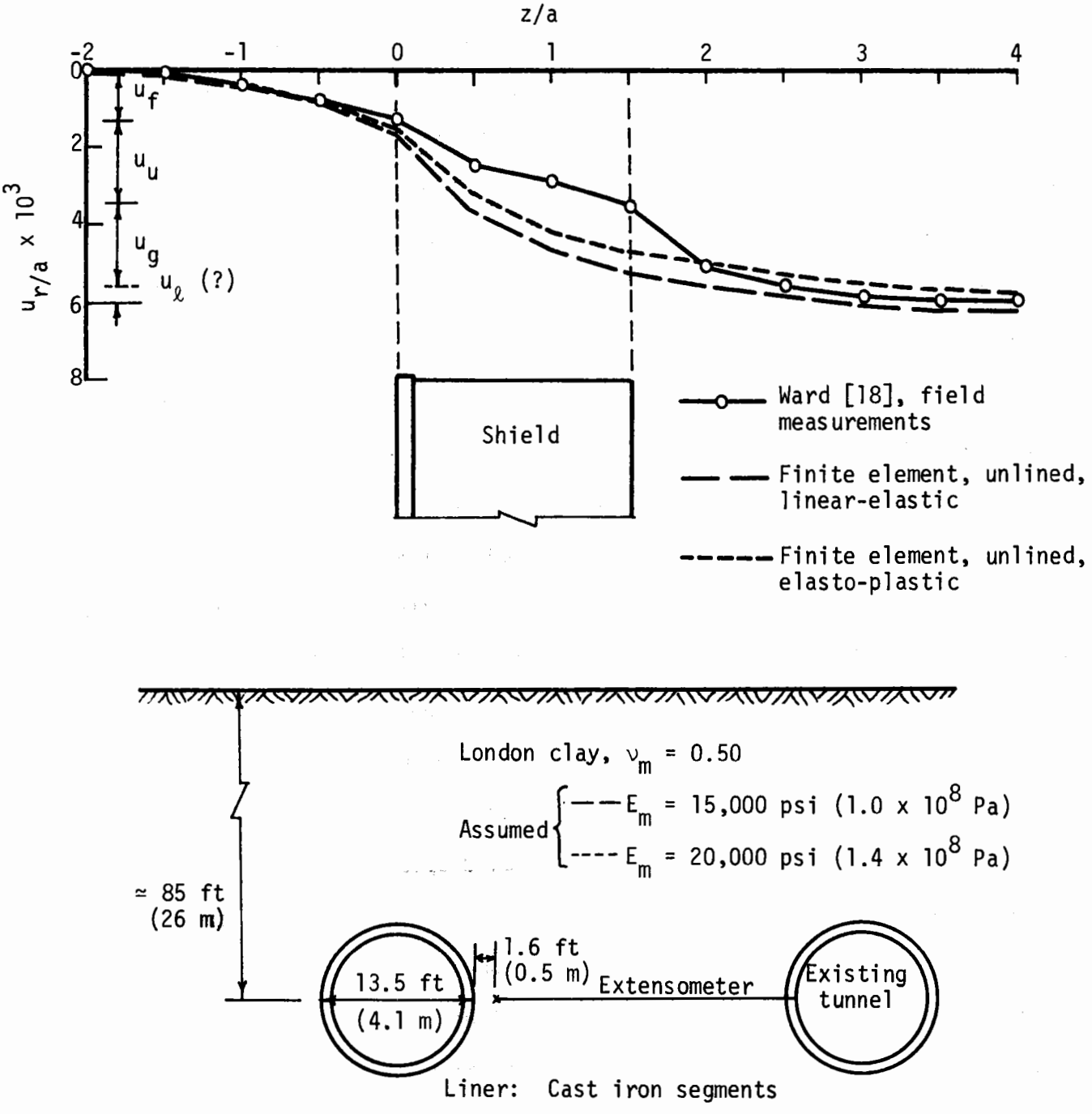

FIGURE 4.9 RADIAL GROUND DISPLACEMENTS: FIELD MEASUREMENTS (WARD [18] AND FINITE ELEMENT RESULTS COMPARED

and begins to take on load. The additional displacements, u_ℓ, of the liner then occurs. It is not clear from the data at what point the liner becomes effective, so it is difficult to estimate u_ℓ from the displacement curve.

The comparison with Muir Wood's data [13] is shown in Fig. 4.10. Here it was found that the best agreement was obtained with the displacements from the partially lined tunnel analyses (liner one radius behind face). Displacements from the fully lined tunnel analyses did not approach the magnitude of the measured displacement unless a very low modulus (2000 psi; 1.4×10^7 Pa) was assumed for the clay. Even then the finite element displacements overestimated the field values ahead of the face and underestimated those behind the face. Typical displacements from the unlined tunnel analyses are shown in Fig. 4.10. It can be seen that they significantly overestimate the displacements behind the tunnel face.

Relative to the maximum measured value, the displacements occurring ahead of the tunnel are quite large. However, as the shield's cutting edge passes the soil is pushed outward again. This suggests the presence of a bead or similar protrusion on the forward end of the shield. In terms of the ground displacement-ground pressure relationship, the reduced radial displacement at the face was taken as u_f rather than the maximum displacement occurring ahead of the face. The subsequent rapid inward displacement over the length of the shield indicates that the clay moved into a void space there. This displacement corresponds to u_u. For this tunnel each ring of precast concrete segments was expanded against the soil after leaving the shield. Thus, the lining becomes effective almost immediately and the potential displacement u_g is essentially eliminated. Almost all displacements occurring behind the shield correspond to u_ℓ.

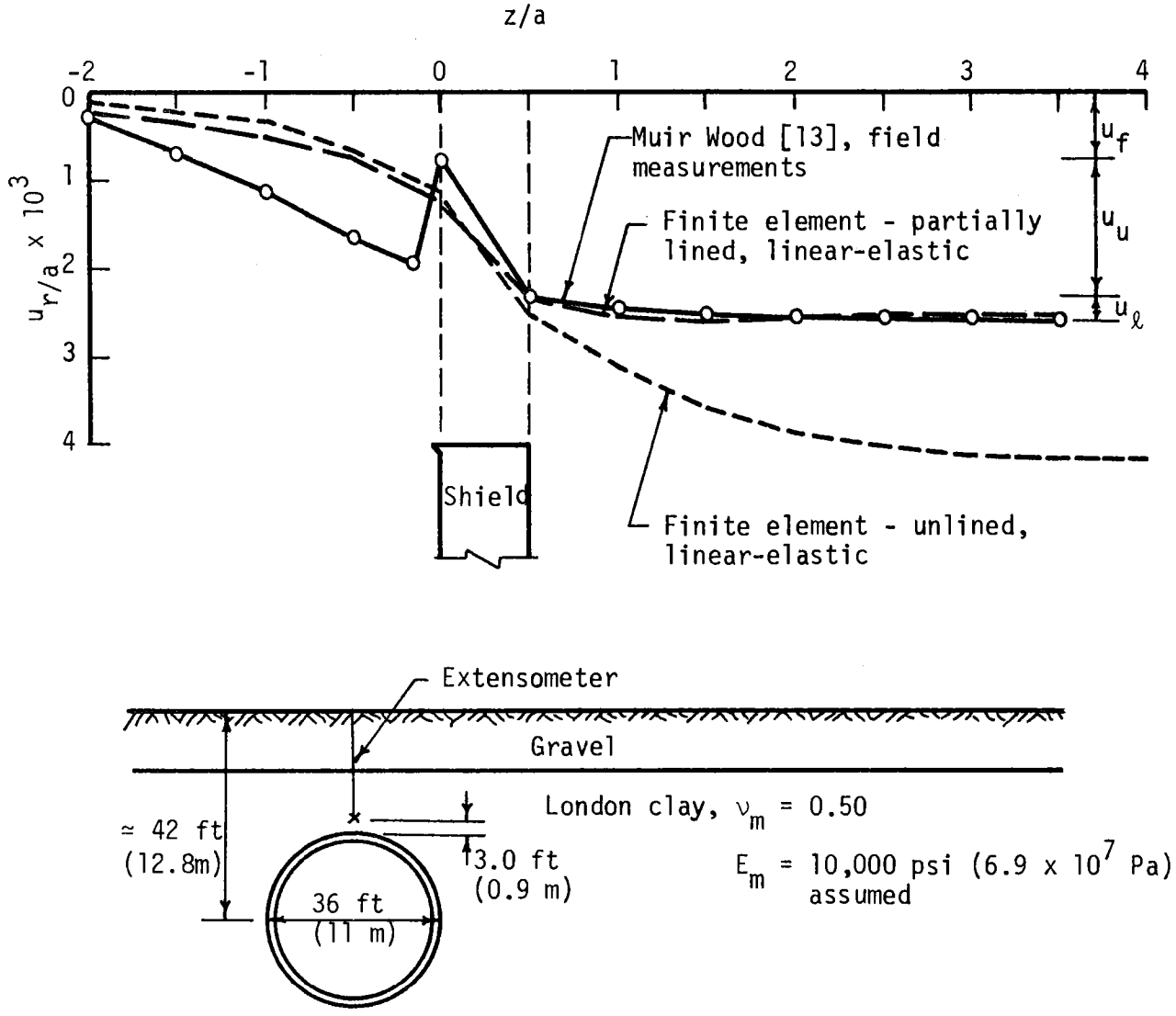

Liner: Precast concrete segments
12 in. (30 cm) thick
27 segments/ring

FIGURE 4.10 RADIAL GROUND DISPLACEMENTS: FIELD MEASUREMENTS (MUIR WOOD [13]) AND FINITE ELEMENT RESULTS COMPARED

It appears that analyses based on the assumption that the shield acts as an extension of the liner (tunnel lined to face) would have underestimated the ground displacements and thus overestimated the initial ground pressures acting on the liner in these two cases.

In general, however, the importance of the above construction details also depends on the behavior of the ground mass. In the above examples the soil was very stiff and possessed a relatively high shear strength. Thus, at the depths considered little or no plastic yielding occurred and the potential total displacement, u_p, was small. The void spaces between the soil and shield-liner were large compared to u_p and thus the shield and liner did little to prevent displacement before a major portion of u_p had occurred. A shield with given bead and tailskin thicknesses (t_b, t_s) will not hold the potential displacements u_u and u_g to less than their maximum values (function of soil properties) unless $(t_b + t_s) < (u_u + u_g)_{max}$. In the first example above, $(t_b + t_s) \geq (u_u + u_g)_{max}$ and thus the shield and liner had almost no effect on the ground displacements. In the second example t_s, and thus u_g, was effectively zero, but $t_b \geq u_u$ and so the shield did little to prevent the displacement u_u.

In summary, the following can be stated. In order to correctly model a given tunneling problem with the finite element method the ground conditions, shield configuration and method of liner installation must be considered. One way of doing this, of course, is to directly model these factors. However, it is a considerable task to effectively model the shield and details of liner installation, and so a reasonable approach is to adjust the position of the liner with respect to the face to correspond to the

anticipated behavior of the real tunnel. The length of unlined tunnel that should be left between the face and liner depends on the relative magnitudes of the two quantities $(t_b + t_s)$ and $(u_u + u_g)_{max}$. It is only when the above factors combine to yield $(t_b + t_s) << (u_u + u_g)_{max}$ that the assumption of the shield acting as an extension of the liner is valid.

4.5 EXTRUDED LINER SYSTEM

The diagram of the conceptual extruded liner system for soft ground tunnels in Fig. 1.1 shows that the forward end of the concrete slipform remains within the tail of the shield at all times. Consequently, concrete pumped into the slipform comes into contact with the surrounding ground at a point immediately behind the shield. Thus, there is no gap between the liner and the soil ($u_g = o$) and the liner (with the aid of the slipform) becomes effective immediately after leaving the shield. Thus, if the shield does nothing at all to prevent radial displacements this system could be modeled by assuming the liner extends to within a shield's length of the tunnel face. At the other extreme, if there are no voids around the shield, or if a void is present but $t_b << u_u$, it could be assumed that the shield acts as an extension of the liner and the system could be modeled by extending the liner up to the face.

Keeping in mind all of the simplifying assumptions that were made in the finite element analyses of this study and the restrictions they impose on the results, it is possible to estimate the liner thrust forces due to the initial ground pressure. Table 4.1 summarizes the various thrust values (in terms of γHa) obtained in this investigation. In general, it is the "final"

TABLE 4.1

VALUES OF THE LINER THRUST COEFFICIENT, $T/\gamma Ha$

Stress-strain behavior	Fully lined			Partially lined			2-D F.E.	Closed form solution
	Leading end	Max.	Final	Leading end	Max.	Final		
Linear-elastic	.570	.950	.875	.425	.425	.290	.983	1.179
Elasto-plastic $\phi = 0$	.725	.925	.800	.780	.780	.450	.983	1.004
Elasto-plastic $\phi \neq 0$	.590	.930	.875	.350	.350	.300	.983	1.179

thrust values that are of importance, because it is these values that would apply at locations behind the shield and slipform where the concrete liner alone would have to support the opening. If the shield effectively prevents most of the potential displacements u_u the fully lined tunnel analyses predict initial liner thrusts of approximately 80 to 85 percent of that due to the full overburden pressure. The thrust is high because the excavation-support system is very effective in holding ground displacements to a minimum. If the liner was less thick than assumed in the analysis and/or had a lower modulus (which it would initially) the stiffness of the liner would be less than that assumed in the analysis, and as a consequence u_ℓ would be increased and the initial thrust would be somewhat lower than the 80 to 85 percent of γH. For a shield of one tunnel radius length that was completely ineffective in preventing the displacement u_u (or for a longer shield that was partially effective in preventing the displacements) the partially lined tunnel analyses would apply.

They predict an initial liner thrust of approximately 30 to 45 percent of that due to the full overburden pressure. The range is greater here because the increased displacements allow a greater range of ground mass response (plastic yielding).

CHAPTER 5

SUMMARY AND CONCLUSIONS

With the general objective being the establishment of guidelines that can be used in the design of extruded concrete tunnel liners, a study had been undertaken to investigate the distribution of stresses and displacements associated with an advancing tunnel. In order to gain a better understanding of this complex problem initial work has been concentrated on the study of unlined and lined tunnels being advanced through soils exhibiting various types of idealized stress-strain behavior.

A series of axisymmetric finite element analyses were performed for a special case, $K_o = 1$, of the general three-dimensional problem. In these analyses the actual advancement of the tunnel through the ground mass was simulated using the excavation and construction option of the finite element program GEOSYS [10].

The unlined tunnel analyses have shown that the extent of the three-dimensional stress and displacement zone around the tunnel face is a function of the stress-strain behavior of the ground mass. For linear-elastic behavior this zone extends only approximately one to two tunnel diameters ahead and behind the face, irrespective of the elastic properties of the ground. If the ground mass exhibits elasto-plastic behavior the extent of the three-dimensional zone is increased when plastic yielding occurs, with the amount of increase being a function of the amount of plastic yield. The greatest increase occurs behind the heading where the three-dimensional zone extends back along the tunnel a distance of approximately three times the radius of the plastic zone.

When a lining is installed in a tunnel the resulting soil-liner interaction yields distributions of stress and displacement that are significantly different from those that would exist around and ahead of an otherwise identical unlined tunnel. However, the interaction (time-independent) occurs only if the liner is installed within the three-dimensional zone that would have existed had the tunnel been unlined. The amount of interaction that does occur varies with the position of liner installation. It is a maximum when the liner is installed at the tunnel face, but decreases rapidly as the point of installation is moved back from the face. The three-dimensional stress-displacement zones around tunnels that are lined to points near the face extend not more than one tunnel diameter behind the end of the liner regardless of soil behavior because of the stabilizing effect of the liner.

The behavior of a lined tunnel is strongly influenced by the ground displacements that occur before the liner comes into contact with the ground mass. These displacements, in turn, are controlled by the behavior of the ground ahead of the liner. Thus, the behavior of a lined tunnel, in response to its construction, cannot be determined from any solution method that does not consider the three-dimensional geometry and the physical advancement of the tunnel through the ground mass.

Also important to tunnel behavior are the interaction of the tunneling shield with the ground mass and the details of liner installation, because these factors determine at what point the ground is first supported and thus the amount of ground displacement that occurs before the liner becomes effective. For tunnels constructed with the extruded liner system, the tunnel opening is effectively provided internal support at some point

between the tunnel face and the tail of the shield. The exact point depends on the soil-shield interaction that occurs.

The finite element analyses performed in this study indicate that if the tunnel opening is supported all the way to the tunnel face the initial ground pressure on the lining results in a liner thrust equivalent to 80 to 85 percent of the overburden weight (γH). If the soil-shield interaction is such that the opening is effectively unsupported over a distance of one tunnel radius behind the face, the increased ground relaxation (displacements) yields a much lower initial liner thrust--only 30 to 45 percent of γH.

The analyses performed to this time, while informative, apply only to certain special cases of the general tunneling problem. Yet to be investigated are such factors as the time-dependent behavior of the ground mass and the extruded concrete liner and, other, more general, loading conditions such as the true ground pressure when $K_o \neq 1$ and the gravity induced loosening pressure.

REFERENCES

1. Abel, J. F. and F. T. Lee, "Stress Changes Ahead of an Advancing Tunnel," Int. Jour. Rock Mech. and Min. Sci. and Geom. Abs., Vol. 10, No. 6, November 1973, pp. 673-698.

2. Analytical Modeling of Rock-Structure Interaction, Vol. 1, Agbabian Assoc., Final Technical Report to U. S. Bureau of Mines, Contract H0220035, April 1973. (Order No. AD-761 648 from NTIS, Springfield, VA 22151).

3. Attewell, P. B. and I. W. Farmer, "Clay Deformations Resulting from Shield Tunneling in London Clay," Canadian Geotechnical Journal, Vol. 11, No. 3, August 1974, pp. 380-395.

4. Burns, J. Q. and R. M. Richard, "Attenuation of Stresses for Buried Cylinders," Proceedings, Symposium on Soil-Structure Interaction, Tucson, 1964, pp. 378-392.

5. Deere, D. U., R. B. Peck, J. E. Monsees and B. Schmidt, Design of Tunnel Liners and Support Systems, Report for U. S. Department of Transportation, OHSGT, Contract 3-0152, February 1969. (Order No. PB183799 from NTIS, Springfield, VA 22151)

6. de la Cruz, R. V. and R. E. Goodman, "Theoretical Basis of the Borehole Deepening Method of Absolute Stress Measurement," in Rock Mechanics - Theory and Practice, Proceedings, 11th Symposium on Rock Mechanics, Berkeley, 1969, pp. 353-374.

7. Descoeudres, F., "Three-Dimensional Analysis of Tunnel Stability Near the Face in an Elasto-Plastic Rock," in Advances in Rock Mechanics, Proceedings, 3rd Cong. Int. Soc. Rock Mech., Denver, 1974, Vol. 2, Part B, pp. 1130-1135.

8. Galle, E. M. and J. C. Wilhoit, Jr., "Stress Around a Wellbore Due to Internal Pressures and Unequal Principal Geostatic Stresses," Soc. Petrol. Engr. Jour., Vol. 2, No. 2, 1969, pp. 145-155.

9. Ghaboussi, J., E. L. Wilson and J. Isenberg, "Finite Element for Rock Joints and Interfaces," Journal of Soil Mechanics and Foundation Division, ASCE, Vol. 99, No. SM10, October 1973, pp. 835-848.

10. Ghaboussi, J. and R. E. Ranken, Tunnel Design Considerations: Analysis of Medium-Support Interaction, Report No. FRA-ORDD 75-24, Federal Railroad Administration, Department of Transportation, November 1974.

11. Hansmire, W. H. and E. J. Cording, "Performance of a Soft Ground Tunnel on the Washington Metro," Proceedings, 1st Rapid Excavation and Tunneling Conference, Chicago, 1972, Vol. 1, pp. 371-389.

12. Höeg, K., "Stresses Against Underground Structural Cylinders," Journal of Soil Mechanics and Foundation Division, ASCE, Vol. 94, No. SM4, 1968, pp. 833-858.

13. Muir Wood, A. M., Discussion of: Peck, R. B., "Deep Excavations and Tunneling in Soft Ground," Proceedings, 7th Int. Conf. Soil Mech. Found. Eng., Mexico City, Vol. 3, 1969, pp. 363-365.

14. Parker, H. W., R. M. Semple, A. Rokhsar, E. Febres-Cordero, D. U. Deere and R. B. Peck, Innovations in Tunnel Support Systems, Report No. FRA-RT-72-17, Office of High Speed Ground Transportation, Federal Railroad Administration, May 1971. (Order No. PB-204-437 from NTIS, Springfield, VA 22151).

15. Paul, S. L., E. H. Gaylord, A. J. Hendron, Jr., C. E. Kesler, B. Mohraz and R. B. Peck, Research to Improve Tunnel Support Systems, Report No. FRA-ORD&D 74-51, Federal Railroad Administration, Department of Transportation, June 1974. (Order No. PB-235-762/AS from NTIS, Springfield, VA 22151)

16. Peck, R. B., "Deep Excavations and Tunneling in Soft Ground," Proceedings, 7th Int. Conf. Soil Mech. Found. Eng., Mexico City, State of the Art Volume, 1969, pp. 225-290.

17. Peck, R. B., A. J. Hendron, Jr. and B. Mohraz, "State of the Art of Soft-Ground Tunneling," Proceedings, 1st Rapid Excavation and Tunneling Conference, Chicago, 1972, Vol. 1, pp. 259-286.

18. Ward, W. H., Discussion of: Peck, R. B., "Deep Excavations and Tunneling in Soft Ground," Proceedings, 7th Int. Conf. Soil Mech. Found. Eng., Mexico City, Vol. 3, 1969, pp. 320-325.

19. Ward, W. H., A. Marsland and S. G. Samuels, "Properties of the London Clay at the Ashford Common Shaft: In-Situ and Undrained Strength Tests," Geotechnique, Vol. 15, No. 4, December 1965, pp. 321-344.

20. Zienkiewicz, O. C., The Finite Element Method in Engineering Science, McGraw-Hill, London, 1971.

☆U.S. GOVERNMENT PRINTING OFFICE: 1976-211-173/484